The influence of gangue minerals on the composition and mineralogy of magnetite in high-grade metamorphic iron ore deposits: Implications for the Warramboo deposit.

Thesis submitted in accordance with the requirements of the University of Adelaide for an Honours Degree in Geology.

Kelsy J Dyer

November 2015

THE UNIVERSITY
of ADELAIDE

THE INFLUENCE OF GANGUE MINERALS ON THE COMPOSITION AND MINERALOGY OF MAGNETITE IN HIGH-GRADE METAMORPHIC IRON ORE DEPOSITS: IMPLICATIONS FOR THE WARRAMBOO DEPOSIT.

ABSTRACT

Understanding the influence that gangue minerals have on the composition and mineralogy of magnetite in high-grade metamorphic deposits is important for the sustainability of iron ore production in Australia. LA-ICP-MS and electron microprobe data from the granulite-facies Warramboo magnetite gneiss and the greenschist-facies Price Metasediments of the southeast Gawler Craton are used to investigate trace element partitioning between the oxide and gangue minerals, with a particular focus on the manganese content of garnet and magnetite. The data indicates that magnetite formed prior to garnet resulting in the partitioning of manganese and iron into magnetite, and consequently restricting these elements from garnet. However, during the development of garnet coronas on magnetite, manganese is redistributed into garnet leaving magnetite comparatively depleted in manganese. The partitioning of manganese during the growth of garnet coronas does not affect the iron content, or impact the ore grade, of the magnetite. Additionally, the proportion of garnet in the Warramboo magnetite gneiss and the Price Metasediments does not correlate with manganese content. The collection of HyLogger spectroscopic data to determine proportion and composition of garnet in the Warramboo gneiss was proven to be an ineffective technique. The HyLogger scanner did not correctly identify the mineral proportions in the samples, nor identify the presence of oxide minerals. By comparing the equivalent lower grade Price Metasediments to the Warramboo gneiss it was confirmed that the enrichment of magnetite through metamorphism did not remove impurities in the form of trace elements from the mineralogy. The results presented here will benefit industry to better understand high-grade magnetite deposits and the effect gangue minerals have on the grade of iron ore deposits.

KEYWORDS

Iron ore, Trace elements, Gawler Craton, LA-ICP-MS, HyLogger, high-grade metamorphism.

Kelsy J Dyer

Gangue mineral influence on magnetite and the implications for Warramboo iron ore deposit.

TABLE OF CONTENTS

LIST OF FIGURES AND TABLES

Figure 1. Geology and TMI aeromagnetic imaging.
Figure 2. TMI aeromagnetic imaging of Warramboo deposit and location of samples.
Figure 3. Cross section of the deposit, showing structure.
Figure 4. Photomicrographs of samples in PPL and RL
Figure 5. HyLogger Data
Figure 6. Graph showing the iron against manganese content (ppm) for the magnetite of each sample and texture from Warramboo and the Price Metasediment.
Figure 7. Graph showing the iron against manganese content (ppm) for the garnet of each sample and texture from Warramboo and the Price Metasediment.
Figure 8. Binary diagrams of Fe55 against Mn57 content of both magnetite and garnet from each sample.
Figure 9. Spider diagram showing the Rare earth element patterns against the Chondrite normalised values for each minerals and its respective textures.
Figure 10. Graph showing the iron against aluminium content (ppm) for the magnetite of each sample and texture from Warramboo and the Price Metasediment.

Table 1. Comparison between HyLogger data and QXRD data.
Table 2.LA-ICP-MS Rare Earth Element data, averaged and normalised to chondrite.
Table 3. Averages of the data used for trace element figures will a full data set in Appendix C.

Kelsy J Dyer

Gangue mineral influence on magnetite and the implications for Warramboo iron ore deposit.

INTRODUCTION

As the growing demand for steel continues globally the mining industry needs to look at ways that they can keep up with the supply of iron ore in an economical way. Australia is the second highest producer of iron ore behind China and in 2014 was the leading exporter with the country exporting 46% of global iron ore (Statista, 2015). The majority of current Australian steel production is supported by iron ore sourced from high-grade hematite deposits (McNab et al., 2009). However, as the quality of Australia's hematite has declined it has resulted in the demand for production from magnetite deposits to be developed in order to sustain the supply of iron ore (MagNet, 2011). Emerging magnetite projects present a viable, long-term alternative source of income and development incentives as opposed to hematite projects (MagNet, 2011).

In contrast to the common high-grade hematite ores, naturally occurring magnetite-dominated systems are usually of lower-grade and are of little value in their raw state (Carpentaria Exploration Ltd, 2011); as they contain impurities (such as trace elements), which can affect the iron product produced (MagNet, 2011). Once it has undergone the beneficiation process it is considered to be a premium quality product with higher grades and lower impurities compared to hematite (Carpentaria Exploration Ltd, 2011).

In the past magnetite trace elements have been used to determine provenance and can be used to characterise mineral deposit types as shown by several studies (Carew, 2004; Beaudoin et al., 2007; Nadoll et al., 2009; Chung et al., 2015). The distribution and partitioning behaviour of the trace elements depend on the metamorphic grade (Evans and Frost, 1975; Van Baalen, 1993; Skulblov and Drugova, 2003: Nadoll et al., 2014) of the deposit. Despite the potential of magnetite systems becoming a more

4

common iron ore source for Australia there have been few studies, if any, that specifically target the significance and relationship between the ore and gangue minerals in the system, instead focusing only on the origin of the ore deposit.

This study will focus specifically on the Warramboo ore deposit, a large Palaeoproterozoic, high-grade magnetite dominated iron ore deposit located in the central Eyre Peninsula, South Australia, developed by Iron Road Limited (Lane et al., 2015). It aims to investigate whether gangue minerals have an influence on the composition of the ore minerals at the high-grade system, and to determine whether the trace elements in the magnetite are correlated to, or affected by the surrounding mineral assemblages, particularly garnet. Hylogger data will also be utilised to determine whether it is an effective tool to identify potential ore deposits and correctly calculate the geochemistry of drill core samples. If the present study can establish the effect that gangue minerals have on the ore in magnetite systems, it will have significant implications for the Warramboo deposit, but also for the future development of the emerging magnetite industry in Australia (Carpentaria Exploration Ltd, 2011).
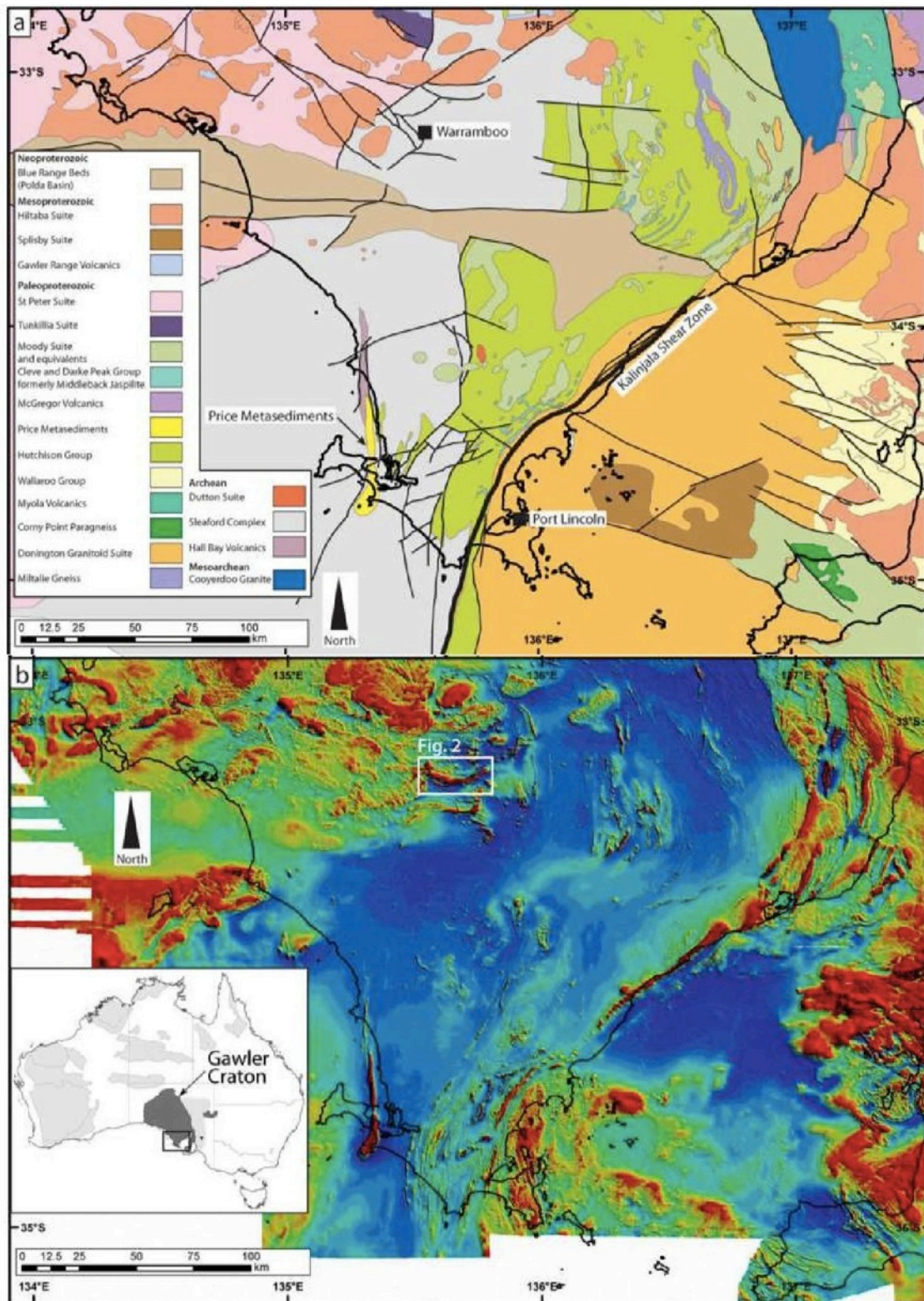
Figure 1. (a) Solid geology interpretation of the South Eastern Gawler Craton, showing Warramboo iron formation location and the Price Metasediment location (Price Island). (b) Shows the TMI aeromagnetic survey of the South Eastern Gawler Craton, with white box correlating to Figure 2. Inset: Overview of the Gawler Craton and the targeted study area (Lane et al., 2015).

Kelsy J Dyer

Gangue mineral influence on magnetite and the implications for Warramboo iron ore deposit.

GEOLOGICAL SETTING

Gawler Craton

The Gawler Craton preserves a complex and prolonged tectonic history spanning the interval *c*. 3150 Ma to *c*. 1450 Ma (Figure 1; Daly et al., 1998; Fraser et al., 2010; Hand et al., 2007; Payne et al., 2008; Reid and Hand, 2012; Morrissey et al., 2015). In general the Gawler Craton is poorly outcropping as it is largely covered by thick Neoproterozoic to Mesozoic sedimentary basins, Cenozoic marine sediments and widespread Neogene to Pleistocene aeolian dune fields (Reid and Hand, 2012; Reid et al., 2014; Lane et al., 2015).

The oldest rocks of the craton are Mesoarchean granitic gneisses with ages of *c*. 3250-3150 Ma, which occur within a shear zone-bounded tectonostratigraphic domain underlying much of the Gawler Craton and outcropping in the southeast (Fraser et al., 2010; Lane et al., 2015; Morrissey et al., 2015).

Neoarchean to early Paleoproterozoic volcano-sedimentary domains of the Gawler Craton are the Sleaford and Mulgathing complexes. The Mulgathing Complex is located in the north-central part of the craton and the Sleaford Complex in the south of the Gawler Craton (Reid et al., 2014). Both complexes comprise volcanic and sedimentary units deposited between *c*. 2560-2480 Ma (Lane et al., 2015).

The Sleaford Complex was metamorphosed and deformed during the 2465-2420 Ma Sleaford Orogeny (Reid et al., 2014; Lane et al.,2015), with low pressure-high temperature conditions of 5-7.5 kbar and 770-810°C recorded in metapelites in the south end of the Gawler Craton (Dutch et al., 2010; Lane et al., 2015).

7

An extensional event at 2000 Ma generated accommodation space for the deposition of the volcanoclastic sediments across the Gawler Craton, and triggered the intrusion of felsic and mafic magmas at 2000 Ma (Fanning et al., 2007; Lane et al., 2015). The Price Metasediments (1760 Ma) are an example of this and are located in central and western Eyre Peninsula (Morrissey et al., 2015).

The Kimban Orogeny was a craton-wide event with metamorphic grades ranging from greenschist to granulite facies (Hand et al., 2007; Payne et al., 2008; Dutch et al., 2010; Lane et al., 2015). The Kimban Orogeny is mostly studied in the southern part of the Craton where the Archean-Paleoproterozoic domains were extensively reworked within transpressional shear zones (Dutch et al., 2010; Lane et al., 2015), and is largely responsible for the macroscopic structural architecture of the Gawler Craton (Reid et al., 2014). Widespread high-grade metamorphism was accompanied by magmatism at *c*. 1580 Ma in the northern and southeastern Gawler Craton (Cutts et al., 2011; Forbes et al., 2012; Morrissey et al., 2013; Morrissey et al., 2015).

Warramboo iron deposit system

The Warramboo deposit is located on the central Eyre Peninsula in South Australia (figure 1), and consists of granulite-facies, magnetite-rich metapelitic gneisses interlayered with felsic gneisses. The deposit is entirely covered by Tertiary to recent cover sequences, with mineralisation projected to occur at depths between 200-600 m (IronRoad, 2014). It is the largest known magnetite deposit in Australia, with a resource estimate of 3.7 billion tonnes at 16% iron (IronRoad, 2014; Morrissey et al., 2015).
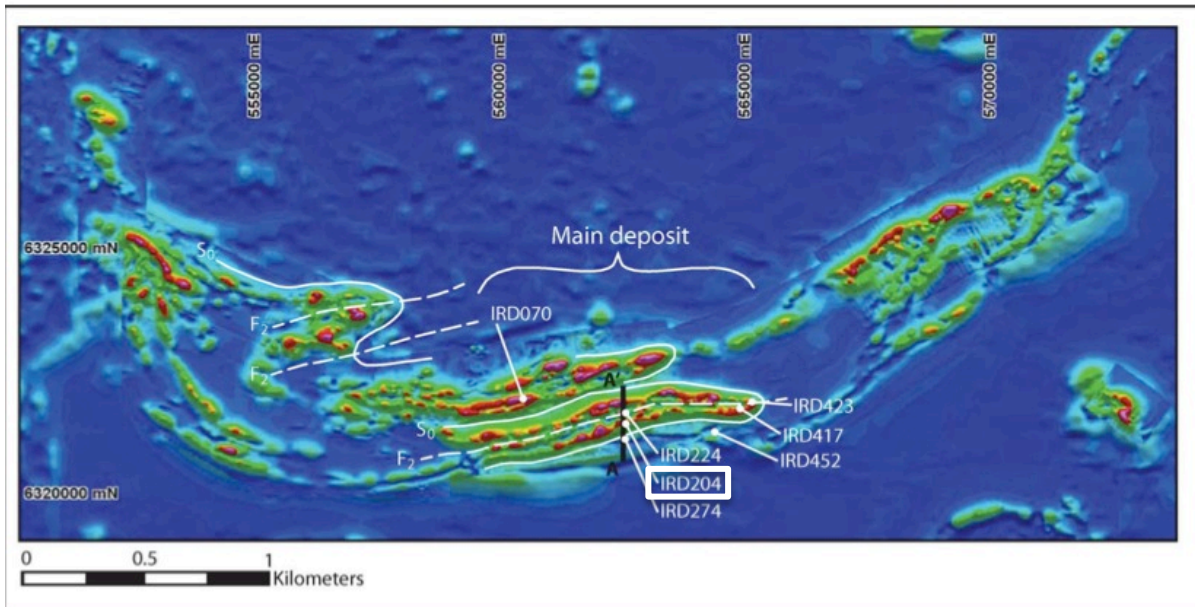
Figure 2. The TMI aeromagnetic image of Warramboo magnetite gneisses, with the main deposit (Murphy South) shown along with selected study drill hole IRD204 in the white box and the A-A' cross section used for 3 (Lane et al., 2015).

The deposit trends east-west and outlines an isoclinal fold system closing to the east. It is identified by a prominent high response on aeromagnetic imagery, which is quite different to the dominant north-south trending structures associated with the Kimban Orogeny, which truncate the east-west fabrics at Warramboo (Figure 2).

As the host rock is granulite facies the mineralisation in the deposit is coarse-grained and therefore easy to concentrate, with an estimated iron beneficiation product of 67% (IronRoad, 2013).

The lithologies are explained in detail by Lane et al. (2015) and have been divided into sub-categories of magnetite-bearing horizons, iron-poor lithologies and magnetite-rich ore zones. The magnetite bearing lithologies are heterogeneous, mineralogically and compositionally, and all have deformed K-feldspar-quartz leucosomes and variable abundances of spessartine-rich garnets and hematite (Lane et al., 2015; Morrissey et al., 2015). These gneisses are interpreted to be a younger cover sequence, deposited

between 1760-1735 Ma, in contrast to the iron-poor lithologies that are considered to

have been deformed and metamorphosed at 2445 Ma, and are interpreted to be a part of

the Sleaford Complex of the southern Gawler Craton (Lane et al,. 2015; Morrissey et

al., 2015). The protolith rocks to the iron-poor lithologies are considered to have been

deposited 2470-2445 Ma coevally with two felsic igneous units with magmatic ages of

2466-2474 Ma (Lane et al., 2015; Morrissey et al., 2015).

Manganese enrichment correlates throughout the deposit in the magnetite-bearing

gneiss, and is interpreted to represent a primary compositional layering (S_0) inherited

from a heterogeneous sedimentary protolith (Lane et al., 2015; Morrissey et al., 2015).

The large-scale structure of the deposit (Figure 3) is interpreted to be a shallowly

southwest-plunging syncline, defined by the gneissic foliation (S_1), which developed

parallel to the original S_0 layering, and dips moderately to gently in a south-southeast

direction. Fold hinges in the drill core are small and plunge shallowly to the east and

west, with a great circle fit of 20/165 (Figure 3; Lane et al., 2015); correlating to the

general east-west trend of the deposit (Figure 2).

The pressure-temperature on the metamorphism of the Warramboo deposit system are

interpreted to be 830-850°C and 5-6.8 kbar (Morrissey et al., 2015). The alignment of

sillimanite within cordierite, and the observation of cordierite enveloping the hematite-

magnetite aggregates, suggests that the earlier evolution may have in fact involved

pressures that were higher than these interpreted values above (Morrissey et al., 2015).

Gangue mineral influence on magnetite and the implications for Warramboo iron ore deposit.
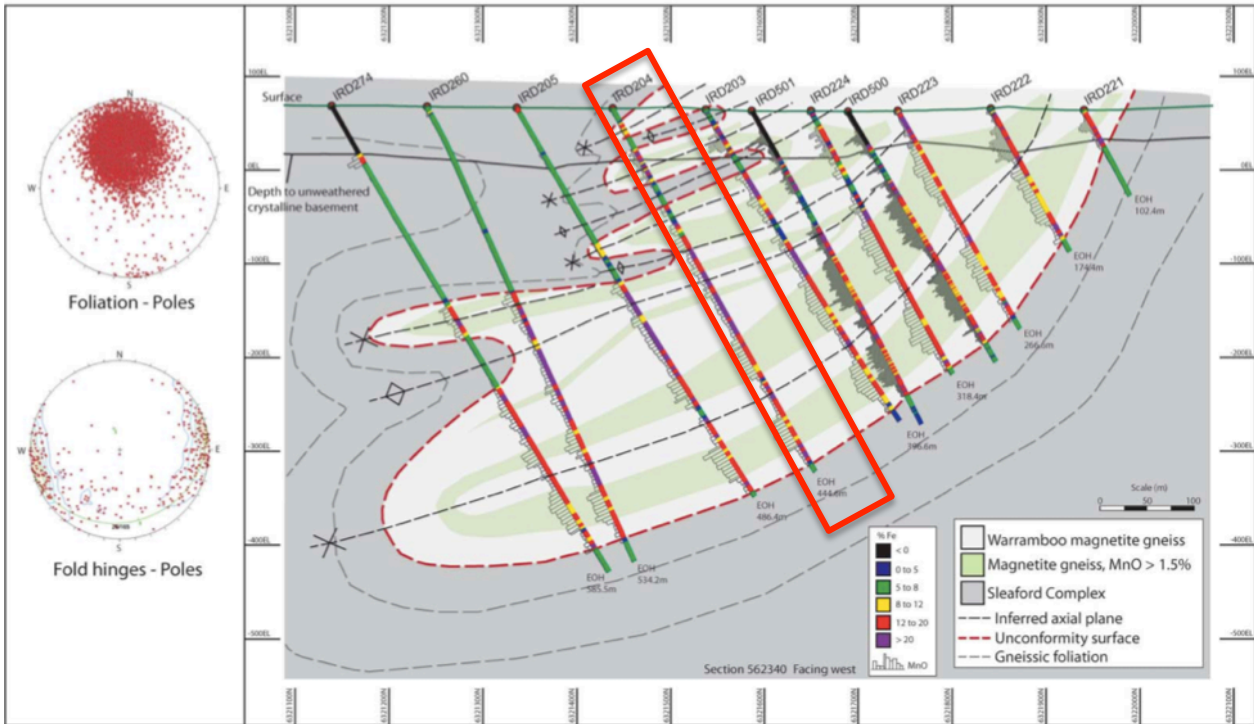
Figure 3. Interpreted cross-section geology and structure of the Warramboo deposit through the A-A' transect from Figure 2. Red box shows IRD204 drill hole, which is the targeted sample in this study. Values of Fe and Mn content are displayed for the drill holes as well as stereonets of the gneissic foliation and fold hinges poles.

METHODS

Petrography

Petrography was conducted at The University of Adelaide using both optical and reflective microscopes.

Laser Ablation Induced Coupling Plasma Mass Spectrometry (LA-ICP-MS) and Electron microprobe (EPMA)

Trace element concentrations were determined by using LA-ICP-MS and EMPA analysis undertaken at Adelaide Microscopy, South Australia. Polished thin sections were ablated in-situ by a laser beam generated by a New Wave UP-213 coupled to an Agilent 7500x ICP-MS (carrier gas of Helium). The acquisition time for each spot was 30s after monitoring the background for 30s. Calibration was conducted using standards of 3x NIST 610, 2x NIST 612 and 3x BHVO-1 and was recalculated after every 15 unknowns to correct for time-dependant drift of sensitivity and mass discrimination (Zhao and Zhou, 2015). Two hundred and seventy five laser spots, each 5 Htz, 55% energy, with a 30μm diameter was ablated from the 7 samples targeting garnet, magnetite and hematite mineral grains. ^{57}Fe was used as the normalising element for multi-standard calibration for the oxides and ^{43}Ca for the garnets. Electron microprobe spot analysis were conducted for all laser spots using a Cameca SXFive Microprobe with beam size of 5μm, 15kV and beam current of 20nA. The elements analysed were ^{24}Mg, ^{27}Al, ^{29}Si, ^{31}P, ^{43}Ca, ^{45}Sc, ^{47}Ti, ^{49}Ti, ^{51}V, ^{53}Cr, ^{55}Mn, ^{57}Fe, ^{59}Co, ^{60}Ni, ^{65}Cu, ^{66}Zn, ^{69}Ga, ^{89}Y, ^{90}Zr, REE's (^{118}Sn-^{175}Lu), ^{178}Hf, ^{208}Pb, ^{232}Th and ^{238}U (Duplis and Beaudoin, 2011; Dare et al., 2014; Huang et al., 2015; Zhao and Zhou, 2015). The raw data from both methods were combined and processed through the program Glitter to produce the

Kelsy J Dyer

Gangue mineral influence on magnetite and the implications for Warramboo iron ore deposit.

Trace Element concentrations MDL filtered and Trace Element concentrations normalised to chondrite for both garnet and magnetite of each sample.

HyLogger

Georgina Gordon at the Geological Survey of South Australia collected the HyLogger data used in this study. Drill core from Murphy South's IRD-204 hole from Warramboo was scanned through the machine in 86 core trays and their spectra collected. The total length of core was 444.6 m. This data was then processed through a program called the spectral geologist (TSG7) where the near-infrared and short wave infrared data was produced. For a detailed methodology contact Georgina Gordon at the GSSA.

Kelsy J Dyer

Gangue mineral influence on magnetite and the implications for Warramboo iron ore deposit.

RESULTS

Samples

SAMPLE 111512

Sample 111512 comes from exploration drill hole IRD204, depth interval 320.89-321.04 m (Figure 4a, b). The sample is classified as a banded ore type, is compositionally layered and contains magnetite, hematite, biotite, garnet, quartz, sillimanite, cordierite, plagioclase and K-feldspar. Magnetite is the dominant ore mineral and occurs as massive banded but irregular shaped grains with a typical size around 500 μm, some with coronas of garnet throughout the sample. Garnet also occurs as euhedral grains up to 200 μm in size with some garnets preserving very fine-grained inclusions of hematite. Biotite occurs as irregular shaped grains, and is weakly aligned to the foliation. Sillimanite occurs mainly in association with cordierite and is aligned to the foliation, with the cordierite showing radiation damage. There is evidence of twinning in the microcline feldspar, and the sample also contains minor plagioclase. Altered hematite grains in the feldspar-biotite occur as rounded disseminated grains up to 100 μm with most preserving ilmenite exsolution. In some magnetite grains there has been Martite replacement of the magnetite to produce hematite/ilmenite. The petrogenesis that can be interpreted from this sample is that the magnetite is early, followed by replacement by martite and then the development of garnet coronas. Euhedral garnets post date the hematite as constrained by the inclusions.

SAMPLE 111516

Sample 111516 comes from exploration drill hole IRD204, depth interval 385.88-385.99 m (Figure 4c, d). The sample is classified as disseminated ore type and contains

hematite, magnetite, garnet, quartz, chlorite and traces of muscovite. Hematite is the main ore mineral and occurs as many different textures in the sample. The first is as large coarse grains with no exsolution occurring up to 1 mm. The second as very advanced martisation of former magnetite grains, as well as developing along cracks in the massive hematite. Irregular shaped hematite occurs in massive muscovite grains, whereas the disseminated hematite occurs in the muscovite-quartz. Magnetite is present as relic grains in the martite as well as disseminated grains up to 100 μm. The garnet forms large, irregular shapes grown predominately next to the oxide minerals, refered to as "Massive" throughout this study. Chlorite is also present as irregularly shaped and/or as rounded grains (up to 400 μm), with some grains preserving inclusions of hematite. There is a lack of cordierite, sillimanite and K-feldspar in the sample. Petrogenically the martite is interpreted to have formed later than the magnetite, as magnetite is present as relics, which would have started as a complete magnetite grain. Hematite formed prior to chlorite with the intrusions present in the sample.

SAMPLE IRD204-31A

Sample IRD204-31A comes from exploration drill hole IRD204, depth interval 293.5-293.7 m (Figure 4e). This sample also has two distinct bands of different mineralogy. The first layer includes magnetite, sillimanite, garnet, biotite, cordierite, plagioclase, K-feldspar and quartz. Biotite occurs as elongate grains defining a fabric with disseminated magnetite, hematite and euhedral garnets. There is evidence of radiation damage in the cordierite as well as "rust" from minerals with high Fe content being oxidised or weathered. The second layer includes magnetite as irregular massive grains defining the foliation, which occasionally are rimmed by garnet and biotite. There are still small amounts of euhedral garnets, but in this layer they mostly occur as corona around the magnetite. The magnetite is the dominant ore mineral, however, few grains

Kelsy J Dyer

Gangue mineral influence on magnetite and the implications for Warramboo iron ore deposit.

of hematite are present also. This layer also contains quartz and feldspar, but is depleted of sillimanite and cordierite. The garnet coronas are interpreted to have formed later than the magnetite.

SAMPLE IRD204-31B

Sample IRD204-31B comes from exploration drill hole IRD204, depth interval 293.5-293.7 m (Figure 4f). This came from the same depth interval of 31A and so the mineralogy is almost identical. This sample can be split into three different layers also, one very garnet rich, one oxide rich and one more felsic layer. The garnet rich layer comprised of small euhedral garnets all overlapping each other, with minor biotite as irregular grains. The oxide rich layer comprised of massive irregular and disseminated magnetite and hematite, with magnetite being the dominant ore mineral. The garnets are quite small (70-100 μm) but larger than the garnet rich layer. The third layer includes quartz, cordierite, plagioclase, sillimanite, feldspar and garnet. The garnets are largest in this band (>100 μm) and some include inclusions of magnetite. There are also a small, infrequent amount of cordierite grains in the band also.

SAMPLE IRD204-02B

Sample IRD204-02B comes from exploration drill hole IRD204, depth interval 90.7-92.6 m (Figure 4g). The sample is from the upper felsic layers with mineralogy of quartz, plagioclase, garnet, magnetite and hematite. The sample lacks cordierite and sillimanite. It is dominant in biotite, which defines a foliation and occurs as elongate and irregular grains. The biotite grains get coarser in association with the magnetite grains and in some areas are banded. Euhedral garnets are present and range in sizes dramatically from 50 μm -1 mm. The larger euhedral garnets have magnetite

Kelsy J Dyer

Gangue mineral influence on magnetite and the implications for Warramboo iron ore deposit.

inclusions up to around 100 μm in some cases. Magnetites also occur as irregular shaped coarse grained in this sample but are restricted to the "band" type alignment in the sample. In areas with magnetite depletion the garnets are smaller in size and do align in a similar direction to the biotite grains. Quartz and plagioclase are also present in this sample.

Price Metasediments

The Price Metasediments occur in the Southern Eyre Peninsula (Figure 1) as prominent, north south trending magnetic high on the aeromagnetic image, and are characterised by fine-grained, grey-green, magnetite-bearing phyllite with a well-developed, spaced cleavage (Oliver and Fanning, 1997; Morrissey et al., 2015). The Price Metasediments are compositionally layered on a mm scale and are finely bedded. The Price Metasediments are similar in age to the Warramboo gneisses and have similar Sm-Nd isotopic compositions, and both contain abundant spessartine garnet, suggesting a common sedimentary source (Oliver and Fanning, 1997; Lane et al., 2015; Morrissey et al., 2015). The two samples chosen to represent the Price Metasediments are comparatively magnetite-rich and magnetite-poor layers within the rock package, which is of greenschist facies.

SAMPLE WDH31541 (GARNET POOR)

Sample WDH 31541 garnet is poor and comprises of muscovite, biotite, quartz, magnetite, garnet, chlorite and plagioclase. It is fine-grained with a weak foliation defined by muscovite and quartz-rich layers with small amounts of plagioclase. Biotite occurs unoriented in small flakes up to around 100 μm and chlorite flakes are aligned with the foliation, or adjacent to magnetite and garnet. Magnetite in the sample is

Kelsy J Dyer

Gangue mineral influence on magnetite and the implications for Warramboo iron ore deposit.

euhedral in shape and ranges in size from 10-100 μm throughout the entire thin section. No hematite is clearly identifiable in the sample but could occur as small grains in the foliation; however the total percentage would be small. Garnet occurs in the sample as grains up to 100 μm euhedral with some having preserving inclusions of fine-grained magnetite.

SAMPLE WDH41368 (GARNET RICH)

Sample WDH41368 is garnet rich and compositionally layered. It is dominantly comprised of two distinct layers of iron-rich and pelitic layers (Figure 4h). There is a weak foliation noticeable in some layers of the sample dominated by magnetite and biotite. The mineralogy is similar to sample WDH41368 garnet poor, and is dominated by muscovite and quartz. Magnetite occurs as euhedral grains up to 200 μm, with small euhedral garnets up to 100 μm in size frequently occurring in the pelitic layer, but also occasionally as porphyroblasts. Inclusions of fine-grained magnetite are present in the garnets. Biotite and chlorite occurs as flakes throughout the sample up to 100 μm in size. The biotite and chlorite forms in contact with or close to magnetite grains. Magnetite is the dominant oxide in the iron-rich layer, occurring as porphyroblasts.
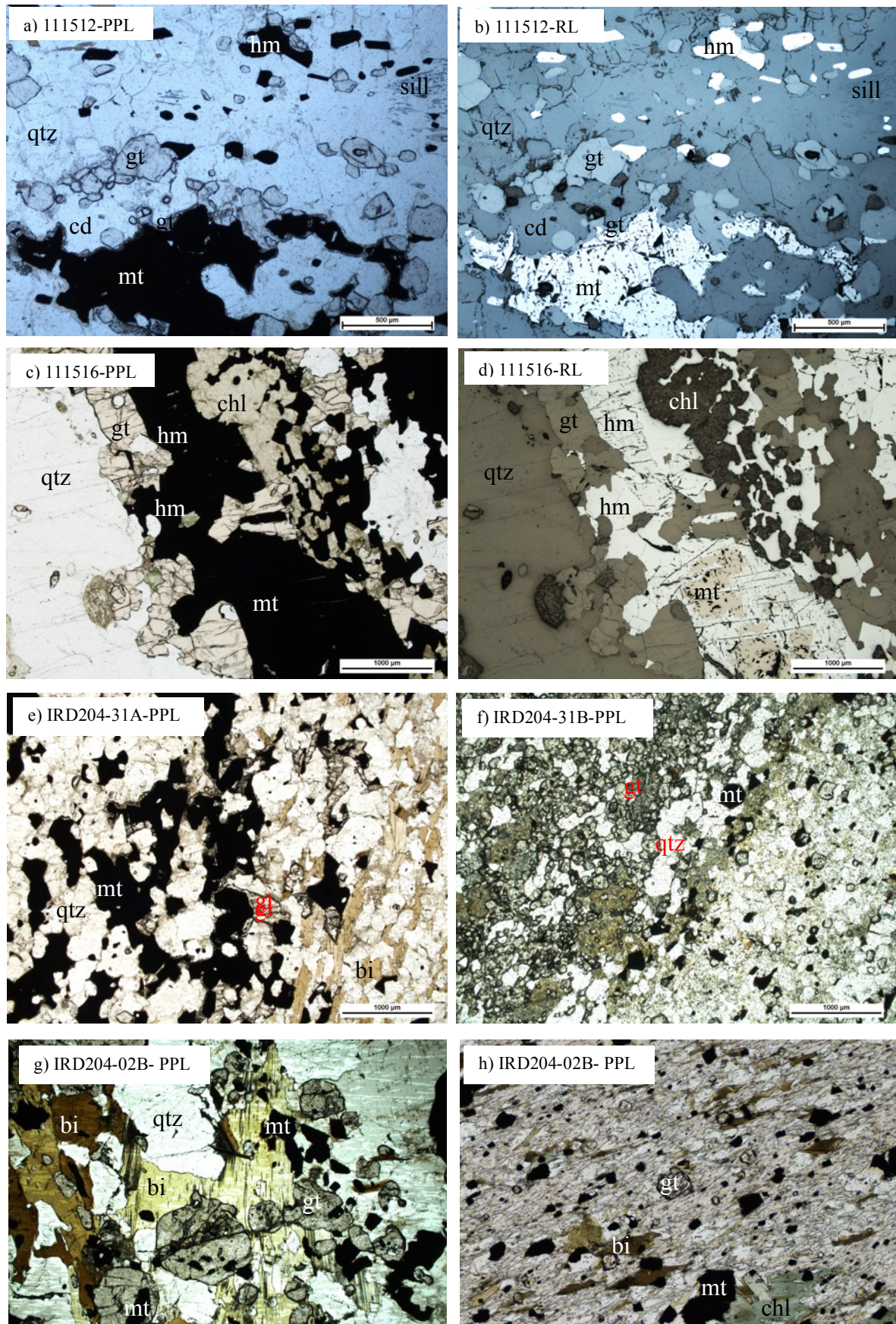
Figure 4. Photomicrographs of the samples. (a) Sample 111512 in PPL. Shows garnet corona on magnetite grain, as well as sillimanite and cordierite mineralogy. (b) Sample 111512 in RL. (c) Sample 111516 in PPL. Martite shown as breakdown of magnetite, chlorite and garnet bordering ore minerals. Hematite dominant. (d) Sample 111516 in RL. (e) Sample IRD204-31A in PPL. Garnet occurring as a corona on magnetite grains. (f) Sample IRD201-31B in PPL. Two different layers within the sample with differing garnet proportions. (g) Sample IRD204-02B in PPL. Large euhedral garnets with inclusions of magnetite and large sheets of biotite. (h). Sample WDH41368 in PPL. Lower grade magnetite, garnet and chlorite. mt=magnetite, gt=garnet, hm=hematite, bi=biotite, chl=chlorite, sill=sillimanite, qtz=quartz and cd=cordierite.

Kelsy J Dyer

Gangue mineral influence on magnetite and the implications for Warramboo iron ore deposit.

HyLogger

In total 444.6 m of drill core were analysed. The entire length of the core was analysed

for short wave infrared and the thermal infrared wavelength before being processed

through the TSG program (Figure 5). The short-wave infrared picked up minerals such

as muscovite, chlorite and biotite (Figure 5a). It shows the sample count in proportion to

the others and does not show a quantitative result. The thermal infrared diagram has the

minerals that are most common in the magnetite gneiss at Warramboo. It was able to

identify quartz, plagioclase, feldspars, garnet, cordierite, the micas, chlorite and few Fe

minerals (Figure 5b). The main point of interest in Figure 5 is that there are a large

portion of oxides (magnetite and hematite) that have not been identified by the

HyLogger machine, with only a small amount detected at around 240-250 m depth

interval. It also does not seem to have identified a wavelength for the sillimanite mineral

in the diagram. While it does not show the percentages of the minerals, it does show the

proportion of the minerals relative to each other. What is clear is that the Hylogger data

is quite different to previous results such as QXRD (Table 1) and petrography

conducted.

Table 1. Comparative table showing the difference between the two techniques, HyLogger and QXRD, for the mineral abundances of samples 111512 and 111516.

Sample 111512 (320-321 m)		Sample 111516 (385-386 m)	
HyLogger	**QXRD (wt%)**	**HyLogger**	**QXRD (wt%)**
Quartz 34%	Quartz 27.4%	Quartz 57%	Quartz 25%
Anorthoclaise 23.6%	Feldspar 25.4%	Anorthoclaise 12.1%	Feldspar 0%
		Microcline 18.8%	
Oligoclaise 8.4%	Plagioclaise 16.2%	Hornblende 12.1%	Hornblende 0%
Spessartine 6.7%	Garnet 7.0%	Garnet 0%	Garnet 13.4%
Almandine 6.4%			
Oxides 0%	Magnetite 9.8%	Oxides 0%	Magnetite 4.9%
	Hematite 2.8%		Hematite 47.4%
Cordierite 20.9%	Cordierite 9.1%		

Kelsy J Dyer

boo iron ore deposit.

Figure 5. HyLogger spectra from IRD204 drill core. (a) Short wave infrared data, with yellow being infrared data, with yellow being muscovite, purple being aspectral and blue being chlorite FeMg. (b) Thermal infrared data spectra with light pink being quartz, orange-feldspars, blue-cordierite, lime green-chlorite, yellow-muscovite and light grey-iron minerals.

21

Kelsy J Dyer

Gangue mineral influence on magnetite and the implications for Warramboo iron ore deposit.

Trace Elements

From the electron microprobe data collected and processed through Glitter, 38 trace elements were analysed for magnetite, hematite and garnet. The Price Metasediment samples were categorised separately from the Warramboo magnetite samples and each mineral was sorted into its respective texture. Inter-elemental relationships between Mn and Fe are examined in binary plots for both magnetite and garnet for all samples and textures.
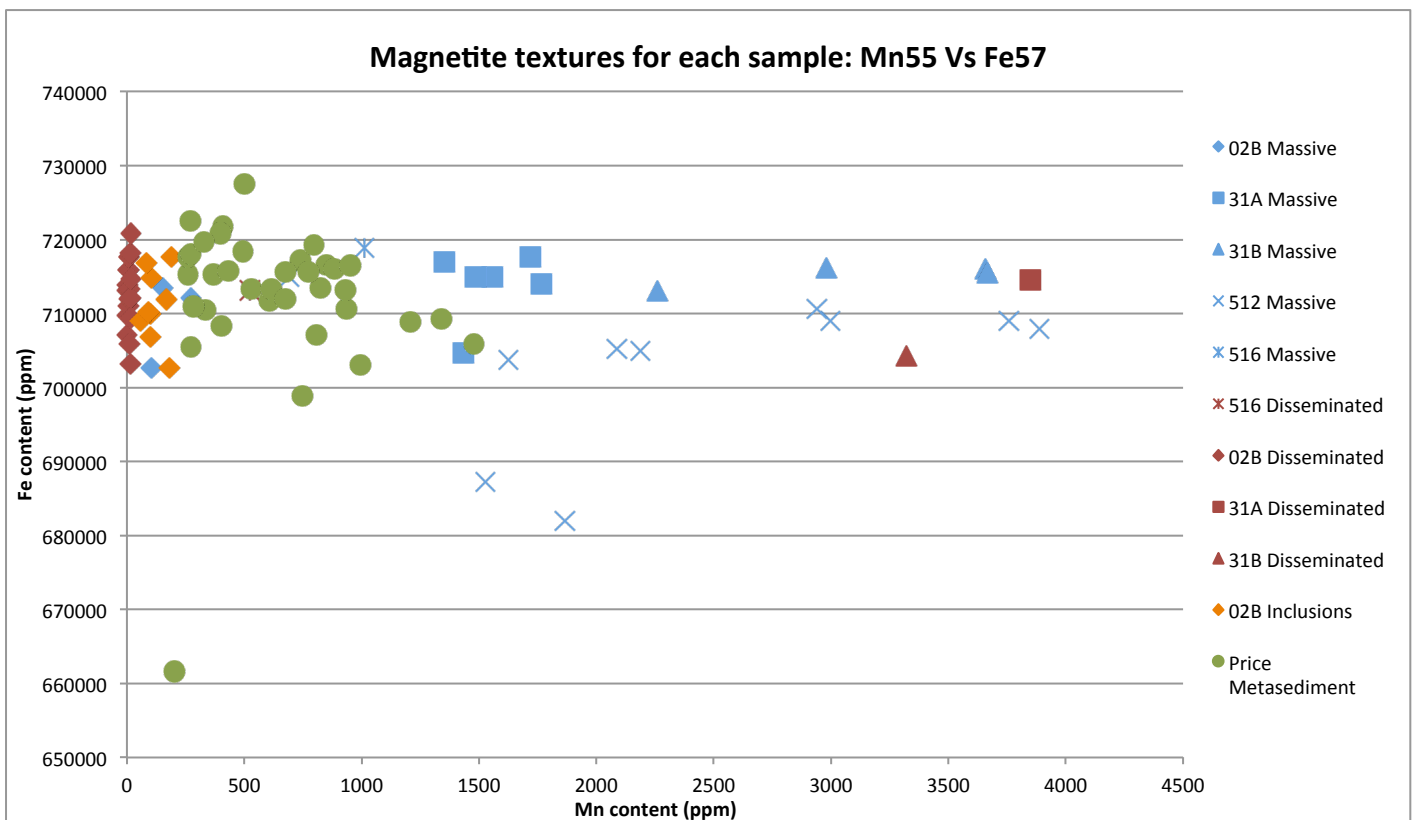
Figure 6. Graph showing the iron against manganese content (ppm) for the magnetite of each sample and texture from Warramboo and the Price Metasediment.

MAGNETITE TEXTURES OVERALL

The general trend for the magnetite textures and each sample shows that most of the massive magnetite grains have a higher Mn content (ppm) than the disseminated and inclusions with the majority being over 1000 ppm. The exception to this is the 204-02B massive magnetite (Figure 6). The Fe content is not jeopardised or affected by changes

in the Mn content, regardless of the textures of the mineral. The samples which contain

large, but few, garnets with magnetite inclusions (204-02B) tend to plot with a lower

Mn content (under 500 ppm) than the samples with a higher percentage of smaller,

garnets such as 204-31B (average 3000 ppm Mn content). The disseminated magnetites,

as well as the inclusion magnetite, generally have a lower Mn content than the massive

magnetite. The Price Metasediment magnetites plot between the

disseminated/inclusions and the massive magnetites in relation to Mn content with

between ~300-1200 ppm with the exception of outliers. Some of the magnetites have

higher Mn values or lower Fe values, but the average has similar Fe values (700000-

725000 ppm) to the rest of the samples.
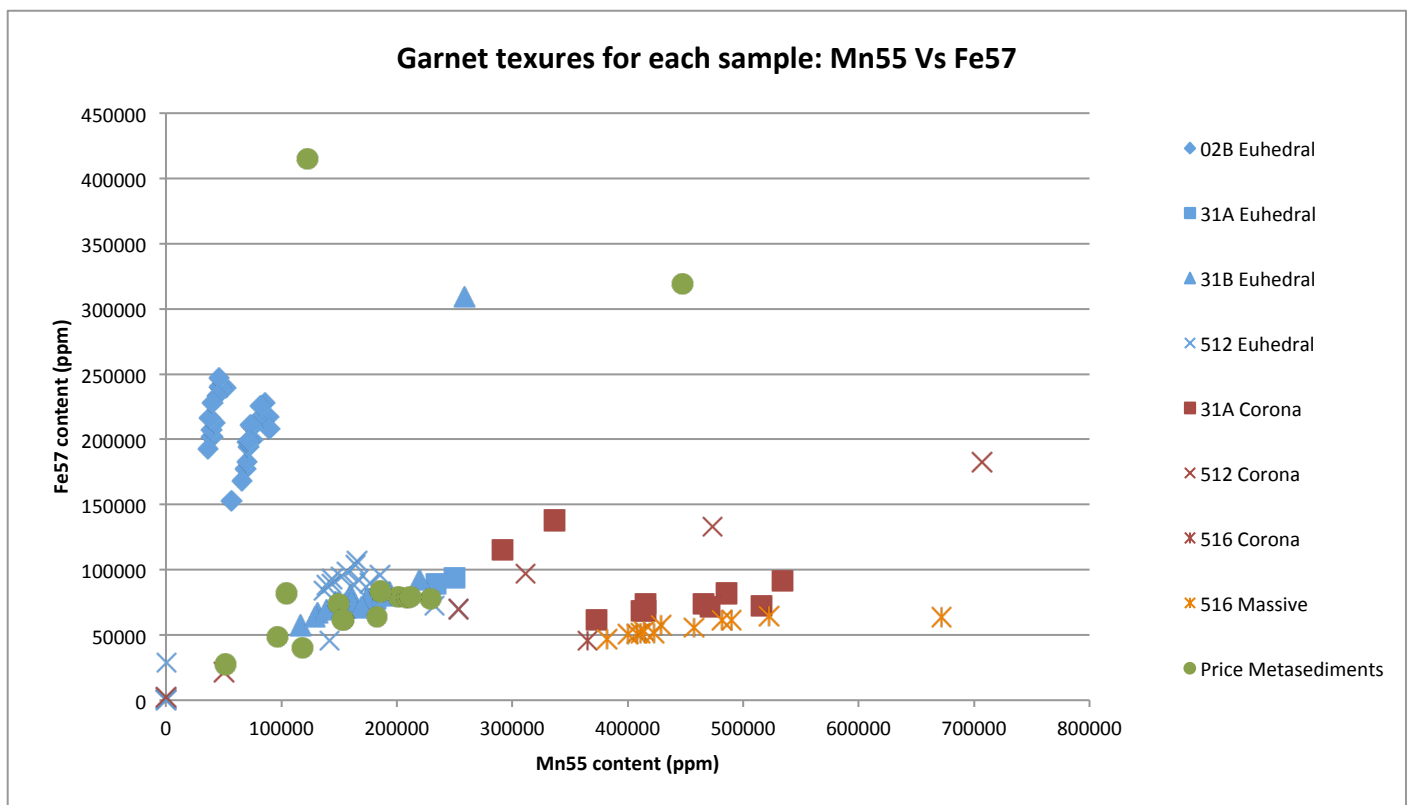
Figure 7. Graph showing the iron against manganese content (ppm) for the garnet of each sample and texture from Warramboo and the Price Metasediment.

Kelsy J Dyer

Gangue mineral influence on magnetite and the implications for Warramboo iron ore deposit.

GARNET TEXTURES OVERALL

The garnet textures from all samples are highly variable (Figure 7). However, there does seem to be distinct patterns with regards to each sample, and the texture of the garnet. Overall, there is a trend with the euhedral garnets and the Price Metasediment garnets (all euhedral also) having a Mn value lower than the corona garnets and the 111516 garnets, which occur in a sample dominated by hematite. The larger garnets of 204-02B with magnetite inclusions are the group that has the highest Fe content of all (150000-250000 ppm). However they have a relatively lower Mn value than the other groups with under 100000ppm. The smallest garnets of 204-31B seem to plot with a positive linear trend, where the Mn and Fe content is positively proportional to each other. Corona garnets of 204-31A plot very similarly, with a few of the corona points plotting with a trend similar to the euhedral garnets which reside in the midrange Mn value (100000-250000 ppm). The Price Metasediment euhedral, 204-31B euhedral and the 111512 euhedral garnets all sit at this mid Mn range and have a similar trend. The majority of the samples plot within this midrange Mn content such as the medium sized euhedral garnets of sample 111512; however, the coronas of this sample have a very odd and diverse pattern with a lot of variation between the values. There does seem to be a rough linear trend that shows that as the Mn content increases, as does the Fe. The garnets that appear in the hematite-dominated sample 111516 plot along the same trend as the 204-31A coronas with a linear positive trend with the highest Mn content of the samples (350000-550000 ppm).

GARNET AGAINST MAGNETITE PER SAMPLE

Magnetite and garnet were plotted against each other for each sample with the minerals in the Warramboo gneiss and the Mn values on a logarithmic scale, to be able to compare the distinctively different minerals (Figure 8). The magnetites all have a

24

Kelsy J Dyer

Gangue mineral influence on magnetite and the implications for Warramboo iron ore deposit.

similar Fe value (700000 ppm) and only vary in the Mn content. The garnets record a

diverse and varied Mn and Fe contents. All garnets have the pattern of the magnetites

having less Mn than garnets and a higher Fe component.

Sample 204-02b has the lowest Mn content of the samples for magnetite and a lower

Mn content than 204-31A and 204-31B. There are similar patterns for both 31A and

31B, with a decrease in Fe and an increase in Mn between the two minerals. All

samples show the same trend that as the magnetite has a lower Mn and higher Fe

content then the garnet has a higher Mn content and a lower Fe content.
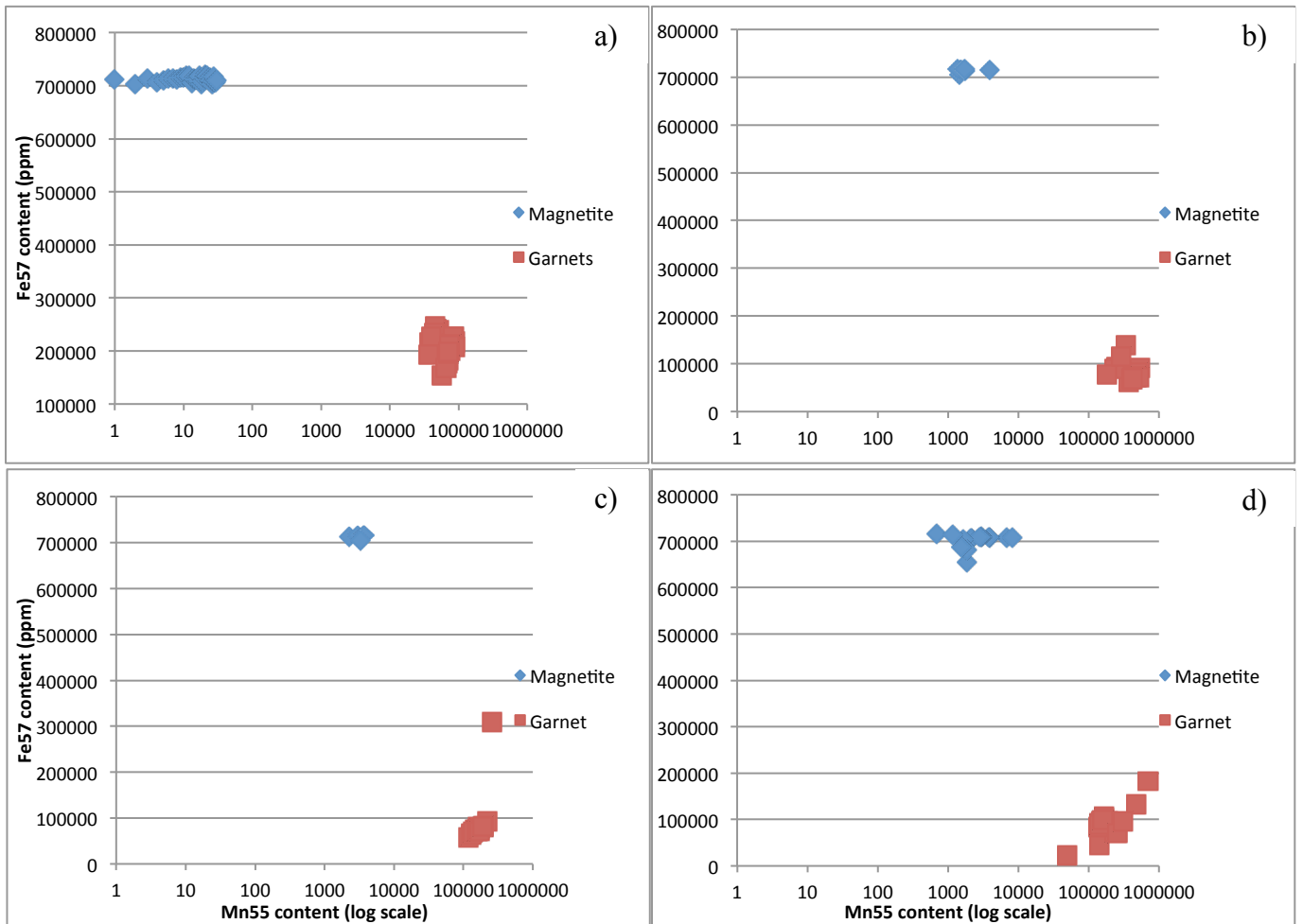
Figure 8. Binary diagrams of Fe55 against Mn57 content of both magnetite and garnet from each sample. (a) Sample 204-02B. (b) Sample 204-31A. (c) Sample 204-31B and (d) Sample 204-512.

Kelsy J Dyer

Gangue mineral influence on magnetite and the implications for Warramboo iron ore deposit.

RARE EARTH ELEMENTS (REE'S) NORMALISED TO CHONDRITE

The REE's for each texture is shown in Figure 9. The garnets all have a very similar trend, being less enriched in the Light Rare Earth Elements (LREE's) than Heavy Rare Earth Elements (HREE's).

The magnetite grain textures tend to have a similar trace element contents with slightly different chondrite-normalised REE patterns. The Magnetite grains are slightly less enriched in the LREE's than the HREE's.

The distance between the magnetite massive and the hematite massive from the LREE's to the HREE's is smaller for lighter REE's than for heavier REE's. The main anomaly comes with 153Eu where at both hematite and magnetite textures spike at a peak (excluding the massive textures).

Magnetite inclusion data is lower than the magnetite grains and indicates that they are depleted in HREE's, whereas the garnets that host the inclusions are not depleted and are highly enriched in these trace elements.

The Price Metasediments both plot at a higher range than the Warramboo magnetites and garnets with a similar patter. The Price Metasediment magnetite has an overall decreasing pattern that is less enriched in the HREE's and slightly more in the LREE's. This is different to the Warramboo that preserves the opposite pattern. Overall, the magnetite has quite a low values plotting under 1.0 for all trace elements, whereas the Price Magnetite plots above 1.0 for all of the REE's.

Gangue mineral influence on magnetite and the implications for Warramboo iron ore deposit.

Table 2. Data used to construct REE spider diagram (Figure 9) averages and then normalised to chondrite.

	Element	La139	Ce140	Pr141	Nd146	Sm147	Eu153	Tb159	Dy163	Ho165	Er166	Yb172	Lu175
Magnetite	Price Metasediment (n=41)	20.51	16.24	11.27	8.21	4.61	2.39	3.34	3.73	3.81	4.38	4.00	3.96
	Massive (n=30)	0.21	0.15	0.16	0.14	0.18	0.08	0.27	0.32	0.47	0.48	0.67	0.68
	Disseminated (n=25)	0.25	0.23	0.21	0.17	0.27	0.53	0.18	0.18	0.13	0.10	0.09	0.13
	Inclusions (n=10)	0.06	0.07	0.08	0.05	0.00	0.00	0.06	0.08	0.02	0.01	0.00	0.00
Hematite	Massive (n=19)	0.07	0.05	0.03	0.03	0.03	0.02	0.00	0.00	0.01	0.01	0.01	0.01
	Disseminated (n=25)	0.73	0.73	0.73	0.24	0.11	0.47	0.16	0.20	0.18	0.20	0.23	0.22
	Martite (n=10)	0.47	0.24	0.16	0.11	0.05	0.30	0.07	0.02	0.01	0.01	0.05	0.12
Garnet	Price Metasediment (n=16)	52.94	41.94	33.34	24.02	28.27	28.15	286.23	736.53	1373.74	2126.66	2731.46	2608.26
	Euhedral (n=73)	0.23	0.24	0.26	1.11	8.74	6.98	40.61	47.80	47.37	49.35	46.49	44.87
	Corona(n=13)	0.31	0.30	0.63	3.74	7.31	13.01	71.92	117.81	181.86	115.22	194.79	227.86
	Massive (n=12)	0.08	0.29	1.48	5.45	17.53	24.05	52.49	65.75	62.56	62.29	53.16	47.59
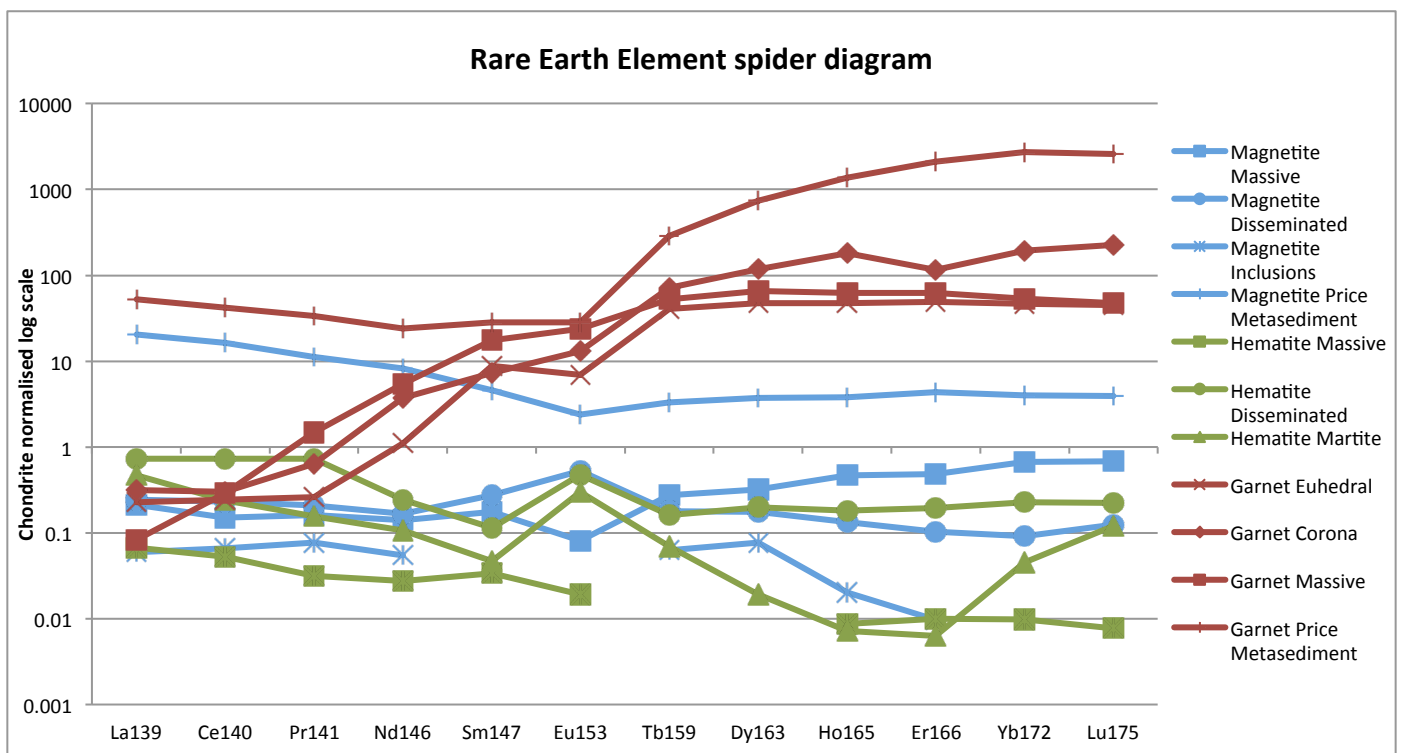
Figure 9. Spider diagram showing the Rare Earth Element patterns against the chondrite normalised values for each minerals and its respective textures. Blue shows the magnetite, green the hematite and red the garnet.

IMPURITIES

One of the main impurities in iron ore that can significantly affect iron ore quality is aluminium. The aluminium content of each texture was plotted against Fe for the Warramboo and the Price Metasediments (Figure 10). There is not a huge discrepancy between the metamorphic grades of the Warramboo Price Metasediments. A consistent trend is that the iron content of magnetite of all texture is similar regardless of the presence of garnets or not.
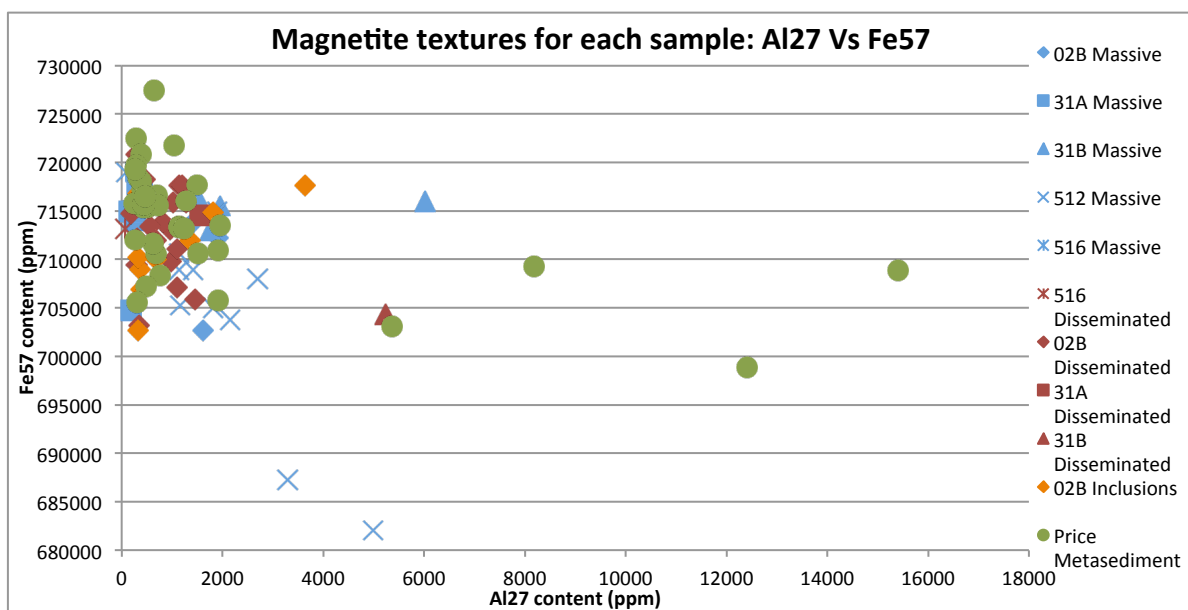
Figure 10 Graph showing the iron against aluminium content (ppm) for the magnetite of each sample and texture from Warramboo and the Price Metasediment.

Gangue mineral influence on magnetite and the implications for Warramboo iron ore deposit.

Table 3. Average data used in the formation of figures 6,7,8 and 10 with values in ppm. The blue highlighted areas are the data that is applicable to this study. For full values used to construct the figures refer to appendix C.

Magnetite

Element	Metasediment (n=39) Average	Max	Min	Massive (n=24) Average	Max	Min	Disseminated (n=21) Average	Max	Min	Inclusions (n=9) Average	Max	Min
Mg24	468.68	7846.71	9.74	409.49	1738.14	1.90	144.17	2028.00	0.59	238.72	1398.07	13.37
Al27	1808.57	15400.97	244.13	1643.87	6021.12	90.05	1002.46	5231.45	67.74	1026.06	3639.27	334.34
Si29	11610.64	18478.97	553.05	3427.89	23271.67	146.65	685.28	4064.38	164.37	1156.63	3749.32	369.95
P31	59.78	111.16	31.41	53.98	126.87	19.29	42.48	65.70	21.04	34.03	52.51	22.90
Ca43	1351.08	8191.99	138.92	837.20	4532.40	68.76	240.98	462.06	72.54	220.30	544.03	113.82
Sc45	2.32	16.62	0.58	1.19	10.19	0.20	0.72	2.02	0.23	0.56	1.28	0.22
Ti47	206.01	1361.51	48.65	175.83	527.40	5.53	599.04	6585.56	5.88	441.23	2066.36	148.89
Ti49	205.25	1392.57	50.11	172.43	524.93	3.91	604.57	6766.48	5.29	429.05	1942.72	147.22
V51	296.01	345.80	222.76	362.41	668.24	63.48	271.48	415.23	54.51	231.25	389.04	132.66
Cr53	236.16	564.24	36.82	234.17	677.00	29.08	205.20	363.88	7.46	157.19	290.49	67.97
Mn55	604.98	1477.99	200.84	1957.85	3885.87	104.48	501.87	3848.11	2.43	118.90	189.78	58.79
Fe57	703953.21	727452.75	543329.56	709414.00	718928.69	682016.00	712555.44	720850.19	703143.13	711103.65	717620.56	702654.94
Co59	61.95	78.60	41.87	106.68	186.25	27.24	35.12	150.84	10.36	14.33	24.74	7.78
Ni60	116.90	151.69	94.88	217.29	468.66	50.42	71.03	463.74	24.03	41.44	79.36	26.76
Cu65	1.47	5.84	0.35	6.91	38.40	0.27	0.51	0.84	0.30	0.70	0.70	0.70
Zn66	173.43	391.76	30.86	27.22	58.11	5.53	33.30	162.43	1.07	9.15	23.39	2.42
Ga69	10.38	19.49	4.24	71.52	143.40	23.57	49.13	82.19	21.70	35.52	58.46	24.00
Y89	16.43	152.15	0.30	1.07	11.85	0.02	0.13	0.52	0.04	0.17	0.41	0.04
Zr90	95.42	934.25	1.14	1168.58	10489.29	0.04	0.07	0.10	0.03	0.03	0.03	0.02
Sn118	22.62	158.91	0.64	30.44	442.07	0.27	38.07	410.71	0.62	21.68	61.61	1.39
La139	64.88	1571.55	0.04	0.09	0.29	0.02	0.09	0.14	0.03	0.19	0.19	0.03
Ce140	106.36	2807.85	0.03	0.17	0.58	0.03	0.16	0.30	0.02	0.56	0.56	0.03
Pr141	15.24	359.82	0.01	0.06	0.10	0.01	N/A	0.00	0.00	0.11	0.11	0.11
Nd146	66.00	1322.61	0.04	0.29	0.65	0.04	0.13	0.21	0.06	0.19	0.34	0.05
Sm147	10.17	192.76	0.06	0.46	0.85	0.08	0.07	0.08	0.07	N/A	0.00	0.05
Eu153	1.38	24.84	0.01	0.05	0.13	0.01	0.03	0.05	0.01	N/A	0.00	0.00
Ho165	0.68	5.53	0.03	0.14	0.30	0.03	0.01	0.02	0.01	0.01	0.01	0.01
Er166	2.08	13.48	0.11	0.30	1.39	0.04	0.04	0.05	0.03	0.02	0.02	0.02
Tm169	0.33	1.82	0.02	0.14	0.24	0.02	0.02	0.02	0.01	0.01	0.01	0.01
Yb172	1.68	10.97	0.09	0.47	2.66	0.07	0.04	0.05	0.03	N/A	0.00	0.00
Gd157	6.97	115.80	0.04	0.12	0.15	0.10	0.06	0.08	0.05	N/A	0.00	0.00
Tb159	0.86	11.11	0.01	0.07	0.17	0.02	0.01	0.01	0.01	0.04	0.04	0.04
Dy163	4.51	41.01	0.07	0.27	1.30	0.03	0.09	0.14	0.06	0.18	0.18	0.02
Lu175	0.26	1.44	0.02	0.10	0.44	0.00	0.01	0.01	0.01	N/A	0.00	0.00
Hf178	3.43	35.78	0.04	46.61	324.45	0.06	0.02	0.02	0.02	0.15	0.15	0.15
Pb208	6.56	122.43	0.06	2.38	22.55	0.44	0.44	4.47	0.02	0.06	0.06	0.02
Th232	16.90	397.82	0.18	0.19	0.79	0.02	0.03	0.04	0.03	0.01	0.01	0.01
U238	2.09	27.81	0.00	1.66	14.71	0.01	0.05	0.09	0.02	0.05	0.05	0.05

Gangue mineral influence on magnetite and the implications for Warramboo iron ore deposit.

Garnet

Element	Price Metasediment (n=15)			Euhedral (n=73)			Corona (n=13)			Massive (n=12)		
	Average	Max	Min	Average	Max	Min	Average	Max	Min	Average	Max	Min
Mg24	27780.37	237427.33	1664.03	40323.87	100867.71	0.23	26230.23	74591.34	48.73	49640.71	85375.29	19840.45
Al27	252252.13	1246433.38	37629.86	190639.18	1778753.00	7333.64	246057.32	431478.19	48973.03	272007.64	517746.00	166710.08
Si29	79339.77	6072468.50	51372.66	161782.91	286970.19	15.00	202031.61	556175.81	749.46	167047.82	289544.16	111951.52
P31	219.92	1044.41	22.62	185.17	390.28	2.02	149.35	269.55	18.91	195.63	297.51	97.95
Ca43	50061.41	369185.25	8434.97	8998.54	12756.41	19.53	6825.67	24589.64	149.54	24296.97	31222.21	19008.12
Sc45	118.71	363.35	16.50	76.97	216.52	0.01	85.53	255.33	0.04	68.26	125.62	28.06
Ti47	4852.22	29094.31	251.94	397.27	16769.54	0.24	223.27	536.84	11.64	256.24	342.85	53.01
Ti49	4947.81	29629.94	237.29	398.51	16579.60	0.21	208.25	489.06	12.08	260.70	348.67	48.96
V51	139.04	872.81	7.94	9.71	151.39	0.03	6.51	14.91	0.22	9.34	18.97	2.98
Cr53	111.53	622.16	7.59	35.44	327.23	3.43	8.29	22.33	2.23	7.39	21.55	2.50
Mn55	174491.81	447329.88	51174.73	139119.91	534009.75	0.04	353980.54	706637.50	39.77	457476.82	672025.56	382094.78
Fe57	106130.94	414827.50	27395.05	129813.37	309068.03	71.49	83589.61	182341.05	2338.71	55658.35	64069.17	46669.30
Co59	28.34	157.95	2.24	27.35	69.15	7.39	51.86	244.51	0.59	22.67	27.12	19.16
Ni60	40.76	242.68	0.22	3.89	39.49	0.44	16.76	64.49	1.07	N/A	0.00	0.00
Cu65	5.33	35.24	0.41	4.11	55.55	0.31	11.85	78.08	0.69	1.45	1.50	1.40
Zn66	126.72	928.91	3.42	162.21	3892.99	0.02	2172.61	10353.34	0.32	29.24	42.70	23.68
Ga69	61.13	437.78	2.09	11.41	167.26	0.80	24.70	121.54	4.31	9.89	18.91	5.64
Y89	1471.23	3716.05	245.22	114.91	266.53	0.07	280.88	2050.11	0.07	141.99	1494.00	0.45
Zr90	318.47	1912.23	7.34	12.66	215.64	0.53	9.48	22.44	0.36	19.25	27.43	8.43
Sn118	56.76	614.28	0.37	13.52	284.01	0.34	45.17	237.98	0.09	1.60	3.07	0.75
La139	23.85	120.83	0.03	0.36	2.96	0.02	0.31	1.54	0.03	0.09	0.15	0.06
Ce140	52.94	225.57	0.07	0.53	7.14	0.02	0.43	2.28	0.04	0.28	0.52	0.13
Pr141	5.98	28.32	0.02	0.08	0.93	0.02	0.13	0.29	0.01	0.20	0.34	0.13
Nd146	22.08	108.86	0.12	0.57	4.20	0.09	1.09	4.65	0.08	3.87	5.37	2.76
Sm147	4.84	20.96	0.20	2.05	5.08	0.23	1.49	2.54	0.04	4.05	13.61	0.45
Eu153	1.47	5.04	0.06	0.69	2.32	0.04	0.98	1.47	0.04	2.09	5.68	0.37
Gd157	11.86	44.21	1.33	9.71	15.77	0.58	6.07	16.26	0.53	11.69	82.75	0.41
Tb159	5.76	13.64	0.63	2.60	5.37	0.03	3.97	11.58	0.14	3.04	27.81	0.03
Dy163	114.31	261.76	14.35	19.97	44.49	0.10	44.51	178.87	0.04	25.05	251.16	0.17
Ho165	55.42	184.62	6.42	4.48	9.73	0.05	18.61	75.63	0.12	9.13	55.05	0.03
Er166	296.10	1192.39	20.48	13.48	30.11	0.09	84.08	388.56	0.23	26.59	161.63	0.10
Tm169	57.54	241.02	2.74	2.08	4.59	0.08	16.55	71.97	0.08	4.30	22.32	0.03
Yb172	453.44	1745.03	18.93	13.36	33.90	0.10	78.50	490.28	0.10	26.37	140.56	0.10
Lu175	68.13	239.26	2.38	1.98	5.69	0.01	18.81	93.46	0.05	3.63	20.05	0.02
Hf178	8.17	47.66	0.23	0.46	9.22	0.08	0.56	0.56	0.08	0.34	0.58	0.21
Pb208	18.40	123.56	0.08	3.08	41.08	0.04	2.04	12.95	0.03	0.11	0.14	0.09
Th232	32.76	316.23	0.04	0.06	0.23	0.02	0.04	0.06	0.02	N/A	0.00	0.00
U238	2.38	13.64	0.09	0.29	4.89	0.02	0.07	0.17	0.02	0.09	0.35	0.04

Kelsy J Dyer

Gangue mineral influence on magnetite and the implications for Warramboo iron ore deposit.

DISCUSSION

HyLogger as an effective tool

The HyLogger is a mineralogical tool developed by the CSIRO and is a reflectance

spectroscopy based analytical technique for measuring ore and rock samples (including

drill-core, rock chips, and pulps) and logging drill-holes (Yang et al., 2011). The current

HyLogging instruments are designed for sensing predominantly gangue minerals,

including sheet silicates, clays, carbonates and shales (Yang et al., 2011). The

automated drill core scanning spectrometer uses visible, near infrared (VNIR) and short

wave infrared (SWIR) spectral regions (400-2500 nm). It is considered a cheap

alternative to other methods of the same calibre and is a non-destructive process.

The HyLogger data collected from the drill hole IRD204 at Warramboo does not pick

up the key minerals and abundances of the major ore minerals, such as magnetite and

hematite. Automated scanners such as the HyLogger machine have been used to

identify zones of hydrothermal alteration, to log core and to grade ore (e.g Gallie et al.,

2002; Keeling et al., 2004; Huntington et al., 2006; Kupsch and Catuneanu, 2007;

Mauger et al., 2007; Tappert et al., 2011). It is primarily used in the context of alteration

minerals, for mineral exploration, or for gangue minerals that are to be separated from

the ore minerals in metallurgy and mineral processing (Yang et al., 2011). As HyLogger

data was collected for ore minerals such as magnetite and hematite, which are not

alteration minerals in this deposit, this could be a contributing reason for why the

proportion of oxides in the TSG graph (Figure 5) does not accurately represent the

abundance of oxides in the drill core itself according to petrography and QXRD data.

Categorisation of the minerals could also present a false mineral identification

depending on the spectral signature received by the instrument, meaning there are

minerals in higher proportions, or possibly not present in the sample at all, recorded in the results due to the spectral signature that the HyLogger is retrieving. Comparing the QXRD data to the HyLogger data for the samples 111512 and 111516 show that there are discrepancies in the minerals identified as well as their proportions. From Table 1 it is shown that 111512 have relatively the same minerals in Hylogger and QXRD and similar values for quartz and feldspar, with the other minerals values varying. However the fact that the correct mineral were categorised is notable. The small percentage of oxides (both magnetite and hematite) recorded in this sample could contribute to why the gangue minerals were categorised correctly from the spectral signatures. However, sample 111516 is dominated by oxides (contains up to 50%), had more issues with the correct identification of minerals. Feldspar and hornblende were the main contributors to the mineral proportions from HyLogger data; however neither are found in this sample. Garnet was not being detected at all, despite forming approximately 15% of the sample. This suggests that when there are a large amount of oxides present the validity of the HyLogger data becomes questionable.

Studies previously conducted on iron ore deposits using HyLogger also conclude that the detection of magnetite and other specular minerals in Banded Iron Formations (BIF's) and hydrothermal deposits are problematic, however the tool was useful for alteration patterns and zonation within the deposit (Tappert et al., 2011; Wells and Ramanaidou, 2015). HyLogger does have its economic benefits within the industry specifically for the identification of alteration minerals determining. However when it comes to determining oxides proportions it is clear from the evidence shown in the present study that it does not always produce correct values. Continued work and new

Kelsy J Dyer

Gangue mineral influence on magnetite and the implications for Warramboo iron ore deposit.

technology could benefit this method and when finally complete will be time effective and cost effective way to log core for companies and exploration projects.

Rare Earth Elements

Rare Earth Elements (REE's) have been widely used to study various geological processes, such as magmatism, metamorphism and hydrothermal activity (Liu and Tang, 1999). This study focuses on the rare earth elements and their distribution in magnetite, hematite and garnet minerals in the Warramboo and Price Metasediment areas. Many studies have shown that factors which control partitioning of

REE's among different minerals include the chemical composition, temperature and pressure of the system as well as the ionic charge and radii of the elements themselves (Liu and Tang, 1999).

REE mineral/melt partition coefficients for magnetite range from 0.003 for La and 0.02 for Lu (Nielsen et al., 1992) with the general trend being that magnetite is more likely to be enriched in HREEs and less in LREEs, (Figure 9). Garnet is generally rich in HREE and depleted in LREE, which is also confirmed by the data (Figure 9).The REE's are much higher in Garnet than magnetite and hematite suggesting that overall garnet is more likely to be heavily enriched in HREE's. The garnets are unlikely to be detrital garnets as they have been affected by metamorphism and the majority of garnet growth occurred during the metamorphism.

The Price Metasediments for both the magnetite and garnet has a higher trend line. This decrease of REE's in the minerals suggests that the REEs were redistributed during metamorphism and that the REE values from the Warramboo samples do not correctly

show the original composition of the protolith rock. However, some of the original elements would have survived the metamorphism due to their high valencies, electronegativities, small radii and strong chemical bonds that get trapped in secondary minerals when primary hosts are destroyed by alteration processes (Singh et al., 2015). The magnetite in these samples are most likely to be recrystallised during metamorphism as they are similar, but not identical to the composition of the Price Metasediments which have been identified to be their lower grade equivalent (Lane et al., 2015). The REE's have been redistributed and diffused into magnetite and garnets in particular. Although there is martitisation (alteration of magnetite to hematite (martite) that occurs in a few samples, it is unlikely that the geochemical changes at an inter-mineral scale will have a significant effect on the element distribution patterns in the system (Nadoll and Koenig, 2011).

In regards to the negative Eu anomaly in the massive textures of both magnetite and hematite, this is most likely caused by discrimination of Eu2+ from the magnetite lattice as also evident in previous studies (Schock, 1979). The positive Eu anomaly for the other textures of magnetite and hematite is unusual in the fact that other literature does not find this trend to be the same and are likely to be unique to this study. Previous studies that involved REE trace elements of magnetite and hematite show similar trends to the data, with hematite being more enriched in LREE and depleted in HREE, and also recording a slight Eu anomaly.

Kelsy J Dyer

Gangue mineral influence on magnetite and the implications for Warramboo iron ore deposit.

Mn correlation and the elemental partitioning during ore genesis

Manganese is the most significant of the analysed trace elements in magnetite from

Warramboo as it can substitute easily for Iron (Frietsch 1970; Loberg & Horndahl 1983;

Kessler &Muller 1988; Nystrom & Heriquez 1994; Muller et al., 2003).

To establish whether there is a correlation between Mn content of the rock and the

proportion of garnet it was approached in two different steps. The first compares two

samples that have the same garnet proportion from petrography analysis to the Mn

content in Figure 7. The two samples selected for this comparison are 111512 and 204-

31A, which do not have identical garnet proportions but are the two samples which have

the most comparable proportions. These samples plot similarly but not identically on the

garnet Mn vs Fe graph and do not conclusively prove a correlation. The second

approach was the inverse of this and investigating two samples that plot with similar

values on the Mn Vs Fe graph and compare these to the petrography analysis

proportions. The samples chosen were 111512 and 204-31B that plot very similar,

however when analysed in petrography 31B has a significantly higher proportion of

garnets, almost entirely covering it in sections. Sample 111512 has a much lower

proportion of garnet with only 7-10%. From this study it shows that the proportion of

garnet in a sample does not correlate with the Manganese content of the rock, when

plotted against iron, for that specific sample.

It is well known that manganese partitions favourably into garnet over magnetite and so

it is essential to establish which mineral grew first and in turn sequested the Mn content.

To determine the elemental partitioning during ore genesis and the relationship between

magnetite and garnet in the deposit the formation of these two minerals needs to be

Kelsy J Dyer

Gangue mineral influence on magnetite and the implications for Warramboo iron ore deposit.

constraint against each other to establish relative timing of growth. From the methods used and the results obtained from trace element data and petrography there is reason to believe that the magnetite formed prior to the garnet, due to garnet coronas on the magnetite grains, distribution of Mn in both minerals as well as inclusions of magnetite in garnet grains throughout the samples.

Comparing Figures 6 and 7 shows that sample 204-02B has to have an overall lower Mn bulk rock value as both the magnetite and the garnets have relatively lower values than the other samples. Suggested reasoning for this could be that as this sample is the shallowest in the drill core, and as the sample is more felsic, contains no sillimanite or cordierite, and is very abundant in biotite it is most likely to be a different lithology to deeper samples and therefore the different bulk Mn content is a plausible idea. Samples 111512, 204-31B have a relatively lower Mn content for the garnet mineral, whereas the Mn content in magnetite is on the higher end of the scale in regards to the other samples. This suggests that the magnetite did grow first and in turn the manganese was partitioned into the magnetite, however not affecting the iron content. As for sample 204-31A, it has a mid-range Mn content in the magnetite textures and relatively high Mn values in the garnets, first suggesting that garnet formed before the magnetite. This was established to not be the case as the garnets analysed in this sample are majority of corona in texture suggesting that as this reaction occurred it depleted the magnetite of the original Mn through elemental exchange and redistribution of elements from this process, which is why we observe a decrease in the magnetite Mn content for this particular sample. Sample 111516 has high Mn values in the garnet also, however as this sample is dominated heavily by hematite the magnetite and garnet relationship cannot be observed effectively with this sample and so it does contribute to the

Kelsy J Dyer

Gangue mineral influence on magnetite and the implications for Warramboo iron ore deposit.

classification of the timing of mineral formation. The Price Metasediments have relatively low Mn in both minerals, again suggesting that these had an original Mn bulk value lower than the Warramboo samples, similarly to 204-02B, and again confirming the idea that it is a different rock lithology, as well as being of lower metamorphic grade.

Therefore, from the data collected in this it can be stated that magnetite formed early and predates the garnet. The original euhedral garnets do not have an effect on the manganese content of the magnetite in these samples, however when coronas are formed surrounding these magnetite grains the redistribution of the manganese into the garnet depletes the magnetite of this element and lower Mn values in the magnetite are observed. The effects of the manganese content on the magnetite does not effect the iron content in the deposit which is a great outcome suggesting the purity of the iron will not be compromised.

Impurities in Magnetite and Future Implications

While it cannot be conclusively proven that the Price Metasediments on southern Eyre Peninsula and the Warramboo magnetite gneiss are the same iron-rich sequence, there have been studies that argue they are, based on the similarity in depositional age, detrital zircon populations and Nd isotopic composition between the two locations (Lane et al., 2015; Morrissey et al., 2015). Mineral equilibria modelling suggests that the granulite-facies metamorphism of the two correlatives (Price Metasediment to the Warramboo magnetite gneiss) is a plausible mechanism to upgrade the sub-economic iron occurrences significantly and possibly to an economic grade (Morrissey et al., 2015). As this mechanism has been shown to enrich the magnetite content of

metasedimentary rocks through melt loss during metamorphism there has not been any study on the implication of the surrounding minerals as well as the trace element distribution and purity of the magnetite produced by this process.

A main impurity in steel and iron is aluminium, which has been plotted show against iron content in Figure 10. There has been no distinctive change between the Price Metasediments of greenschist facies to the Warramboo gneisses of granulite facies. This suggests that during metamorphism and the subsequent melt, it does not take away impurities however they are simply redistributed during recrystallization. There have not been any studies thus far which discuss impurities in magnetite and their subsequent effect on the quality of steel produced. The manganese content of the minerals also does not affect the iron content of the samples, which is a great outcome for the company and the industry as it means that the magnetite is not becoming less pure or less economical with increased manganese content. The full impact of the trace elements on the quality of steel is still a debated concept, and whether ore deposits with large amounts of trace elements jeopardise steel quality is still to be determined. Future work could include continued investigation using this data to determine whether having trace elements in ore minerals is actually a bad thing or whether their presence does not have an effect on the quality of the steel produced.

CONCLUSIONS

- The HyLogger is not an effective technique to determine the proportion of minerals and is limited by the amount of spectral detail and data it can correctly identify when the drill core is highly abundant in specular minerals (specifically magnetite) in the Warramboo deposit.

- There is no correlation between the Mn content of the rock and the proportion of garnet.

- Magnetite growth predates garnet and in turn is manganese rich, however when corona reactions take place on the magnetite grain the manganese value is decreased as the element is partitioned into the garnet. The change in the manganese content of the magnetite does not have an effect on the iron content.

- The enrichment of magnetite content through melt loss and metamorphism from greenschist to granulite facies does not clean up or remove impurities from the resulting minerals, specifically magnetite.

ACKNOWLEDGMENTS

REFERENCES

BEAUDOIN G., DUPUIS C., GOSSELIN P. & JÉBRAK M. 2007. Mineral chemistry of iron oxides: application to mineral exploration. Ninth Biennial SGA meeting. *SGA, Dublin,* p.497-500.

CAREW M. J. 2004 Controls on Cu-Au mineralisation and Fe oxide metasomatism in the Eastern Fold Belt, NW Queensland, Australia. James Cook University.

CARPENTARIA EXPLORATION LTD. 2011. *Magnetite-What you may not know.* http://www.carpentariaex.com.au/uploads/files/Magnetite-Information-Sheet.pdf.

CHUNG D., ZHOU M.-F., GAO J.-F. & CHEN W. T. 2015. In-situ LA–ICP-MS trace elemental analyses of magnetite: The late Palaeoproterozoic Sokoman Iron Formation in the Labrador Trough, Canada. *Ore Geology Reviews,* **65**, 917-928.

CUTTS K., HAND M. & KELSEY D. 2011. Evidence for early Mesoproterozoic (ca. 1590Ma) ultrahigh-temperature metamorphism in southern Australia. *Lithos,* **124**, 1-16.

DALY S., FANNING G. & FAIRCLOUGH M. 1998. Tectonic evolution and exploration potential of the Gawler Craton, South Australia. *AGSO Journal of Australian Geology and Geophysics,* **17**, 145-168.

DARE S. A. S., BARNES S. J., BEAUDOIN G., MERIC J., BOUTROY E. & POTVIN-DOUCET C. 2014. Trace elements in magnetite as petrogenetic indicators. *Mineralium Deposita,* **49**, 785-796.

DUPUIS C. & BEAUDOIN G. 2011. Discriminant diagrams for iron oxide trace element fingerprinting of mineral deposit types. *Mineralium Deposita,* **46**, 319-335.

DUTCH R., HAND M. & KELSEY D. 2010. Unravelling the tectonothermal evolution of reworked Archean granulite facies metapelites using in situ geochronology: an example from the Gawler Craton, Australia. *Journal of Metamorphic Geology,* **28**, 293-316.

EVANS B. W. & FROST B. R. 1975. Chrome-spinel in progressive metamorphism—a preliminary analysis. *Geochimica et Cosmochimica Acta,* **39**, 959-972.

FANNING C., REID A. & TEALE G. 2007. A geochronological framework for the Gawler Craton, South Australia. *South Australia Geological Survey Bulletin,* **55**, p.80.

FORBES C., GILES D., JOURDAN F., SATO K., OMORI S. & BUNCH M. 2012. Cooling and exhumation history of the northeastern Gawler Craton, South Australia. *Precambrian Research,* **200**, 209-238.

FRASER G., MCAVANEY S., NEUMANN N., SZPUNAR M. & REID A. 2010. Discovery of early Mesoarchean crust in the eastern Gawler Craton, South Australia. *Precambrian Research,* **179**, 1-21.

FRIETSCH R. & LUNDEGÅRDH P. H. 1970 Trace elements in magnetite & hematite mainly from northern Sweden.

GALLIE E., MCARDLE S., RIVARD B. & FRANCIS H. 2002. Estimating sulphide ore grade in broken rock using visible/infrared hyperspectral reflectance spectra. *International Journal of Remote Sensing,* **23**, 2229-2246.

HAND M., REID A. & JAGODZINSKI L. 2007. Tectonic framework and evolution of the Gawler Craton, southern Australia. *Economic Geology,* **102**, 1377-1395.

HUANG X.-W., ZHOU M.-F., QIU Y.-Z. & QI L. 2015. In-situ LA-ICP-MS trace elemental analyses of magnetite: The Bayan Obo Fe-REE-Nb deposit, North China. *Ore Geology Reviews,* **65**, 884-899.

HUNTINGTON J. F., MAUGER A. J., SKIRROW R. G., BASTRAKOV E. N., CONNOR P., MASON P., KEELING J. L., COWARD D. A., BERMAN M. & PHILLIPS R. 2006. Automated mineralogical core logging at the Emmie Bluff iron oxide–copper–gold prospect. *MESA Journal,* **41**, 38-44.

IRON ROAD. 2013. *Annual Report.* Iron Road Ltd. http://www.ironroadlimited.com.au/investor-centre/reports/annual-reports.

IRON ROAD. 2014. *Presentation; Central Eyre Iron Project- Our Technical Journey.* Iron Road Ltd. http://www.ironroadlimited.com.au/images/files/preserntations/20141029%20IRD%20CEIP%20Our%20Journey%20.pdf.

KEELING J., MAUGER A. & HUNTINGTON J. 2004. Spectral core logger update—preliminary results from the Barns gold prospect. *MESA Journal,* **33**, 32-36.

KESSLER W. & MÜLLER G. 1988. Minor and trace-element data of iron oxides from iron-formations of the Iron Quadrangle, Minas Gerais, Brazil. *Mineralogy and Petrology,* **39**, 245-250.

KUPSCH B. & CATUNEANU O. 2007. Alteration features and geochemical signatures of the Maybelle River uranium zone, Athabasca Basin, Alberta. *BULLETIN-GEOLOGICAL SURVEY OF CANADA,* **588**, p.347.

LANE K., JAGODZINSKI E. A., DUTCH R., REID A. J. & HAND M. 2015. Age constraints on the timing of iron ore mineralisation in the southeastern Gawler Craton. *Australian Journal of Earth Sciences,* **62**, 55-75.

LIU C. & TANG H. 1999. Redistribution of REEs during metamorphism and its indicative significance for fluid processes. *Science in China Series D: Earth Sciences,* **42**, 646-654.

LOBERG B. E. & HORNDAHL A.-K. 1983. Ferride geochemistry of Swedish Precambrian iron ores. *Mineralium Deposita,* **18**, 487-504.

MAGNET. 2011. *Magnetite Facts and Figures.* http://www.magnetitenetwork.com.au/who-we-are/magnetite/.

MAUGER A., KEELING J. & HUNTINGTON J. 2007. Alteration mapping of the Tarcoola Goldfield (South Australia) using a suite of hyperspectral methods. *Applied Earth Science: Transactions of the Institutions of Mining and Metallurgy: Section B,* **116**, 2-12.

MCNAB B., JANKOVIC A., DAVID D. & PAYNE P. 2009 Processing of Magnetite Iron Ores–Comparing Grinding Options. Proceedings of Iron Ore 2009 Conference, Perth, Australia*.* pp. 27-29.

MORRISSEY L., HAND M., WADE B. & SZPUNAR M. 2013. Early Mesoproterozoic metamorphism in the Barossa Complex, South Australia: links with the eastern margin of Proterozoic Australia. *Australian Journal of Earth Sciences,* **60**, 769-795.

MORRISSEY L., HAND M., LANE K., KELSEY D. & DUTCH R. 2015. Upgrading iron-rich sequences to economic grade iron-ore deposits by melt loss during granulite-facies metamorphism. *Under Review*.

MÜLLER B., AXELSSON M. D. & ÖHLANDER B. 2003. Trace elements in magnetite from Kiruna, northern Sweden, as determined by LA-ICP-MS. *Gff,* **125**, 1-5.

NADOLL P., MAUK J., HAYES T., KOENIG A., HOFSTRA A. & BOX S. 2009 Geochemistry of magnetite from hydrothermal ore deposits and their host rocks in the Proterozoic Belt Supergroup, USA. Smart science for exploration and mining, Proc 10th Biennial Meeting, Townsville*.* pp. 129-131.

NADOLL P. & KOENIG A. E. 2011. LA-ICP-MS of magnetite: methods and reference materials. *Journal of Analytical Atomic Spectrometry,* **26**, 1872-1877.

NADOLL P., ANGERER T., MAUK J. L., FRENCH D. & WALSHE J. 2014. The chemistry of hydrothermal magnetite: A review. *Ore Geology Reviews,* **61**, 1-32.

NIELSEN R. L., GALLAHAN W. E. & NEWBERGER F. 1992. Experimentally determined mineral-melt partition coefficients for Sc, Y and REE for olivine, orthopyroxene, pigeonite, magnetite and ilmenite. *Contributions to Mineralogy and Petrology,* **110**, 488-499.

NYSTROEM J. O. & HENRIQUEZ F. 1994. Magmatic features of iron ores of the Kiruna type in Chile and Sweden; ore textures and magnetite geochemistry. *Economic Geology,* **89**, 820-839.

OLIVER R. & FANNING C. 1997. Australia and Antarctica: precise correlation of Palaeoproterozoic terrains. *The Antarctic Region: geological evolution and processes. Sienna, Terra Antartica Publication*, 163-172.

PAYNE J., HAND M., BAROVICH K. & WADE B. 2008. Temporal constraints on the timing of high-grade metamorphism in the northern Gawler Craton: implications for assembly of the Australian Proterozoic. *Australian Journal of Earth Sciences,* **55**, 623-640.

REID A. J. & HAND M. 2012. Mesoarchean to Mesoproterozoic evolution of the southern Gawler Craton, South Australia. *Episodes,* **35**, 216-225.

REID A. J., JAGODZINSKI E. A., FRASER G. L. & PAWLEY M. J. 2014. SHRIMP U–Pb zircon age constraints on the tectonics of the Neoarchean to early Paleoproterozoic transition within the Mulgathing Complex, Gawler Craton, South Australia. *Precambrian Research,* **250**, 27-49.

SCHOCK H. H. 1979. Distribution of rare-earth and other trace elements in magnetites. *Chemical Geology,* **26**, 119-133.

SINGH M. R., MANIKYAMBA C., RAY J., GANGULY S., SANTOSH M., SAHA A., RAMBABU S. & SAWANT S. 2015. Major, trace and platinum group element (PGE) geochemistry of Archean Iron Ore Group and Proterozoic Malangtoli metavolcanic rocks of Singhbhum Craton, Eastern India: Inferences on mantle melting and sulphur saturation history. *Ore Geology Reviews*.

SKUBLOV S. & DRUGOVA G. 2003. Patterns of trace-element distribution in calcic amphiboles as a function of metamorphic grade. *The Canadian Mineralogist,* **41**, 383-392.

STATISTA. 2015. *Major countries in ore mine production worldwide from 2010 to 2014(million metric tons).* http://www.statista.com/statistics/267380/iron-ore-mine-production-by-country/

TAPPERT M., RIVARD B., GILES D., TAPPERT R. & MAUGER A. 2011. Automated drill core logging using visible and near-infrared reflectance spectroscopy: a case study from the Olympic Dam IOCG deposit, South Australia. *Economic Geology,* **106**, 289-296.

TAPPERT M. C., RIVARD B., GILES D., TAPPERT R. & MAUGER A. 2013. The mineral chemistry, near-infrared, and mid-infrared reflectance spectroscopy of phengite from the Olympic Dam IOCG deposit, South Australia. *Ore Geology Reviews,* **53**, 26-38.

VAN BAALEN M. 1993. Titanium mobility in metamorphic systems: a review. *Chemical Geology,* **110**, 233-249.

WELLS M. & RAMANAIDOU E. 2015 Raman Spectroscopic Core Scanning for Iron Ore and BIF Characterization. Proceedings of the 11th International Congress for Applied Mineralogy (ICAM). pp. 387-396. Springer.

YANG K., HUNTINGTON J., EHRIG K., WHITBOURN L., MASON P. & MUNDAY T. 2011. HyLogging for quantifying gangue minerals for geometallurgy.

ZHAO W. W. & ZHOU M.-F. 2015. In-situ LA–ICP-MS trace elemental analyses of magnetite: The Mesozoic Tengtie skarn Fe deposit in the Nanling Range, South China. *Ore Geology Reviews,* **65**, 872-883.

APPENDIX A: SAMPLES-THIN SECTION SLIDES
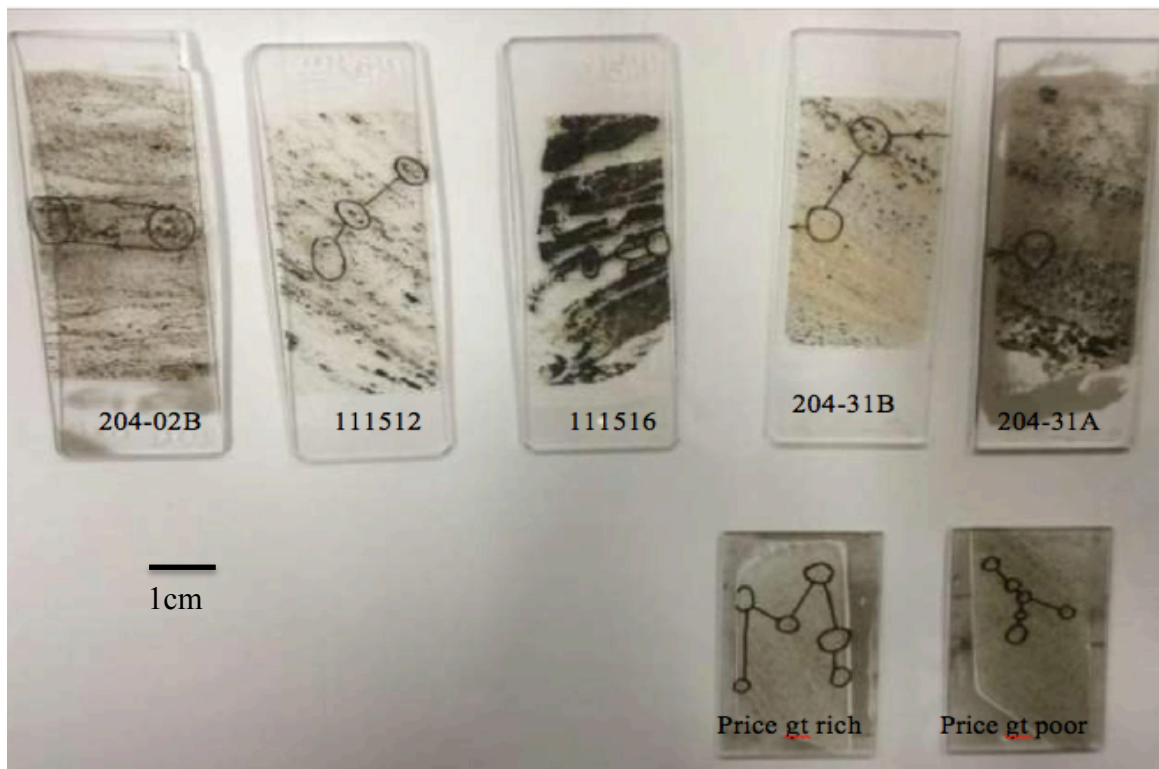
APPENDIX B: IMAGES SHOWING LASER ANALYSIS SITES ON ALL SAMPLES
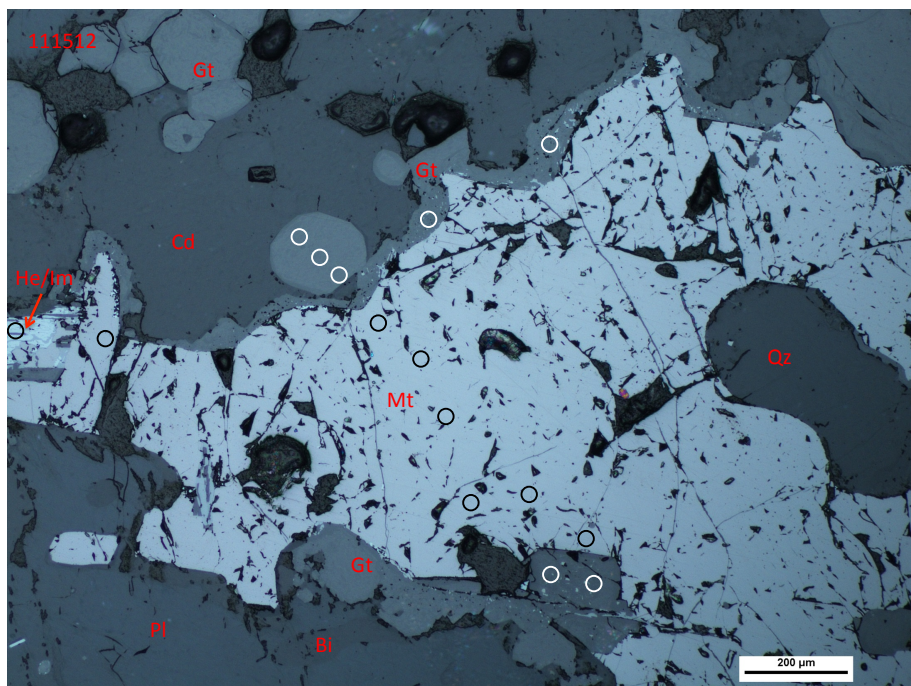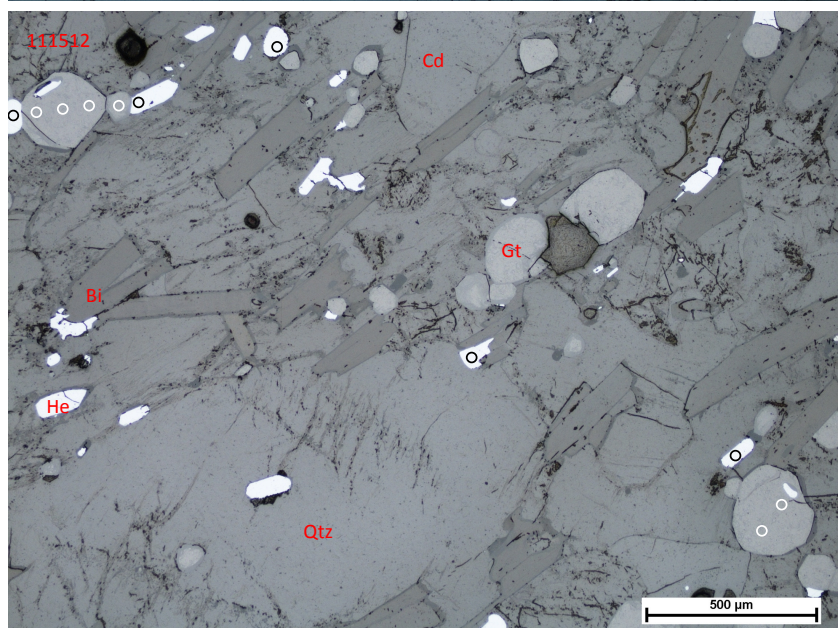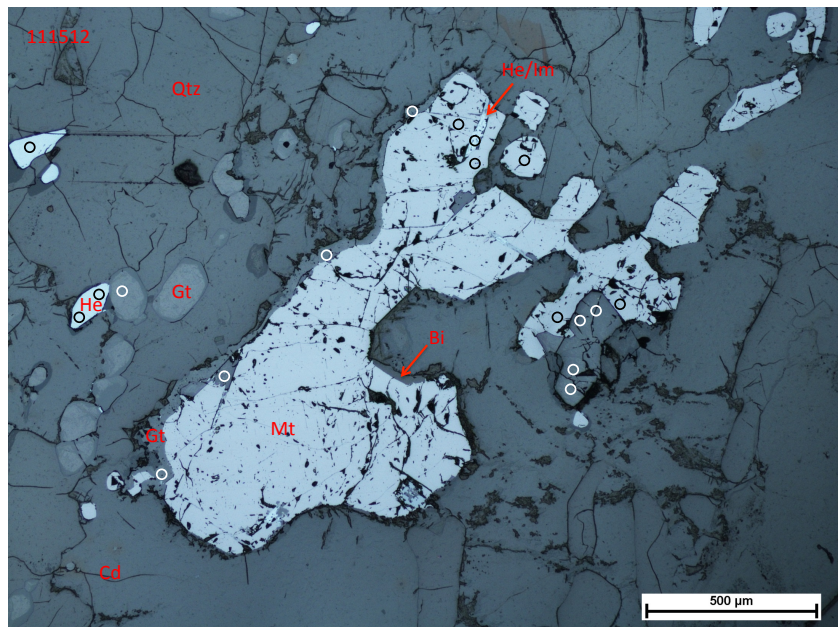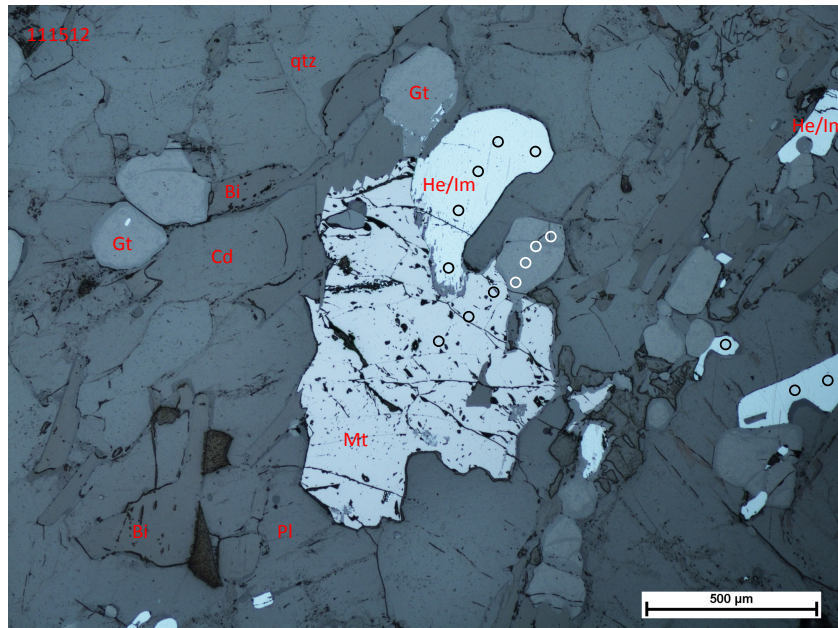
Gangue mineral influence on magnetite and the implications for Warramboo iron ore deposit.

Gangue mineral influence on magnetite and the implications for Warramboo iron ore deposit.

Gangue mineral influence on magnetite and the implications for Warramboo iron ore deposit.

Gangue mineral influence on magnetite and the implications for Warramboo iron ore deposit.

Kelsy J Dyer
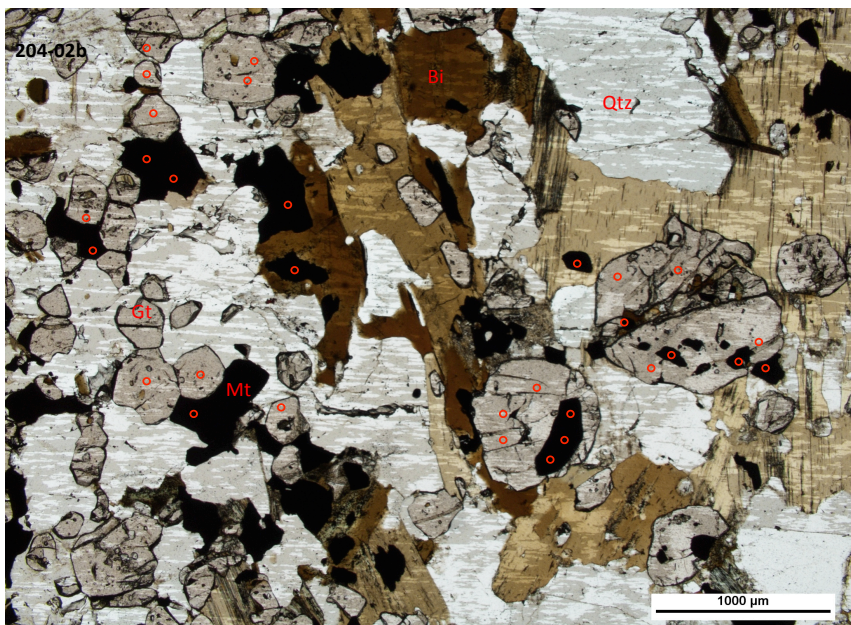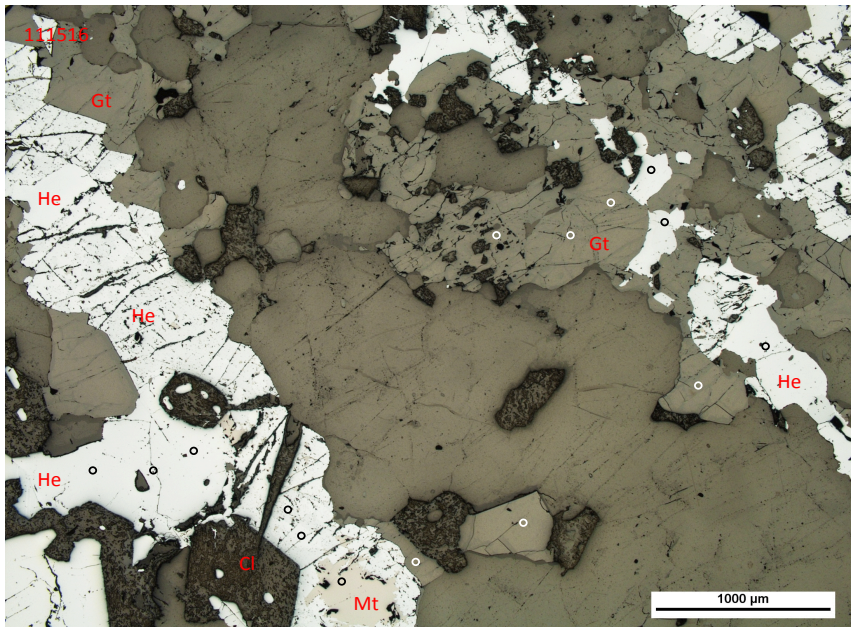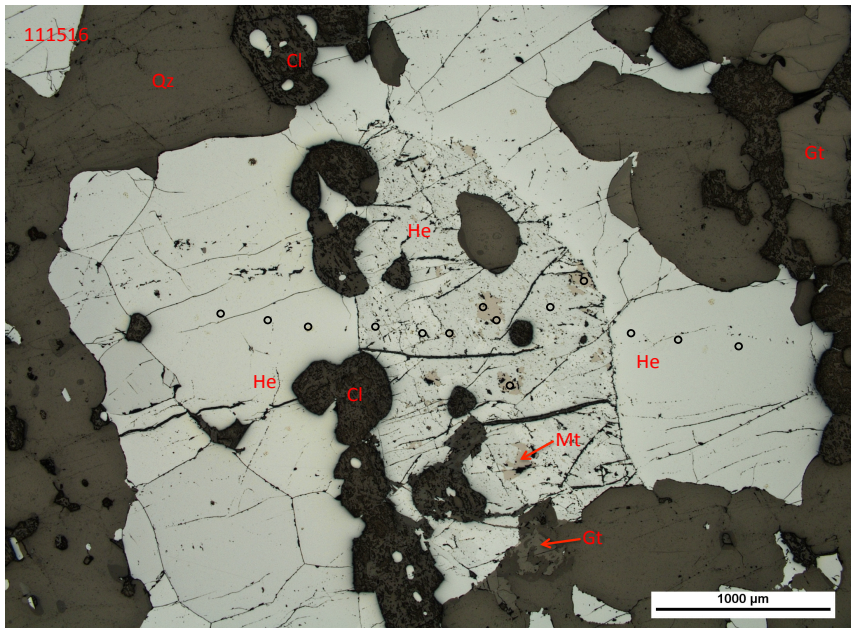
Gangue mineral influence on magnetite and the implications for Warramboo iron ore deposit.
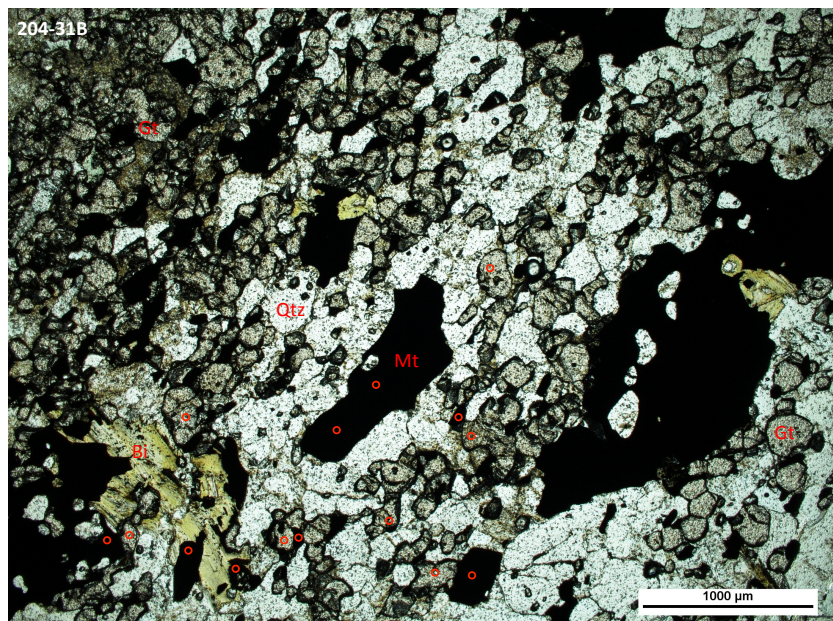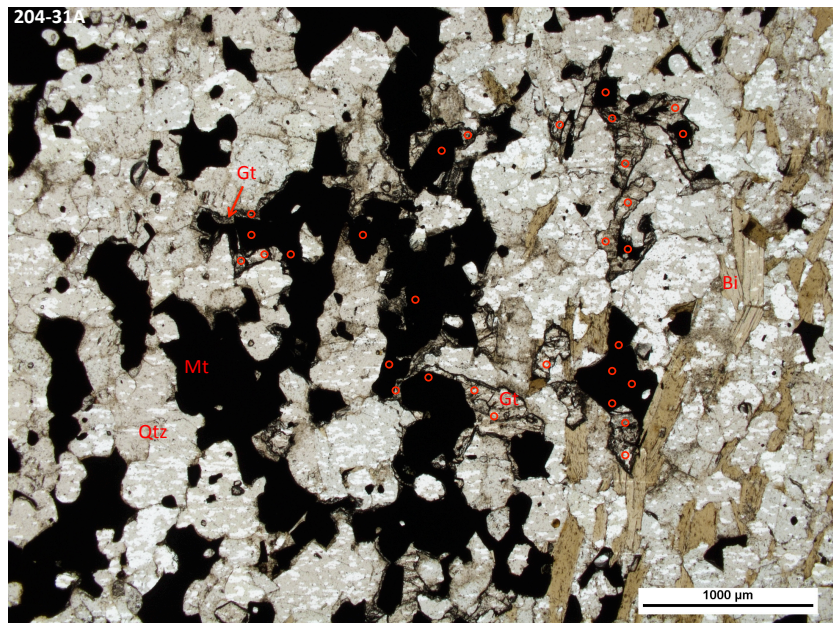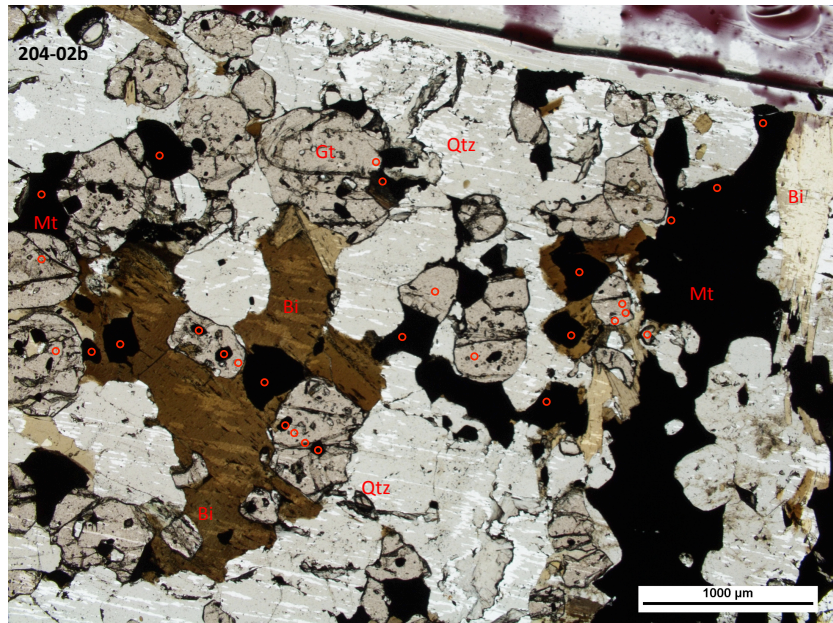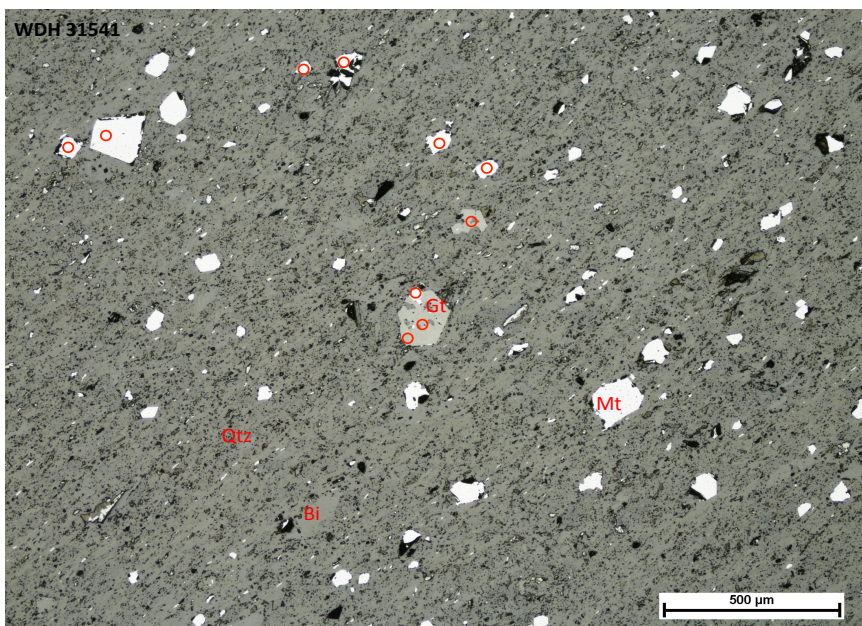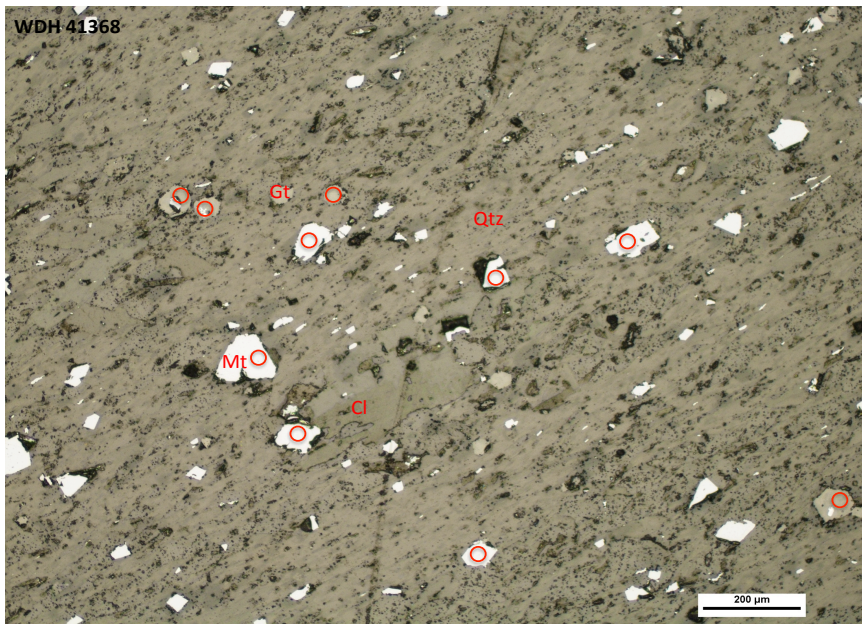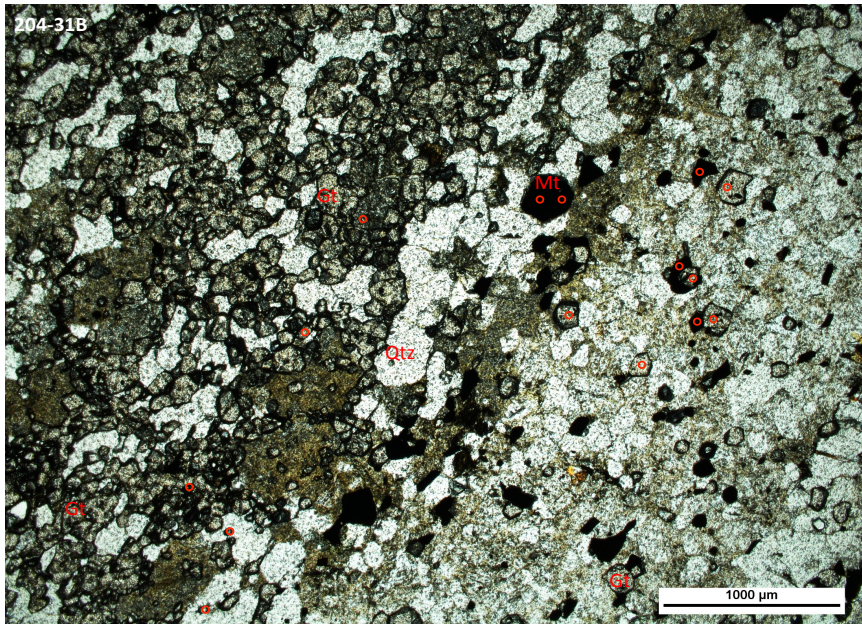
APPENDIX C: RAW LA-ICP-MS DATA PROCESSED THROUGH GLITTER (PPM)

Garnet

Euhedral

Element	Mg24	Al27	Si29	P31	Ca43	Sc45	Ti47	Ti49	V51	Cr53	Mn55	Fe57	Co59	Ni60	Cu65	Zn66	Ga69	Y89
02B-06	41649.58	127171.48	143149.72	195.93	9321.06	72.92	40.18	43.80	5.35	31.38	51860.54	239648.86	20.65	<0.81	<0.70	27.75	3.84	141.58
02B-07	48710.00	130224.06	143199.86	145.34	9846.79	72.53	44.82	47.68	6.61	32.36	46684.90	240522.67	21.53	<0.72	<0.66	35.85	4.54	133.69
02B-08	49279.27	137354.33	157345.84	143.81	9846.79	76.01	79.58	73.20	9.37	35.61	47401.51	240609.11	22.79	<0.73	<0.71	31.63	6.08	131.66
02B-09	40731.78	115316.52	124749.03	144.94	9105.72	57.86	49.75	52.73	7.17	75.68	40155.55	202067.39	17.05	<0.67	<0.62	24.71	5.03	131.85
02B-10	47232.49	120607.99	172294.44	172.94	9606.94	65.83	50.05	50.49	5.41	23.31	43949.57	202092.95	20.21	<0.72	<0.63	35.68	3.09	79.04
02B-11	53081.52	136860.83	151607.97	151.19	9877.95	78.79	76.92	76.92	8.38	23.16	45608.92	246719.78	23.16	<0.75	<0.69	35.51	5.51	119.55
02B-13	54384.86	139833.50	151642.75	150.74	9820.92	72.80	47.35	45.75	6.34	5.76	43957.68	233103.69	21.62	1.11	<0.68	34.22	4.21	108.15
02B-14	46655.28	125925.14	151119.44	137.01	8956.99	67.70	44.64	44.03	6.01	5.12	39665.45	207007.36	18.42	<0.60	<0.57	30.51	3.70	99.93
02B-17	44934.46	135019.28	147736.06	140.46	8993.80	76.68	45.81	37.67	4.53	7.15	42310.36	212350.59	17.12	<0.69	<0.61	30.18	3.18	82.53
02B-22	58610.59	137500.20	157857.48	123.14	10120.95	59.27	55.67	43.52	4.71	15.26	37799.63	216232.53	18.26	<0.77	<0.73	22.02	3.32	70.83
02B-23	60350.63	156592.05	171940.02	175.82	9918.41	62.10	68.67	55.70	4.04	33.26	40130.38	227748.77	20.65	<0.80	0.88	29.37	3.38	62.03
02B-30	44569.07	139926.56	144535.28	168.38	8318.48	61.30	34.42	29.94	3.72	4.62	36243.80	193094.42	15.24	<0.66	<0.56	23.16	2.50	73.37
02B-31	79656.70	199670.17	149670.17	164.72	8674.25	55.30	53.35	51.69	8.19	10.49	56888.48	153023.83	16.95	0.88	<0.68	27.65	5.41	117.99
02B-32	84862.12	225354.02	142356.95	170.04	8816.19	44.34	44.71	53.35	6.42	50.42	68892.13	177560.77	20.34	0.85	<0.82	38.35	4.74	138.17
02B-33	88061.70	246367.19	152399.36	169.47	8808.03	74.74	53.76	63.34	9.53	25.49	94930.93	199732.25	21.89	<0.82	<0.82	36.10	6.55	163.08
02B-34	100867.71	274320.34	174371.06	214.84	9538.47	82.86	53.96	52.37	9.61	73.56	85554.50	227900.55	24.56	<1.13	<1.12	43.55	6.71	179.22
02B-35	78158.60	174371.06	172213.95	157.97	8722.35	72.82	47.15	45.95	6.31	25.71	70160.16	182592.88	19.16	<0.82	<1.12	33.30	5.44	106.67
02B-38	72095.91	227821.41	157656.95	218.84	8643.66	91.94	44.81	55.40	7.56	20.84	88467.33	216724.22	21.19	<1.08	<1.02	35.73	5.70	146.19
02B-40	82646.63	264774.75	157656.95	211.55	9599.08	56.65	34.21	43.76	6.40	18.44	65757.14	167580.22	18.26	<1.23	<0.97	30.37	6.65	128.57
02B-41	86824.70	269972.53	176276.14	197.71	9779.83	80.65	63.64	65.84	8.58	42.05	79151.46	214169.09	22.16	<1.14	<0.88	39.10	4.30	98.89
02B-45	78991.49	271378.13	169530.75	200.26	8764.02	84.95	30.96	23.23	5.74	38.23	82063.91	225847.52	21.95	<1.20	<1.40	38.53	5.37	154.38
02B-48	86897.07	269906.88	180646.17	175.29	10034.76	70.70	41.56	48.99	4.54	30.61	89642.46	208295.38	21.87	1.34	<0.96	27.86	3.93	154.84
02B-50	25833.99	135512.23	130309.19	141.79	9943.49	72.65	72.65	53.80	8.23	7.58	68892.13	192395.38	16.91	<1.37	<0.96	24.64	4.46	220.34
02B-54	64504.34	268233.56	163981.94	175.74	9104.50	63.42	62.28	62.28	3.35	23.94	57434.93	194210.94	22.81	<1.01	<1.07	34.55	4.46	158.49
02B-55	88973.66	302084.97	190066.05	221.73	8662.75	59.88	59.88	60.24	3.50	3.95	63703.00	197967.38	25.09	0.62	0.41	36.27	4.16	149.25
02B-56	92735.63	303805.69	197384.81	305.57	8818.34	46.35	47.03	79.59	5.03	8.36	75447.62	211095.47	21.37	0.67	0.49	44.02	6.00	98.52
02B-57	90941.65	314408.16	196741.91	350.42	9961.43	63.86	46.84	51.40	4.51	10.07	73090.95	211095.47	21.98	<1.16	<1.16	34.73	3.25	94.04
31B-03	77996.93	290940.50	182423.58	300.02	9321.34	59.25	47.32	41.91	4.57	5.88	71857.77	198688.48	18.57	<1.09	<0.94	32.82	2.93	90.14
31B-04	27344.13	121830.66	170222.02	174.44	9628.67	37.45	68.90	71.72	4.05	15.85	149713.94	74845.98	29.40	0.62	0.31	37.56	6.18	80.65
31B-15	14062.02	147737.63	204785.48	148.98	9614.08	20.35	84.65	93.85	7.91	14.43	258567.88	309068.03	36.56	<0.56	0.82	49.11	30.33	1.86
31B-16	30214.26	114027.51	166004.70	147.49	9525.46	38.35	81.94	81.79	4.57	15.08	139185.14	69285.20	28.65	<0.56	<0.51	41.15	6.85	90.05
31B-19	33693.87	126672.83	179849.39	189.97	8818.34	47.03	83.19	79.59	5.03	31.83	146562.77	75447.62	32.01	0.67	<0.52	44.02	6.00	98.52
31B-22	31848.78	145933.36	177849.39	170.62	12407.42	28.06	119.22	124.24	7.52	30.81	169647.59	92172.07	58.71	2.72	<0.72	71.61	10.03	62.46
31B-23	25215.96	115959.87	174341.00	193.50	12194.51	23.51	89.63	85.92	4.21	40.91	169647.59	71319.55	45.85	1.78	0.49	84.65	10.90	71.71
31B-26	27553.85	130448.64	188043.14	174.15	11960.38	33.53	114.02	119.07	5.20	44.68	174157.07	77120.94	50.57	1.44	<0.69	67.29	16.14	144.26
31B-27	28774.55	122021.95	173665.09	119.33	11624.54	94.14	95.03	96.63	7.16	58.17	160572.03	74508.47	47.16	1.96	<0.69	64.98	14.59	138.01
31B-28	24388.64	102330.13	147784.08	161.56	11960.38	34.27	63.42	62.28	3.35	23.94	116895.19	57434.93	22.79	<0.36	<0.37	24.64	7.77	70.36
31B-29	29408.62	131057.00	147784.08	189.97	8818.34	47.03	83.19	79.59	5.03	31.83	146562.77	75447.62	32.01	0.67	<0.52	44.02	6.00	98.52
31B-30	28672.00	127317.55	196251.53	170.62	11983.67	35.76	106.92	91.22	5.90	51.87	193389.56	82719.67	52.90	1.97	<0.76	79.47	12.42	74.48
31A-05	16112.34	233324.56	161240.34	215.88	9332.78	41.58	209.10	197.08	6.26	182.16	415063.81	73620.23	13.69	1.39	0.99	21.44	13.68	89.55
31A-06	18592.21	295865.88	199330.97	243.98	10147.39	69.31	218.18	243.77	6.11	4.72	534009.75	81812.45	17.59	1.10	<0.89	24.69	14.59	74.48
31A-07	20943.18	275357.47	183577.58	321.04	9497.66	104.55	265.67	315.32	5.55	4.22	485811.03	81722.69	17.80	<1.19	<0.95	23.40	5.02	8.76
31A-08	19842.50	212589.75	144002.17	272.79	8774.38	105.38	208.92	218.70	4.72	<2.06	372901.38	62034.23	13.52	<0.85	0.94	21.68	5.26	39.77

| Zr90	Sn118	La139	Ce140	Pr141	Nd146	Sm147	Eu153	Gd157	Tb159	Dy163	Ho165	Er166	Tm169	Yb172	Lu175	Hf178	Pb208	Th232	U238
6.75	2.03	<0.054	<0.051	<0.052	0.41	0.99	0.15	7.59	2.30	20.40	4.86	14.36	1.77	10.17	1.43	0.23	<0.142	<0.070	<0.067
6.66	1.53	<0.053	<0.049	<0.038	1.34	0.31	0.31	8.42	2.62	21.25	4.62	12.39	1.55	8.93	1.18	<0.21	<0.113	<0.059	<0.067
5.23	12.51	<0.053	<0.054	<0.049	<0.29	1.34	0.47	9.84	2.63	20.94	4.49	13.83	1.90	13.40	1.86	0.21	<0.126	<0.062	<0.059
4.36	7.05	<0.045	<0.043	<0.050	<0.21	1.56	0.25	7.29	1.92	19.36	4.44	14.35	2.00	13.30	2.12	0.12	<0.113	<0.053	<0.055
6.42	<0.40	<0.052	<0.041	<0.038	0.34	1.17	0.28	7.63	1.87	13.63	2.63	7.66	0.99	6.15	0.92	<0.15	<0.118	<0.041	<0.058
5.61	0.73	<0.054	<0.052	<0.050	0.42	1.49	0.40	10.81	2.56	18.63	3.92	10.38	1.36	8.14	1.07	<0.20	<0.143	<0.058	0.06
5.97	16.14	<0.052	0.42	0.42	1.38	1.38	0.56	18.63	2.56	18.63	3.92	10.38	1.36	8.14	1.07	<0.178	<0.118	<0.058	<0.058
5.09	0.95	<0.047	<0.048	<0.041	1.39	1.39	0.24	17.12	2.28	17.12	3.66	11.66	1.72	12.53	2.22	<0.188	<0.054	<0.054	0.06
5.91	1.10	<0.040	<0.045	<0.032	0.94	0.94	0.31	16.48	2.20	16.48	3.45	10.46	1.73	12.25	2.23	0.17	<0.188	<0.048	<0.055
4.55	<0.040	<0.040	<0.039	<0.037	<0.19	0.93	0.24	13.20	1.72	13.20	2.39	6.20	0.76	4.62	0.54	0.23	<0.076	<0.038	0.23
4.79	0.85	<0.042	<0.041	<0.037	0.23	1.04	0.18	6.40	1.66	9.99	2.09	5.00	0.65	3.76	0.68	<0.124	<0.091	<0.042	<0.042
4.88	0.99	<0.032	<0.034	<0.032	0.62	0.62	0.12	4.34	1.29	10.83	2.33	6.04	0.81	4.87	0.66	<0.152	<0.085	<0.043	0.05
5.52	3.14	<0.025	<0.025	<0.024	1.59	1.59	0.39	6.95	1.72	21.60	4.95	16.23	2.74	17.85	2.83	<0.116	<0.062	<0.036	0.12
6.93	0.78	0.03	<0.031	<0.027	0.37	1.67	0.46	13.77	3.81	27.72	5.55	15.94	2.03	11.82	1.73	0.14	<0.037	<0.033	0.10
6.44	1.55	<0.034	<0.034	<0.028	0.35	2.82	0.46	14.74	4.08	30.79	5.55	21.32	3.28	20.34	3.42	0.12	<0.080	<0.024	0.04
6.70	1.04	<0.039	<0.025	<0.024	0.24	2.37	0.56	15.64	4.38	33.44	7.90	23.70	3.84	27.79	4.82	0.14	<0.087	<0.039	0.04
7.19	<0.49	<0.028	<0.027	<0.026	<0.143	2.11	0.46	12.69	3.56	23.23	4.60	11.10	1.53	8.69	1.09	<0.13	<0.076	<0.033	<0.024
7.66	10.92	<0.040	<0.045	<0.041	0.24	2.69	0.85	7.94	2.20	16.48	3.45	10.46	1.72	12.53	2.22	<0.13	<0.087	<0.054	0.06
7.02	<0.66	<0.039	<0.039	<0.036	0.46	2.05	0.36	5.85	1.72	13.20	2.39	6.20	0.76	4.62	0.54	0.10	<0.076	<0.038	0.23
5.97	0.55	<0.036	<0.036	<0.029	0.15	1.67	0.46	7.14	1.66	12.52	2.04	4.31	0.52	2.14	0.25	0.10	<0.039	<0.042	<0.038
7.02	284.01	0.04	0.04	0.02	0.42	2.81	0.62	15.77	4.07	27.08	5.71	15.40	2.13	13.29	2.01	0.19	<0.092	<0.044	0.04
7.73	<0.54	<0.033	<0.032	<0.026	<0.20	0.99	0.29	11.32	3.95	32.10	6.74	17.12	2.41	12.76	1.45	0.19	<0.087	<0.032	<0.028
8.83	<0.56	<0.026	<0.024	<0.030	<0.167	1.84	0.51	12.74	4.03	31.57	6.83	18.54	2.68	15.22	2.30	0.23	<0.084	<0.024	<0.032
35.90	0.72	<0.037	<0.031	<0.030	0.35	2.35	0.50	15.77	3.82	37.99	9.55	24.21	3.30	18.01	2.52	2.59	<0.080	<0.037	0.61
8.78	1.36	<0.029	<0.024	<0.026	0.37	2.35	0.50	12.74	4.08	29.68	7.05	19.73	2.78	15.03	1.96	0.18	<0.079	<0.032	<0.024
10.31	<0.50	<0.036	<0.025	<0.018	0.46	3.46	0.53	13.01	4.17	30.82	6.34	15.29	1.83	10.34	1.17	0.18	<0.064	<0.024	<0.022
8.83	0.61	<0.026	<0.028	0.03	0.35	1.65	0.31	11.18	3.09	22.07	4.92	15.36	2.24	12.93	1.91	0.34	<0.089	<0.017	0.04
11.79	0.55	<0.031	<0.024	<0.042	0.21	2.22	0.49	10.12	2.84	19.02	4.19	11.38	1.58	9.26	1.40	0.31	<0.075	<0.019	0.03
10.50	0.55	<0.029	<0.031	<0.021	0.35	1.57	0.36	9.86	2.64	18.56	3.98	10.88	1.57	9.02	1.24	0.32	<0.023	<0.026	0.03
12.64	<0.57	<0.021	<0.021	<0.026	0.25	2.22	0.36	9.09	2.21	14.59	3.07	8.96	1.32	6.66	1.01	0.33	<0.069	<0.023	<0.026
11.58	<0.49	0.06	0.06	<0.027	1.57	1.57	1.57	10.28	2.64	13.72	2.89	9.55	1.41	11.30	1.65	0.28	<0.044	<0.038	0.04
215.64	<0.49	<0.0299	<0.031	<0.026	2.91	2.91	0.90	10.28	1.98	21.21	4.30	11.50	1.75	10.97	1.45	0.31	<0.047	<0.015	0.03
11.89	<0.58	<0.034	0.03	<0.023	2.64	2.64	0.90	12.27	2.51	21.21	4.30	9.55	1.41	9.53	1.52	0.29	<0.040	<0.0188	0.03
12.36	<0.47	<0.016	0.02	0.09	0.79	2.11	1.05	8.83	1.72	13.84	2.97	7.54	0.96	6.36	0.90	9.22	<0.061	<0.0180	0.07
14.41	<0.58	0.15	0.40	0.53	2.32	2.35	0.85	7.85	2.19	11.96	2.47	8.63	1.14	7.61	1.13	0.27	<0.052	0.02	0.03
10.72	<0.52	<0.0249	<0.033	0.04	0.25	2.12	0.84	10.68	2.39	16.37	3.69	10.51	1.44	9.35	1.30	0.21	<0.064	<0.030	0.03
10.58	<0.55	<0.037	0.05	0.03	0.72	3.27	1.05	10.54	2.47	16.00	4.92	16.00	2.53	18.47	3.11	0.14	<0.051	<0.020	0.07
10.58	<0.48	<0.033	0.05	0.03	0.33	3.52	0.72	11.70	2.56	23.88	5.85	19.29	3.24	23.68	3.65	<0.083	<0.054	<0.040	0.06
5.06	12.36	2.96	7.14	0.93	4.20	4.20	2.32	1.28	0.16	0.57	0.05	0.17	<0.044	<0.154	0.01	1.18	<0.047	<0.022	4.89
11.67	<0.52	<0.033	<0.033	<0.021	0.46	2.12	0.83	9.96	2.12	15.95	3.20	9.83	1.45	9.22	1.26	0.26	<0.064	<0.030	0.03
10.55	0.61	<0.023	0.05	<0.033	1.06	3.03	1.07	10.91	2.48	22.01	5.43	19.28	3.15	20.82	3.23	0.20	<0.050	<0.0234	0.07
10.72	<0.55	0.04	0.15	0.08	0.72	2.75	0.92	10.54	2.66	21.16	5.20	18.61	3.09	21.80	3.81	0.11	<0.051	0.03	0.13
10.55	<0.55	<0.037	0.03	0.10	0.92	3.26	1.09	13.99	2.31	12.45	2.39	6.09	0.89	5.97	0.74	0.42	<0.051	<0.033	0.11
10.77	0.84	<0.0214	0.06	0.06	2.05	4.95	1.44	11.30	1.70	10.59	2.10	6.85	0.85	5.76	0.82	0.31	<0.0260	<0.033	0.07
21.16	0.84	<0.033	0.05	0.03	1.04	3.03	1.26	9.96	2.48	22.14	5.20	18.61	3.15	9.35	1.30	0.20	<0.050	<0.0234	0.13
17.73	<0.54	<0.049	<0.049	<0.035	0.95	2.86	1.27	13.99	2.18	13.85	2.67	8.08	1.19	7.46	0.80	0.64	<0.078	<0.0275	0.12
18.85	0.80	<0.031	0.21	0.03	1.08	5.08	1.24	13.99	2.18	13.85	2.45	8.47	1.10	9.63	1.25	0.42	<0.062	0.03	0.10
22.37	<0.70	<0.037	0.08	0.04	1.04	3.85	1.09	9.36	1.93	12.48	2.45	8.47	1.10	9.63	1.25	0.42	<0.078	0.03	0.10
15.99	0.77	<0.031	<0.024	<0.029	0.95	2.86	1.26	10.45	2.21	15.26	3.15	11.24	1.71	11.07	1.73	0.27	<0.067	<0.029	0.06
9.55	118.78	<0.031	<0.046	<0.029	<0.134	0.63	0.99	3.64	1.24	9.40	1.37	6.09	0.10	11.07	1.73	0.44	<0.067	<0.035	0.05
3.82	23.70	<0.031	<0.046	0.04	0.85	0.63	0.99	3.60	0.71	3.19	0.42	0.80	<0.030	0.29	0.02	0.12	<0.082	<0.033	0.02
7.97	6.58	<0.047	<0.042	<0.027	0.20	1.53	1.29	2.77	0.45	1.96	0.32	0.36	<0.033	<0.137	0.23	0.23	<0.087	0.03	<0.031
14.89	5.48	<0.034	0.10	0.03	0.74	1.53	1.23	2.88	0.85	6.23	1.50	3.66	0.46	2.08	0.24	0.30	<0.057	<0.027	0.06

Gangue mineral influence on magnetite and the implications for Warramboo iron ore deposit.

Element	Mg24	Al27	Si29	P31	Ca43	Sc45	Ti47	Ti49	V51	Cr53	Mn55	Fe57	Co59	Ni60	Cu65	Zn66	Ga69	Y89
31A-09	16746.07	253609.39	166186.23	199.16	8840.49	126.02	340.28	343.34	6.68	3.93	465826.78	73949.34	16.37	1.30	<0.95	24.09	7.83	48.49
31A-27	50485.95	274854.25	182711.11	80.08	9894.32	80.08	416.13	489.06	9.23	<4.59	249880.11	93631.22	18.77	1.30	<1.43	28.21	5.46	22.19
31A-28	52624.27	278335.44	210396.41	97.90	9386.02	101.30	305.09	242.70	5.82	<2.01	233955.56	89279.24	18.77	1.34	<4.01	23.20	5.51	0.71
31A-29	55881.37	232808.34	286970.19	305.09	9630.45	72.14	731.41	683.32	11.24	7.43	181809.45	77982.87	25.71	<0.75	<0.94	21.05	5.94	5.94
512-01	24293.22	201226.92	201111.70	267.82	8653.53	155.27	102.24	100.96	10.06	38.85	176739.53	88944.66	35.62	<0.28	<0.72	57.64	9.11	0.71
512-02	22316.80	179243.91	146.80	146.80	8774.81	80.36	84.82	84.82	13.20	31.08	162872.20	88470.23	31.80	0.71	<2.77	38.21	6.12	0.92
512-03	24217.64	125741.04	201226.92	213.83	8774.81	137.20	100.51	94.99	12.50	26.36	185838.56	95443.77	34.05	<0.31	<1.07	40.58	8.88	240.71
512-04	4052.87	48299.76	96813.72	334.88	6157.11	110.28	186.44	94.99	23.27	26.36	141652.77	95808.17	46.18	<0.31	<0.94	90.72	9.29	71.08
512-05	11737.80	125997.29	182054.22	146.67	8230.42	31.76	962.81	978.01	14.01	3.72	232710.89	72775.54	34.05	<0.29	<0.76	56.12	7.25	1.45
512-21	18621.03	100687.01	159469.55	173.65	8495.22	102.18	1207.74	1305.62	21.68	44.47	136692.52	83847.92	22.59	0.80	<0.68	34.49	6.60	167.87
512-22	23952.08	113659.63	163954.63	169.38	8330.34	126.78	761.99	831.29	15.74	36.67	143320.19	89079.99	22.59	0.89	<0.68	34.49	7.53	196.81
512-23	22887.65	117161.20	177872.20	190.34	8257.44	117.25	76.10	76.10	7.93	56.11	143967.17	92658.98	25.90	0.49	<0.62	39.91	6.69	174.51
512-24	24531.43	171258.17	166488.42	219.51	8401.17	133.10	528.17	619.36	17.72	32.31	151880.30	94902.93	25.77	0.54	<0.94	39.91	6.69	151.38
512-31	21096.48	125693.95	183392.17	238.52	8224.35	223.11	216.11	216.11	10.02	27.33	139089.59	88477.16	27.22	0.67	<0.54	42.90	4.47	217.15
512-32	0.23	7333.64	238.52	19.53	238.52	128.63	223.11	141.00	0.21	22.96	166651.05	92336.34	26.75	0.44	<0.27	41.03	5.17	234.70
512-33	2.57	85020.27	340.07	21.43	194.66	16.46	15.96	15.96	0.03	4.07	656.04	71.49	<0.0033	0.64	42.90	<0.20	0.80	<0.00146
512-34	2.73	147795.19	705.71	46.88	19.53	<0.075	0.24	0.21	0.41	29.27	0.19	656.04	<0.033	<0.016	<0.0151	0.02	7.73	<0.0130
512-41	380.81	1778753.00	5944.88	390.28	5944.88	<0.90	184.15	166.52	19.91	46.59	275.19	1255.67	<0.050	<0.170	55.55	<0.32	15.07	<0.021
512-49	12227.36	14782.88	194367.88	125.96	8281.88	216.52	489.06	1033.16	14.91	6.38	253052.78	29035.26	43.02	0.68	0.69	34.05	6.60	0.07
512-51	28095.97	199628.56	199628.56	186.53	8608.14	130.50	536.84	421.26	17.72	32.67	165523.02	69882.34	32.67	0.75	7.67	25.92	4.31	247.37
512-52	22932.72	146873.55	177872.20	219.51	8401.17	117.25	82.17	120.84	7.22	56.11	143967.17	88477.16	25.77	0.41	7.53	39.91	6.69	190.27
512-53	24819.78	157518.45	194298.13	222.19	8396.09	121.55	120.84	141.00	8.97	27.33	103641.85	103641.85	28.99	0.34	<0.34	40.58	5.40	151.38
512-54	21484.80	121084.28	181901.97	199.95	7946.05	122.79	114.21	112.26	8.79	45.54	156610.73	98733.70	26.16	<0.38	<0.32	38.47	5.81	222.55

31A-11	13172.07	220807.86	141274.50	254.99	8969.92	61.61	203.67	231.35	6.81	<2.56	411717.66	68173.12	13.66	1.56	<0.85	17.96	5.73	52.12
31A-16	15292.34	265704.19	146873.55	124.47	8608.14	255.33	90.67	46.22	3.11	4.15	470983.34	71150.80	14.06	<1.22	<0.67	17.61	4.31	2050.11
31A-17	13190.77	272674.81	157518.45	178.08	8416.82	101.30	145.76	149.38	3.91	<2.35	516334.59	72655.70	14.35	<1.07	<0.68	16.70	6.60	974.64
31A-19	12659.18	253815.86	155695.95	211.69	8283.10	67.20	50.84	62.29	3.44	2.23	414951.97	68907.95	15.19	2.21	1.40	21.84	9.56	217.45
31A-22	74591.34	427973.81	20267.10	166.45	10161.98	166.45	424.31	302.91	8.85	<7.62	336631.56	137959.88	28.73	2.54	<0.72	31.22	6.81	8.18
31A-24	64623.38	334223.47	226817.28	<418.04	9752.09	116.59	497.57	441.26	9.34	<5.92	291277.31	115078.17	23.69	3.23	<0.95	35.62	7.42	65.48
512-12	48.73	65149.67	749.46	18.91	149.54	0.04	58.85	59.54	2.89	22.33	2338.71	39.77	0.59	1.07	<0.80	0.32	10.49	<0.0095
512-41	12227.36	147824.88	194367.88	125.96	890.70	216.52	536.84	489.06	14.91	6.38	253052.78	69882.34	43.02	9.80	<0.64	2563.71	25.92	0.07
512-42	33010.08	360882.84	173.25	173.25	2203.79	28.93	137.93	156.83	10.65	<1.77	473437.63	132810.47	167.33	41.26	<0.64	10168.35	66.45	0.12
512-43	48795.70	278060.91	259377.42	269.55	269.55	30.64	331.73	337.95	7.62	6.68	706637.50	182341.05	244.51	64.49	4.18	10353.34	121.54	0.18
512-44	24237.73	437751.08	136.02	136.02	2145.90	13.45	131.18	121.85	4.27	<1.37	311369.34	97250.56	80.17	21.59	78.08	4912.21	41.10	0.11
512-45	10516.94	259377.42	70067.95	26.58	2448.67	1.16	11.64	12.08	0.22	<0.30	50188.96	21705.00	10.63	2.72	4.72	85.10	6.75	0.08
516-37	18627.36	264307.41	154578.22	123.39	24589.64	52.71	281.46	296.53	8.63	7.99	365124.59	45811.17	18.25	<1.36	<1.16	19.91	8.42	2.00

516-01	66915.73	190298.45	128792.80	197.74	26218.23	50.24	308.25	293.57	10.04	21.55	457047.81	55625.41	21.61	<0.73	<0.68	24.71	9.47	0.60
516-02	60731.75	170984.39	115805.09	189.10	25105.01	68.22	273.48	284.70	10.13	<2.01	407753.69	51167.96	20.01	<0.78	<0.67	26.12	8.39	0.45
516-03	56530.75	166710.08	111951.52	174.71	25551.63	28.06	238.56	242.70	9.86	<2.07	400099.75	50657.61	19.16	<0.76	<0.68	24.35	8.99	0.72
516-04	70955.03	202127.17	134389.69	222.84	27581.24	61.66	296.74	309.88	11.06	4.61	481638.09	61236.98	26.57	<0.94	1.40	38.93	10.64	0.90
516-05	62513.81	122053.98	188.00	188.00	26015.75	62.75	281.36	268.25	9.42	4.18	411196.06	51511.53	19.82	<0.72	<0.62	23.68	9.11	0.71
516-08	64907.51	189561.28	124402.87	184.92	23798.90	36.11	299.57	291.69	9.53	2.50	414079.97	53190.55	24.34	<0.95	<0.80	42.70	10.90	0.92
516-13	85375.29	212068.39	139947.52	212.00	22614.85	83.96	48.96	48.96	2.98	<2.77	428911.84	57279.46	23.14	<1.07	<0.94	24.83	5.64	1494.00
516-38	31278.83	369126.94	215706.25	297.51	19613.32	125.62	339.77	340.16	6.21	<3.88	489987.59	61278.60	25.74	<1.84	<2.11	31.18	8.74	92.86
516-39	30822.40	351137.78	229959.00	150.88	19008.12	117.54	342.85	348.67	5.68	8.64	522005.38	64069.17	27.12	<1.40	<1.91	31.15	10.34	98.20
516-43	23740.96	326746.94	201735.03	147.83	22969.35	72.61	284.18	330.70	9.27	4.71	422881.31	51533.39	19.73	<1.22	1.50	23.82	8.81	8.01
516-44	22076.06	289544.16	190285.97	97.95	21864.99	280.11	293.00	8.96	18.97...	5.54	382094.78	46669.30	22.16	1.22	1.13	34.03	8.70	6.04
516-45	19840.45	517746.00	289544.16	284.00	31222.21	<1.23	77.05	76.06	18.97	<3.35	672025.56	63680.18	22.64	<1.86	<1.88	25.35	18.91	0.50

Gangue mineral influence on magnetite and the implications for Warramboo iron ore deposit.

Isotope	Values
Zr90	17.21, 8.04, 6.94, 3.19, 10.68, 7.71, 0.40, 11.61, 0.57, 16.60, 9.64, 0.53, 4.23, 11.55, 5.19, 5.85, 16.04, 0.34, <0.0032, <0.026, <0.044, <0.48, 3.71, 10.44, 8.33, 3.00, 14.34, 7.20, 17.41, 17.74, 18.40, 5.15, 5.54, 8.03, 8.36, 3.71, 0.36, <0.22, 1.45, 5.20, 22.44, 20.52, 19.69, 15.35, 20.53, 17.32, 20.38, 8.43, 27.43, 23.15, 21.82, 19.96, 16.42
Sn118	6.78, 38.32, 58.80, 5.97, 0.34, 0.40, 0.57, 9.64, 4.23, 0.98, 0.92, 0.34, <0.0138, <0.140, <0.21, 5.48, 17.84, 1.67, 0.35, 3.15, 4.11, 2.88, 17.84, 0.09, 7.51, 17.18, 237.98, 235.06, 25.06, 33.87, 0.77, 1.70, 1.70, 1.96, 1.11, 1.81, 1.67, 1.04, 0.63, 0.76, 3.07, 1.22, 1.66, 0.75
La139	0.21, 0.069, 0.04, <0.064, <0.039, 0.23, <0.029, 0.57, 1.08, 0.07, 0.02, 0.02, <0.0107, <0.0097, <0.0132, <0.18, <0.026, 1.67, <0.021, 0.19, 0.19, <0.045, <0.026, <0.0063, <0.00, 0.03, 1.54, <0.064, 0.12, <0.058, 0.10, 0.16, 0.09, 0.19, <0.026, 0.09, 0.06, 0.07, 0.09, 0.16, 0.06, 0.15, <0.031, <0.043, <0.029, <0.039, <0.027, <0.045, <0.039, <0.029, <0.026, 0.21, 0.20, 0.24
Ce140	0.67, <0.039, <0.064, 0.23, 3.33, 0.04, 0.19, 2.07, 0.07, 0.02, 0.03, <0.00096, <0.0086, <0.013, <0.17, <0.052, 2.28, 0.04, 0.16, 0.16, 0.18, 0.42, 0.18, 0.16, <0.0052, <0.058, 0.04, 0.11, 0.29, 0.18, 0.30, 0.20, 0.24, 0.37, 0.31, 0.18, 0.43, 0.28, 0.52, 0.13, 0.16, 0.19
Pr141	0.07, 0.04, <0.029, 0.19, <0.29, 0.03, 0.19, <0.0115, <0.0076, <0.00085, 0.02, <0.017, <0.037, <0.040, <0.14, <0.038, <0.71, <0.041, 0.25, 0.28, <0.79, <0.0046, <0.0164, <0.0120, 0.05, 0.03, 0.03, 0.02, 0.07, 0.15, 0.19, 0.16, 0.20, 0.21, 0.19, 0.13, 0.19, 0.23, 0.01, 0.29, 0.21, 0.24
Nd146	1.35, 0.23, <0.14, 0.47, 0.16, 0.11, <1.76, <2.08, 0.49, 0.35, 0.49, <0.0050, <0.046, <0.139, <0.79, 0.09, 1.22, 0.28, 0.58, 0.84, 0.82, 0.90, 0.49, 0.56, <0.027, <0.139, 2.90, 3.56, 3.11, 4.49, 0.45, 2.90, 2.20, 3.49, 4.14, 3.28, 4.65, 3.86, 4.90, 4.63, 2.76, 0.08, 0.56, 2.11, 2.17
Sm147	1.94, 2.21, 3.16, 0.60, 1.62, 1.20, 2.08, 2.02, 1.84, 2.20, 2.06, <0.0055, <0.049, <0.079, <0.96, <0.154, 2.04, 0.59, 1.20, 2.54, 2.16, <0.24, 1.14, 2.57, 0.04, 1.19, 1.37, 0.85, 0.45, 2.20, 0.72, 2.24, 2.97, 8.55, 10.68, 1.02, 5.37, 1.16, 3.95, 4.04, 2.11
Eu153	1.42, 1.37, 4.63, <0.17, 0.62, 0.49, 1.39, 0.18, 0.03, 0.73, 0.66, <0.00158, <0.0149, <0.020, <0.26, <0.020, 1.18, 1.16, 1.12, 1.47, 1.41, 0.53, 0.46, 0.56, <0.0087, 1.10, 0.69, 0.53, 0.37, 0.92, 0.44, 0.80, 0.66, 5.50, 5.68, 0.93, 4.82, 0.61, 2.47, 2.16, 1.29, 0.05, <0.053
Gd157	4.35, 3.16, <0.00, 0.58, 12.72, 15.71, 4.73, 9.57, 1.84, 10.40, 11.71, <0.0060, <0.065, <0.089, <1.04, <0.16, 7.55, 0.54, 3.31, 16.26, 15.71, 0.53, 2.98, 10.62, <0.038, 3.53, 0.55, 0.41, 0.42, 0.97, <0.213, 12.31, 11.24, 20.86, 27.03, 0.61, 82.75, 3.86, 2.49, 2.96, 0.75, <0.053
Tb159	1.12, 0.71, <0.00, 0.15, 4.38, 5.37, 1.30, 2.82, 0.03, 2.98, 3.55, <0.00083, <0.0092, <0.0130, <0.14, <0.022, 4.05, 0.38, 0.89, 11.58, 9.31, 0.53, 2.29, 2.29, <0.0051, 1.47, 0.09, 0.05, 0.04, 0.06, <0.060, 3.41, 3.88, 22.34, 22.11, 0.09, 27.81, 0.07, 0.28, 0.39, 0.07, <0.0065
Dy163	8.82, 4.63, 0.32, 1.60, 12.72, 15.71, 13.93, 25.29, 1.84, 30.18, 31.66, <0.0034, <0.036, <0.072, <0.62, <0.025, 36.42, 1.88, 8.86, 178.87, 118.61, 0.53, 26.32, 20.56, <0.022, 10.69, 0.28, 0.17, 0.25, 0.19, <0.29, 29.11, 34.27, 22.34, 22.11, 0.28, 251.16, 0.70, 1.38, 2.00, 0.17, 0.04
Ho165	1.67, 0.71, <0.048, 0.25, 9.01, 9.73, 1.30, 5.84, 0.08, 7.79, 8.05, <0.00106, <0.0097, <0.0134, <0.16, <0.025, 8.20, 0.18, 2.46, 75.63, 41.58, <0.074, 6.28, 5.71, <0.0056, 2.10, 0.05, 0.03, <0.027, <0.021, <0.048, 23.23, 8.41, 12.59, 9.31, <0.032, 55.05, 0.12, 0.23, 4.28, <0.035, <0.037
Er166	4.77, 1.16, <0.125, 0.40, 28.89, 28.24, 10.54, 17.80, 0.09, 26.51, 28.85, <0.0033, <0.026, <0.037, <0.47, <0.067, 23.99, 0.29, 9.05, 388.56, 163.33, <0.24, 21.77, 20.21, <0.0194, 3.09, 0.10, 0.11, <0.082, <0.080, <0.124, 23.23, 4.37, 12.59, 10.46, <0.077, 161.63, 0.23, 0.50, 12.59, <0.078, <0.089
Tm169	0.58, 0.11, <0.021, <0.026, 3.68, 4.14, 1.69, 2.65, 0.08, 3.40, 3.14, <0.00073, <0.0082, <0.0148, <0.17, <0.021, 10.78, 0.08, 1.51, 71.97, 22.48, <0.040, 3.25, 3.14, <0.0055, 0.36, 0.08, 0.03, <0.029, <0.028, <0.071, 22.44, 3.62, 7.47, 1.56, <0.026, 22.32, 0.29, 0.10, 1.73, <0.023, <0.034
Yb172	3.43, 0.38, <0.00, <0.098, 26.89, 24.40, 6.65, 18.10, 0.19, 30.84, 31.42, <0.0036, <0.044, <0.063, <0.64, <0.025, 16.36, 0.28, 10.13, 490.28, 114.43, <0.34, 23.14, 22.44, <0.026, 1.73, 0.10, 0.10, <0.111, <0.116, <0.18, 25.97, 32.69, 7.47, 140.56, <0.126, 140.56, 0.29, 0.35, 9.31, <0.133, <0.036
Lu175	0.30, 0.38, <0.039, <0.020, 3.84, 3.48, 4.21, 2.42, 0.19, 4.67, 4.87, <0.00091, <0.0083, <0.0158, <0.18, <0.025, 1.36, <0.00, 1.47, 93.46, 16.36, <0.043, 3.13, 3.18, <0.0053, 0.16, <0.00, 0.05, <0.025, <0.028, <0.077, 3.83, 4.89, 20.05, 0.92, <0.026, 20.05, 0.05, 0.02, 0.69, <0.035, <0.030
Hf178	0.13, 0.27, 0.18, 0.35, 0.23, 0.22, 0.99, 0.08, 1.39, 0.14, 0.07, <0.00035, <0.034, <0.047, <0.058, <0.068, <0.14, <0.059, 0.36, 0.36, 0.56, 0.31, 0.14, 0.26, 0.33, <0.15, 0.08, 0.35, 0.28, 0.33, 0.15, 0.30, 0.31, 0.58, 0.49, 0.21, 0.31, 0.48, 0.15, 0.36, 0.40, 0.35, 0.23
Pb208	0.51, 0.19, 0.18, 0.14, 0.35, 0.23, 41.08, 0.07, 1.13, 0.07, 0.10, <0.00104, <0.050, <0.022, 0.04, <0.064, <3.02, 12.95, 0.09, 0.26, 3.89, 0.66, 0.07, <0.050, 0.03, <0.047, 1.34, <0.18, 0.28, 0.53, 0.03, 0.07, 0.08, 0.66, 0.09, 0.14, 0.08, <0.069, 0.02, 1.92, 0.58, 0.40, 0.21
Th232	0.11, <0.00, <0.045, 0.07, <0.026, <0.023, 0.68, <0.024, 0.48, <0.026, <0.023, <0.00102, <0.0113, <0.0131, <0.017, <0.074, <0.19, <0.047, 0.06, <0.034, <0.053, <0.089, <0.028, <0.023, <0.0077, <0.047, <0.028, <0.056, <0.037, <0.029, <0.053, <0.024, <0.026, <0.100, 0.09, 0.14, <0.102, <0.0199, <0.033, 0.03, <0.083, <0.052, <0.021, <0.0134, <0.035, <0.036, <0.025, <0.021, <0.018, <0.0171
U238	0.11, <0.042, 0.03, 0.04, 0.08, 0.05, 0.68, 0.04, 0.07, 0.04, 0.04, 0.08, 0.16, 0.06, 0.17, 0.35, 0.09, 0.05, 0.04, 0.06, 0.08, 0.10, 0.35, 0.09, 0.05, 0.10, 0.05, 0.05, 0.09, 0.07, 0.09, 0.05, 0.05, 0.06, 0.15, 0.10, 0.02, 0.10, 0.08, 0.16, 0.06, 0.17, 0.35

PM Element	Mg24	Al27	Si29	P31	Ca43	Sc45	Ti47	Ti49	V51	Cr53	Mn55	Fe57	Co59	Ni60	Cu65	Zn66	Ga69	Y89
P1-06	5409.78	105901.55	180167.83	131.02	9597.08	22.28	545.43	548.68	15.44	21.65	149503.14	73937.02	7.61	0.63	0.41	14.55	4.84	2079.11
P1-07	1664.03	37629.86	51372.66	22.62	8434.97	31.53	251.94	237.29	7.94	7.59	51174.73	27395.05	2.24	0.22	<0.147	3.42	2.09	296.28
P1-09	3206.96	64636.36	97586.42	43.86	11525.77	16.50	398.55	439.42	13.93	30.65	96136.62	48507.26	4.64	<1.52	<0.24	10.33	2.96	1138.09
P2-01	5735.53	122568.96	189189.94	79.79	35879.42	107.84	2336.31	2391.56	48.55	53.63	201924.28	79444.13	12.39	2.16	1.09	25.37	7.21	2350.26
P2-02	108029.20	1246433.38	3690044.25	788.64	36064.89	293.81	26529.68	27362.90	795.86	522.56	447329.88	319638.63	147.55	192.03	6.37	928.91	437.78	1539.89
P2-06	237427.33	1157938.63	6072468.50	1044.41	369185.25	363.35	29094.31	29629.94	872.81	622.16	122248.46	414827.50	157.95	242.68	35.24	402.46	245.22	245.22
P2-10	4607.40	116710.60	176507.58	62.04	35625.27	113.77	2908.42	2934.24	46.05	59.00	209621.59	78688.78	11.68	3.23	<0.30	20.43	6.81	2177.76
P2-11	4969.64	102204.38	157092.13	406.36	36448.39	135.69	1737.64	1739.40	37.29	49.55	182938.30	63853.51	12.84	4.56	1.34	27.90	6.31	1089.07
P2-13	7590.45	137121.41	182375.41	209.94	24568.14	174.13	1743.49	1663.32	43.43	86.58	185867.78	83606.18	10.44	1.24	<0.62	15.33	9.59	3716.05
P2-14	6976.46	166773.30	218398.66	130.27	36221.69	114.29	2215.38	2273.31	36.20	49.51	228649.84	77742.68	10.52	0.58	0.98	28.87	8.43	2065.49
P2-16	4816.60	98301.83	164585.17	69.83	22796.46	63.40	1030.87	1068.62	27.03	35.25	154227.72	61460.77	9.55	0.47	<0.58	22.40	5.41	250.14
P2-24	3224.47	83632.40	117752.08	44.22	22823.05	90.41	1027.35	981.66	25.09	24.63	118362.02	40265.69	5.53	0.54	<0.41	13.20	4.35	633.36
P2-26	5147.25	112596.36	171453.69	61.52	29740.28	66.52	975.34	938.14	23.71	21.93	153074.41	61315.42	8.55	<0.56	0.53	14.51	5.00	2077.69
P2-27	5888.14	134068.17	259201.23	123.12	37374.36	86.13	1321.68	1329.55	31.50	41.46	211838.13	79126.25	11.60	<0.91	0.89	26.81	7.83	474.73
P2-28	12012.34	97264.71	171901.00	81.22	34636.20	100.98	666.89	679.19	60.77	46.77	104480.22	82155.30	12.05	<0.71	1.10	34.35	5.90	1935.35

Kelsy J Dyer

Gangue mineral influence on magnetite and the implications for Warramboo iron ore deposit.

Element	S1	S2	S3	S4	S5	S6	S7	S8	S9	S10	S11	S12	S13	S14	S15	S16	S17
Zr90	29.73	7.34	66.27	145.76	6.86	1912.23	1372.38	614.28	80.47	956.88	14.80	24.81	24.27	15.56	16.25	98.37	11.93
Sn118	<0.55	0.37	1.13	<0.00	2.98	3.40	120.87	13.74	6.79	3.77	2.55	4.90	14.33	1.82	13.21	2.14	1.66
La139	<0.038	1.79	<0.00	0.40	2.98	13.74	40.65	22.61	9.17	3.67	0.07	38.22	82.63	120.83	0.12	84.21	0.03
Ce140	<0.00	3.00	0.07	5.82	13.04	22.61	69.66	9.39	8.05	5.13	<0.00	82.63	37.69	225.57	0.12	204.16	<0.044
Pr141	0.03	0.40	<0.0118	0.61	1.36	2.34	9.17	28.26	0.98	5.13	<0.0219	9.08	0.07	28.32	108.86	19.33	<0.0166
Nd146	0.45	1.48	0.12	2.40	5.90	13.04	9.39	28.26	5.13	0.82	<0.183	37.69	<0.19	108.86	<0.00	64.98	0.27
Sm147	2.34	0.49	0.27	1.05	11.54	3.21	6.58	1.57	2.23	0.82	8.06	0.61	20.96	4.19	0.20	14.04	0.26
Eu153	1.07	0.06	0.38	0.47	5.04	2.48	1.57	0.77	0.28	1.75	0.32	4.19	0.39	3.25	5.99	3.25	0.07
Gd157	12.64	1.33	3.37	7.92	44.21	13.64	6.64	13.39	9.82	5.19	21.20	4.22	24.90	5.99	13.80	13.80	3.28
Tb159	10.61	0.63	3.56	5.85	13.64	1.59	5.79	4.97	7.68	9.65	2.45	6.25	5.38	5.05	5.38	5.05	3.30
Dy163	202.96	14.35	73.37	144.74	179.31	22.66	117.39	79.16	261.76	211.16	31.54	73.04	131.49	55.10	76.16	52.55	116.68
Ho165	87.08	9.92	39.90	75.07	35.56	6.42	58.91	27.71	184.62	109.79	10.20	23.05	75.11	11.43	74.69	16.56	70.34
Er166	427.22	101.47	288.82	378.12	132.39	20.48	287.68	106.49	1192.39	542.99	36.82	75.11	415.92	72.07	480.33	52.55	383.04
Tm169	90.35	42.19	87.72	62.73	17.65	2.74	48.10	14.82	241.02	92.71	5.22	11.43	72.07	8.24	46.32	6.75	66.07
Yb172	729.47	614.90	1044.63	416.19	128.02	18.93	307.11	95.37	1745.03	619.77	40.49	74.69	480.33	46.32	66.56	6.75	440.38
Lu175	105.44	124.46	194.35	56.13	20.28	2.38	42.09	14.24	239.26	77.32	5.40	10.59	66.56	6.75	66.56	6.75	56.65
Hf178	1.52	0.28	0.19	1.45	2.27	47.66	42.69	1.36	17.80	0.23	1.34	0.64	1.05	0.44	0.57	4.17	0.41
Pb208	0.08	0.29	0.66	0.19	2.37	122.65	123.56	0.78	29.24	1.61	0.64	4.97	0.80	10.90	0.78	7.08	0.37
Th232	0.07	1.80	1.53	0.66	316.23	13.64	7.74	0.77	29.24	11.11	15.74	26.67	1.02	60.43	0.17	25.72	0.04
U238	0.47	0.09	0.81	1.53	2.37	13.64	7.74	0.77	2.26	0.60	1.03	0.94	2.61	0.25	2.61	2.77	0.25

Magnetite

Element	Mg24	Al27	Si29	P31	Ca43	Sc45	Ti47	Ti49	V51	Cr53	Mn55	Fe57	Co59	Ni60	Cu65	Zn66	Ga69	Y89
Massive																		
02B-01	83.24	1909.45	437.09	<18.13	249.64	0.833	527.4	523.45	384.19	304.21	273.42	712194.13	28.6	66.11	<0.39	16.4	72.25	<0.057
02B-02	136.57	1619.49	1121.88	24.09	<84.20	0.554	275.54	249.95	374.52	281.45	104.48	702637.88	27.24	64.8	<0.42	14.47	65.88	0.069
02B-03	75.13	1368.71	420.82	29.06	<101.70	0.313	508.52	524.93	379.99	317.2	153.61	713514.81	27.66	65.78	<0.41	17.89	68.95	0.062
31A-01	1.9	145.94	303.96	26.63	<61.31	0.204	43.11	45.11	317.2	35.77	1558.07	714904.38	36.66	50.42	<0.195	8.82	38.85	<0.0132
31A-02	3.87	177.03	210.4	27.11	<75.21	<0.135	61.5	59.63	94.38	34.41	1433.55	704746.63	38.15	52.29	<0.24	10.74	37.09	0.02
31A-10	9.74	251.48	342.14	32.12	<85.09	<0.184	55.44	94.25	94.25	29.08	1763.73	713985.69	45.92	55.46	<0.27	13.52	32.56	0.117
31A-12	7.76	222.76	321.44	20.02	<59.48	<0.165	34.69	37.38	93.46	34.25	1483.65	714966.63	42.9	54.02	<0.24	40.36	37.09	0.097
31A-13	182.44	411.56	1104.76	19.29	<105.64	0.315	27.53	30.55	96.79	30.06	1351.89	716976.75	41.85	56.03	<0.25	26.91	32.56	0.46
31A-20	2.98	310.53	146.65	<12.21	<105.64	0.28	62.66	66.84	94.57	32.86	1718.88	717688.13	42.54	53.67	<0.32	21.78	34.71	0.73
31B-02	53.57	1131.57	189.52	45.06	189.52	0.38	181.29	170.72	248.58	128.73	2258.38	713023.63	170.89	462.26	<0.33	51.8	83.3	<0.052
31B-05	69.04	1756.58	300.85	69.78	102.78	<0.29	178.61	181.03	254.93	107.07	2980.81	716189.63	186.25	461.93	<0.46	43.36	76.58	0.063
31B-06	1411.65	1532.26	601.12	72.87	170.23	<0.33	102.78	101.7	256	101.7	3656.58	715974.31	171.29	468.66	1.14	58.11	96.47	0.948
31B-10	176.41	1951.95	1280.28	76.26	243.74	0.4	217.75	227.4	281.8	98.15	3666.4	715540.63	162.01	443.02	<0.43	72.63	143.4	0.043
512-07	635.29	2691.51	5632.44	61.32	232.97	1.57	263.33	263.17	245.47	294.76	3885.87	707960.38	170.69	308.33	0.34	34.56	72.63	0.85
512-08	405.36	1407.24	2066.93	65.14	269.17	1.28	269.17	163.78	281.8	296.77	3759.97	708936.69	164.45	318.29	0.34	29.31	143.4	0.117
512-09	317.86	1151.54	2562.97	70.89	163.78	1.21	163.78	201.59	307.39	307.39	2998.35	708936.69	159.88	310.27	<0.20	25.63	97.92	0.097
512-10	1738.14	1141.94	70.82	57.49	70.82	0.69	201.59	181.97	307.39	261.17	2940.56	710620.38	161.54	364.58	0.31	31.19	80.97	<1.15
512-11	487.91	1807.05	4532.4	69.78	79.29	10.19	122.51	122.51	525	79.29	2188.28	705016.69	148.78	310	<1.15	33.87	80.89	0.46
512-14	480.95	1159.13	119.42	126.87	122.51	1.08	179.27	201.59	617.33	380.41	2087.09	705291.81	178.09	329.52	0.77	10.82	71.88	11.85
512-26	1726.57	2153.32	3152.81	72.87	277.20	1.02	217.75	217.75	608.76	288.69	1626.45	703750.38	98.98	200.62	11.6	32.47	114.33	0.65
512-27	206.07	1896.99	170.23	70.4	170.4	0.386	243.74	211.75	665.56	677	694.24	704921.13	93.42	196.62	38.4	39.16	96.47	0.094
512-37	507.1	1399.09	57.95	57.95	<52.07	0.472	179.34	179.34	502.9	296.77	1865.66	687213.94	122.5	228.28	0.27	42.38	94.83	0.027
512-38	1089.64	3295.57	121.73	73.61	121.73	0.314	102.44	177.06	502.9	450.23	1526.98	687213.94	129.13	230.06	2.48	24.25	100.88	<0.031
516-36	18.56	308.05	308.05	33.91	<111.54	<0.28	5.53	3.91	63.48	46.65	1011.62	718928.69	110.87	63.87	<0.48	5.53	38.65	<0.0218
Disseminated																		
516-14	0.589	67.74	369.77	<20.18	<84.63	<0.147	5.88	5.29	54.51	7.46	524.97	713167.19	109.27	60.13	<0.32	53.06	21.7	0.06
02B-04	58.87	1108.72	773.62	34.45	<94.10	0.607	468.73	466.32	357.88	259.56	157.91	707127.63	32.18	58.39	0.45	33.32	64.36	<0.054
02B-05	34	984.73	328.13	<18.12	<97.55	0.512	570.16	566.53	364.53	308.27	134.1	709769.75	30.97	59.64	0.44	67.03	35.55	<0.055
02B-16	35.02	961.94	282.25	<18.47	<118.47	0.578	278.38	268.87	365.04	317.89	101.57	713102.81	27.4	56.11	<0.41	2.3	59.58	<0.045
02B-20	42.29	822.85	304.47	59.15	<106.99	0.555	517.08	524.41	264.34	264.34	164.96	713835.06	30.12	55.55	0.62	36.14	54.6	<0.044
02B-21	40.95	1097.91	780.03	50.08	112.44	0.81	723.97	697.66	386.23	363.88	105.04	711072.5	19.42	57.94	<0.45	83.72	54.97	<0.050
02B-24	152.46	1018.68	<132.03	44.77	462.06	1.59	305.74	309.64	367.27	212.18	209.64	715884.81	28.74	58.61	0.43	23.68	54.6	<0.044
02B-25	34.48	1267.67	476.47	65.7	<119.92	2.02	399.55	392.02	369.66	252.49	114.55	715884.81	24.15	57.82	<0.41	62.3	64.19	<0.050
02B-27	54.64	1131.49	694.69	58.01	160.37	0.389	404.07	396.1	374.94	249.21	115.73	717620.56	25.47	59.42	2.69	64.19	54.8	0.042
02B-28	51.77	1195.11	634.16	48.99	<114.05	0.48	356.43	349.33	415.23	280.76	147.33	717620.56	30.02	61.69	3.93	3.93	59.81	<0.041
02B-29	90.67	1446.81	700.18	34.49	<128.69	1.17	470.26	487.18	307.39	249.21	89	705846.63	17.97	59.37	2.54	33.61	54.94	0.071
02B-36	71.2	879.96	879.96	26.01	<79.96	0.626	104.71	105.62	192.24	169.99	166.79	713377.25	12.84	33.61	33.61	54.94	35.55	0.52
02B-37	47.28	563.54	286.9	21.04	104.71	1.2	6585.56	6766.48	189.79	190.03	872.4	711964.06	13.54	32.31	<0.30	5.29	38.27	0.156
02B-39	<0.89	686.9	164.37	<16.75	<73.01	0.3	153.1	147.37	190.03	160.82	<2.43	712159.94	12.1	29.08	0.3	162.43	32.53	<0.044
02B-42	70.92	307.58	780.89	35.42	<87.68	0.45	184.57	184.92	194.27	141.43	267.22	718250.19	12.61	25.81	<0.32	3.02	35.68	0.204
02B-43	20.91	347.77	260.34	<17.20	72.54	<0.158	181.72	182.64	199.11	160.82	51.57	703143.13	14.13	28.78	<0.29	66.97	41.63	0.052
02B-44	4.87	301.52	264.45	28.55	<78.17	0.225	186.73	191.06	190.99	159.53	54.73	709412.19	10.36	28.11	<0.33	1.53	34.26	<0.0194
02B-46	5.07	193.88	435.81	34.58	<78.27	0.37	183.2	171.96	185.5	175.22	35.11	714728.88	12.87	24.03	<0.38	4	29.26	<0.0177
02B-53	13.84	285.65	539.36	37.47	294.22	<0.22	129.99	130.15	197.62	219.86	54.48	720850.19	10.85	28.15	<0.35	11.85	30.41	<0.0190
31A-23	25.64	1559.7	1594.37	<725.90	344.25	<12.09	78.26	74.79	154.59	86.95	3848.11	714543.13	111.57	156.05	<3.20	47.71	53.75	0.13
31B-01	2028	5231.45	4064.38	50.54	<124.16	0.39	291.83	277.63	249.83	113.48	3321.73	704302.94	150.84	463.74	0.84	96.56	82.19	<0.062

15

Gangue mineral influence on magnetite and the implications for Warramboo iron ore deposit.

Element	Values
Zr90	25.02, <0.033, 6.5, 1.73, 2.79, <0.0078, 19.12, 442.07, 43.35, 28.45, 50.24, <0.61, 1.04, <0.64, 1.05, 0.59, 0.65, 1.7, 8.78, 10489.29, 1.12, 16.22, 0.83, 0.6, <0.123, <0.056, <0.038, <0.030, <0.112, <0.102, 0.099, <0.088, <0.083, <0.068, 0.097, <0.077, <0.094, <0.086, <0.042, 0.061, <0.040, <0.029, <0.036, 0.034, <0.041, <0.035, 0.052, <0.106
Sm118	25.02, 6.5, 1.73, 2.79, 19.12, 442.07, 43.35, 28.45, 50.24, <0.61, 1.04, <0.64, 1.05, 0.59, 0.65, 1.7, 8.78, 6.69, 4.92, 0.65, 0.29, 0.6, 0.83, 16.22, 1.12, 35.07, 42.92, 51.85, 21.91, 28.33, <0.75, 2.5, 4.75, 7.36, 20.64, 4.24, 3.66, <1.71, 1.91, 0.67, 0.78, 0.62, 9.35, 410.71, <0.66, 0.27, <0.28
La139	0.055, 0.068, 0.157, <0.034, <0.034, 0.091, 0.435, 0.039, 0.326, <0.10, 0.166, 0.089, 0.29, 0.022, 0.033, 0.028, <0.016, <0.015, 0.041, 0.03, <0.028, <0.0092, 0.098, <0.0083, <0.0100, <0.0107, 0.036, <0.0108, 0.142, <0.0131, 0.115, <0.0112, <0.036, <0.024, <0.026, <0.023, <0.024, <0.021, <0.023, <0.025, <0.038, <0.036, 0.034, <0.0103, <0.0127, 0.061, 0.141, <0.00, <0.0091, <0.0089
Ce140	<0.033, 0.157, <0.034, <0.034, 0.041, 0.435, 0.039, 0.326, <0.079, 0.575, 0.065, 0.033, 0.028, 0.048, 0.044, 0.024, <0.022, <0.024, <0.025, <0.034, <0.030, <0.128, <0.0081, 0.115, 0.142, <0.0131, <0.028, <0.0092, <0.0100, <0.0100, <0.0104, <0.0072, <0.0113, <0.0090, <0.0100, <0.0086, <0.025, <0.028, 0.024, 0.034, <0.0071, <0.00, 0.296
Pr141	<0.033, <0.034, 0.039, <0.0151, 0.05, 0.1, 0.044, 0.094, <0.014, <0.012, 0.013, <0.015, <0.0158, <0.0120, <0.0128, <0.0058, <0.0096, <0.030, <0.024, <0.034, <0.024, <0.020, <0.022, <0.019, <0.021, <0.021, <0.0207, <0.0197, <0.0092, <0.0102, <0.0087, <0.0065, <0.0096, <0.0083, <0.0065, <0.0064, <0.096, <0.031, 0.2, <0.0225, <0.0130, 0.0119, <0.0084, <0.0067, <0.0049, <0.0052, <0.0091, <0.035
Nd146	0.2, 0.23, <0.24, 0.29, 0.308, <0.084, <0.151, <0.084, 0.263, 0.65, 0.3, 0.094, 0.036, 0.028, <0.081, <0.075, <0.077, <0.112, <0.103, <0.138, <0.135, <0.170, <0.165, <0.143, <0.187, <0.182, <0.133, <0.130, <0.129, <0.051, <0.046, <0.049, <0.039, <0.040, <0.054, <0.048, <0.034, 0.063, 0.205, <0.113, <0.045, <0.053, <0.037, <0.065, <0.041, <0.036, <0.030, <0.029
Sm147	<0.30, <0.25, 0.29, 0.078, <0.164, 0.85, <0.085, <0.56, <0.112, <0.103, 0.098, <0.098, <0.106, <0.097, <0.023, <0.081, <0.049, <0.067, <0.25, <0.26, <0.170, <0.165, <0.143, <0.187, <0.182, <0.139, <0.130, <0.046, <0.054, <0.071, <0.050, <0.063, <0.038, <0.126, <0.127, <0.070, <0.065, <0.050, <0.065, <0.036, <0.039, <0.057, <0.060
Eu153	<0.073, <0.060, 0.073, 0.32, <0.028, 0.14, 0.126, <0.12, <0.023, <0.026, 0.12, <0.024, <0.032, <0.020, <0.023, <0.0172, <0.0196, <0.056, <0.062, <0.036, <0.039, <0.044, <0.036, <0.040, <0.035, <0.037, <0.040, <0.185, <0.0155, 0.013, <0.054, <0.046, <0.040, <0.094, <0.0101, <0.0094, <0.0131, <0.024, <0.0107, <0.0109, <0.0121, <0.0106, <0.0067, <0.0055, <0.0052
Gd157	<0.32, <0.34, 0.32, 0.079, <0.171, <0.65, 0.15, <0.57, <0.102, <0.0173, 0.12, 0.091, <0.112, 0.101, <0.095, <0.064, <0.063, <0.25, <0.24, <0.166, <0.149, <0.160, <0.134, <0.16, <0.134, <0.144, <0.146, <0.132, <0.093, <0.102, <0.068, <0.071, <0.048, <0.130, <0.131, <0.099, <0.041, <0.057, <0.053, <0.050, <0.052, <0.066, <0.070
Tb159	<0.056, <0.052, 0.32, <0.0201, 0.174, 0.15, <0.095, 0.015, <0.0173, <0.026, <0.023, <0.015, <0.0157, <0.018, <0.095, <0.0060, 0.0105, <0.046, <0.046, <0.030, <0.027, <0.044, <0.022, <0.024, <0.022, <0.021, <0.023, <0.025, <0.133, <0.106, <0.068, <0.0109, <0.0074, <0.0097, <0.0066, <0.0077, <0.077, <0.024, <0.0171, <0.0098, <0.0065, <0.0077, <0.0055, <0.0077, <0.0124
Dy163	<0.22, <0.177, 0.22, 0.082, <0.062, 0.42, <0.35, 0.07, <0.061, <0.017, 0.166, 0.079, <0.082, <0.067, <0.066, <0.033, <0.040, <0.169, <0.166, <0.100, <0.122, <0.093, <0.078, <0.14, <0.078, <0.088, <0.093, <0.102, <0.132, 0.081, 0.078, <0.048, <0.014, 0.055, <0.029, <0.035, <0.022, 0.029, <0.023, <0.024, <0.025, <0.027, <0.022
Ho165	<0.046, <0.050, 0.046, 0.03, <0.026, 0.24, 0.296, 0.11, <0.018, <0.018, 0.05, 0.041, <0.021, 0.021, <0.017, <0.0070, <0.0104, <0.043, <0.047, <0.025, <0.029, <0.029, <0.024, <0.022, <0.024, <0.023, <0.022, <0.023, <0.022, 0.197, <0.081, <0.014, 0.0115, 0.078, <0.0059, <0.0093, <0.0077, 0.029, <0.022, <0.024, <0.025, <0.0055, 0.012, <0.0112
Er166	<0.157, <0.161, 0.157, <0.051, <0.067, 0.30, 1.39, 0.073, 0.051, <0.014, 0.137, 0.166, <0.054, <0.019, 0.05, <0.059, <0.028, <0.124, <0.136, <0.075, <0.080, <0.090, <0.064, <0.092, <0.064, <0.065, <0.066, <0.065, <0.086, <0.065, 0.048, <0.026, 0.027, <0.048, 0.027, <0.030, <0.026, 0.087, <0.024, <0.023, <0.045, <0.018, <0.00, <0.081
Tm169	<0.057, <0.061, 0.057, <0.031, <0.043, 0.10, 2.66, <0.079, <0.017, <0.014, 0.041, 0.082, <0.019, <0.019, 0.072, <0.061, <0.099, <0.053, <0.045, <0.029, <0.025, <0.024, <0.023, <0.021, <0.023, <0.022, <0.027, <0.025, <0.025, <0.0115, <0.012, <0.043, <0.0095, 0.031, <0.0064, <0.0063, <0.0105, 0.032, <0.028, <0.029, <0.032, <0.0105, <0.00, 0.022
Yb172	<0.22, <0.21, 0.22, 0.0042, <0.043, 0.45, 2.66, <0.38, <0.061, 0.032, 0.152, <0.061, <0.020, <0.020, 0.088, <0.032, <0.059, <0.171, <0.193, <0.111, <0.112, <0.118, <0.092, <0.101, <0.092, <0.093, <0.102, <0.102, <0.093, 0.047, 0.013, <0.040, <0.043, 0.031, <0.036, <0.032, <0.029, 0.223, <0.021, <0.029, <0.030, <0.0071, <0.42, <0.047
Lu175	<0.058, <0.049, 0.058, 0.0042, <0.0200, 0.11, 324.45, <0.100, <0.018, 0.032, 0.021, 0.065, <0.0171, <0.018, 0.061, <0.0147, <0.0177, <0.044, <0.045, <0.030, <0.025, <0.029, <0.021, <0.079, <0.023, <0.087, <0.081, <0.081, <0.026, <0.022, <0.0094, <0.035, <0.038, 0.0112, 0.024, <0.0093, <0.0071, 0.099, <0.024, <0.027, <0.025, <0.0096, <0.00, <0.028
Hf178	<0.215, <0.19, 0.215, 0.0042, <0.0200, 0.46, 1.04, <0.108, 0.015, 0.338, 0.105, 0.409, 0.174, 0.08, 0.056, <0.020, <0.0227, <0.167, <0.180, <0.092, <0.097, <0.092, <0.079, <0.065, <0.079, <0.083, <0.087, <0.081, <0.029, 0.048, 0.036, <0.052, <0.035, 0.115, <0.038, <0.027, <0.024, 0.223, <0.024, <0.029, 0.032, <0.0071, <0.38, <0.072
Pb208	0.101, 0.094, <0.072, <0.061, 0.033, 2.85, 22.55, 20.58, 0.015, 0.026, 0.105, 0.409, 0.174, 0.212, 0.111, 0.030, 0.056, 0.164, 0.104, 0.083, 0.115, 0.223, 0.115, 0.79, 0.026, 0.042, 0.089, 0.129, 0.048, 0.072, 0.047, <0.057, 0.036, 0.115, 0.043, 0.024, 0.036, 0.087, 0.029, 0.032, 0.101, 0.164, 0.82, 2.85, 20.58, 22.55, 0.23, 0.309
Th232	<0.049, <0.072, <0.061, <0.053, 0.0113, 0.06, 14.71, <0.074, <0.0150, 0.014, 0.038, 0.033, 0.028, 0.033, <0.025, <0.031, <0.0135, <0.0095, <0.085, <0.0062, <0.0063, <0.0091, <0.0067, <0.0075, <0.0083, <0.0078, <0.024, <0.026, <0.026, <0.026, <0.0087, <0.052, <0.032, 0.036, <0.0082, <0.0075, <0.0090, <0.0080, <0.0090, <0.017
U238	<0.049, <0.053, <0.049, <0.0025, <0.0063, <0.0056, <0.015, <0.0138, <0.0150, 0.038, 0.033, 0.028, 0.0113, <0.0072, <0.0095, <0.0135, 0.089, 0.129, <0.0171, <0.085, <0.0092, <0.0061, <0.0063, <0.0082, <0.0075, <0.0078, <0.0210, <0.022, <0.026, 0.0198, <0.0100, <0.044, <0.032, 0.029, <0.0090, <0.0067, <0.0090, <0.024, <0.0075, <0.0060, <0.0082, <0.0076, <0.00, 0.073

Gangue mineral influence on magnetite and the implications for Warramboo iron ore deposit.

Inclusions

Element	Mg24	Al27	Si29	P31	Ca43	Sc45	Ti47	Ti49	V51	Cr53	Mn55	Fe57	Co59	Ni60	Cu65	Zn66	Ga69	Y89
P2-30	36.3	476.56	1156.52	80.5	127.69	<0.67	127.69	138.45	260.17	214.31	952.96	716493.56	78.6	142.25	0.71	315	12.31	0.45
P2-29	35.56	432.85	5836.87	72.42	<283.94	<0.62	185.43	170.18	249.26	177.03	771.71	715619.75	74.87	151.69	<0.60	167.59	7.88	0.3
P2-25	212.45	1239.12	3630.34	68.04	<261.72	<0.53	147.31	148.28	248.47	564.24	930.8	713203.13	70.83	125.82	<0.67	346.02	10.42	7.49
P2-23	15.43	275.05	1952.32	77.64	<249.22	<0.45	87.88	83.31	222.76	291.63	676.93	712035.56	64.99	105.62	0.35	41.25	6.57	7.92
P2-19	76.86	1272.11	3247.73	65.95	<209.83	0.58	168.39	161.76	256.08	227.05	882.89	716015.5	68.49	111.1	5.84	227.34	11.25	16.46
P2-18	60.22	267.56	1241.22	70.41	<235.71	0.98	52.67	54.35	252.08	268.85	673.68	719599.63	68.37	116.53	<0.34	155.5	8.69	31.02
P2-17	14.4	719.8	1963.8	92.67	463.16	<0.45	94.58	98.11	249.2	268.85	796.16	719285.63	68.83	120.53	<0.60	95.62	9.36	1.41
P2-15	169.3	1516.49	1466.43	111.16	<249.41	<0.45	162.21	153.49	248.31	157.51	936.86	710625.63	67.45	110.53	<0.49	388.75	14.62	5.54
P2-12	228.87	8188.92	7697.06	<49.84	2361.85	16.62	228.54	208.87	243.17	202.53	1339.98	709280.06	62.53	99.43	<0.60	271.42	19.49	76.77
P2-09	1239.57	12408.65	2086.29	51.22	208.1	2.81	1361.51	1392.57	269.51	362.7	748.78	698840.81	65.47	114.27	0.68	34.34	10.78	4.25
P2-08	7846.71	15400.97	119755.06	76.58	8191.99	6.43	672.32	633.29	276.67	432.79	1207.99	708848.69	71.76	135.27	1.83	46.56	12.37	152.15
P2-05	181	1917.56	4830.11	48.27	138.92	0.687	155.75	143.69	256.76	321.35	1477.99	705824.13	65.05	112.78	0.37	77.04	8.53	71.18
P2-04	4214.95	5359.74	184786.97	81.73	6273.72	4.07	464.63	458.47	229.99	315.42	995.5	703064.81	64.6	96.47	2.08	30.86	8.36	6.73
P1-30	13.62	286.1	<591.00	57.38	357.91	<0.54	71.71	80.49	316.02	147.23	328.81	719695.19	56.51	103.14	<0.43	187.06	8.81	<0.092
P1-29	75.66	1150.86	1280.83	49.64	288.51	0.59	697.13	668.74	335.22	115.17	614.53	731318.13	64.66	99.16	<0.68	166.35	9.52	1.05
P1-28	29.47	619.86	<612.89	65.92	300.88	1.06	160.13	151.48	340.16	92.31	608.2	716698.25	64.12	120.12	<0.35	204.92	10.53	0.68
P1-27	12.79	310.68	<551.21	52.46	207	<0.46	102.42	101.61	319.19	277.56	273.18	705519.38	51.75	114.38	1.73	125.13	6.43	3.85
P1-26	19.8	389.19	1479.43	53.3	<225.25	<0.46	90.82	99.16	310.66	278.06	273.86	718100.19	52.39	104.56	<0.28	85.18	7.63	4.4
P1-25	111.48	1505.66	1599.07	61.67	<193.94	0.9	95.29	102.47	316.01	280.33	258.98	717726.31	53.57	107.29	0.4	76.31	9.5	42.45
P1-24	23.09	1593.07	553.05	48.1	<166.19	0.7	83.71	90.88	276.63	227	284.36	614006.5	48.86	94.88	<0.44	157.04	7.66	6.24
P1-23	113.39	506.13	<166.19	83.71	379.81	<0.54	130.23	128.18	316.32	194.15	398.98	720815.31	56.44	111.4	<0.41	166.35	1.05	1.05
P1-22	117.03	920.98	379.81	49.67	<247.31	0.85	102.49	113.27	331.2	168.28	433.48	715780.69	65.59	120.12	<0.35	204.92	10.53	0.68
P1-21	337.44	380.89	920.98	64.78	<204.09	<0.54	113.6	113.6	331.2	168.28	739.83	717210.13	71.32	118.78	<0.38	277.85	15.9	3.24
P1-20	20.38	244.13	<204.09	56.19	<228.72	<0.52	114.85	184.13	323.81	127.54	739.83	716593.75	70.18	118.78	<0.38	277.85	15.9	0.24
P1-19	541.03	1642.88	818.05	49.61	114.85	<0.52	181.72	178.42	323.15	127.54	847.74	707195.25	68.16	130.37	<0.47	391.76	16.57	3.45
P1-18	1044.58	1465.52	3548.19	68.52	181.72	<0.55	183.24	154.55	327.57	38.87	807.78	722456.19	55.32	129.93	<0.54	303.35	4.52	5.02
P1-17	166.14	390.97	2319.01	35.01	500.42	0.59	130.36	122	318.7	242.22	271.12	713510.94	56.08	129.37	0.92	189.73	11.3	2.62
P1-16	684.58	702.12	818.05	81.54	<205.65	0.65	816.28	837.04	329.66	183.34	824.91	661627.75	49.31	118.95	<0.46	42.69	5.54	7.03
P1-15	1523.85	484.66	2054.3	257.52	500.42	0.7	48.65	50.11	291.21	365.44	200.84	715311.25	60.8	128.1	<0.43	134.9	7.5	4.67
P1-14	785.12	2234.77	785.12	360.86	360.86	<0.55	167.33	155.81	336.38	282.64	528.92	713378	63.52	136.4	<0.53	303.12	11.8	22.22
P1-13	2054.3	1926.79	428.28	167.33	<260.32	0.59	95.74	82.67	401.8	401.8	710923.25	710923.25	57.25	118.06	3.09	62.7	8.51	1.94
P1-12	1140.71	3548.19	2042.68	155.81	<245.26	<0.57	53.36	161.73	326.91	225.49	334.37	710564.94	56.94	129.04	1.63	109.57	1.52	1.88
P1-11	428.28	2319.01	2234.77	319.96	<210.53	<0.50	49.02	60.98	304.23	376.02	401.47	710838.69	56.94	116.94	<0.43	104.29	6.24	1.88
P1-10	2042.68	1959.5	1926.79	35.01	<186.49	<0.39	58.43	61.21	248.34	232.67	221.67	543329.56	41.87	103.09	0.47	45.62	4.24	9.22
P1-05	134.67	1927.38	756.82	31.41	220.26	<0.54	110.08	122	294.56	245	234.25	649402.19	49.67	103.1	<0.57	47.46	7.16	1.27
P1-04	148.66	511.07	3637.82	74.62	<157.35	<0.56	118.41	101.85	335.1	161.48	368.03	715313.5	55.54	107.73	<0.41	173.61	7.87	0.99
P1-03	22.95	651.27	1692.35	43.4	<143.79	<0.54	162.77	153	334.23	175.68	498.96	727452.75	66.11	118.26	<0.44	287.18	12.96	0.73
P1-02	39.46	1033.12	1668.38	65.58	1106.34	0.61	115.71	129.38	345.8	279.68	410.09	721774.5	66.65	128.84	0.45	109.22	13.76	9.03
PM P1-01	9.74	327.04	<738.24	<34.74	<134.61	0.64	126.58	104.18	332.3	36.82	494.89	718395.56	64.59	123.52	<0.44	327.01	12.97	<0.00
02B-12	1398.07	3749.27	1927.38	44.63	544.03	0.62	479.78	494.25	332.3	173.37	189.78	717620.56	15.46	55.43	0.7	23.39	52.94	0.41
02B-15	139.68	1353.41	1811.26	52.51	168.27	0.38	188.4	186.77	389.04	290.49	165.84	711953.19	24.74	58.26	3.02	52.94	58.46	0.245
02B-18	165.35	1811.26	1798.16	33.44	113.82	0.562	378.72	198.8	334.23	75.27	498.96	714829.25	19.16	79.36	<0.44	58.46	24	<0.050
02B-49	308.89	672.67	911.41	35.39	374.35	0.6	374.35	247.7	198.8	247.7	104.61	709951.56	7.78	7.27	<0.45	7.27	0.73	0.131
02B-51	47.57	336.24	771.42	25.1	<81.43	0.62	217.55	222.15	335.1	75.27	98.51	702654.94	26.76	79.36	<0.41	23.09	12.96	0.176
02B-52	14.16	369.23	369.95	<20.90	<106.64	<0.215	2066.36	132.66	294.56	67.97	179.23	708962.06	11.92	33.34	<0.33	27.16	30.53	<0.0188
02B-58	13.37	338.2	756.76	22.9	169.79	0.47	169.79	168.54	188.89	112.43	58.79	716819.94	11.94	31.44	<0.38	30.53	33.17	0.042
02B-59	38.83	379.91	524.74	25.41	161.48	0.22	161.48	160.87	216.48	155.64	82.71	706939.5	11.23	30.11	<0.35	31.02	31.02	0.064
02B-60	22.53	334.34	625.76	32.86	<85.77	0.31	160.06	164.56	208.96	147	93.21	710201.88	14.61	29.53	<0.40	4.34	31.56	0.102

17

Gangue mineral influence on magnetite and the implications for Warramboo iron ore deposit.

Zr90	Sn118	La139	Ce140	Pr141	Nd146	Sm147	Eu153	Gd157	Tb159	Dy163	Ho165	Er166	Tm169	Yb172	Lu175	Hf178	Pb208	Th232	U238
<0.107	37.76	0.187	0.56	0.106	0.34	<0.19	0.046	0.22	0.036	0.18	0.040	0.052	0.052	0.166	0.043	0.144	0.163	0.050	0.054
<0.099	12.75	<0.030	<0.032	<0.027	<0.163	<0.197	<0.052	<0.18	<0.123	<0.040	<0.114	<0.102	<0.035	<0.166	<0.043	<0.067	<0.041	<0.050	<0.054
<0.108	11.25	<0.043	<0.025	<0.026	<0.146	<0.178	<0.049	<0.119	<0.030	<0.123	<0.087	<0.087	<0.032	<0.123	<0.028	<0.056	<0.067	<0.041	<0.034
0.034	32.52	<0.030	<0.025	<0.026	<0.104	<0.197	<0.052	<0.18	<0.119	<0.123	<0.035	<0.102	<0.035	<0.146	<0.028	<0.067	0.056	<0.041	<0.027
<0.033	1.39	0.032	0.0298	<0.0097	<0.039	<0.059	<0.0163	<0.061	<0.072	0.045	<0.026	<0.026	<0.038	<0.038	<0.0110	0.071	<0.063	<0.034	<0.0083
<0.032	<0.091	<0.0091	0.032	<0.0069	0.045	<0.045	<0.0120	<0.059	0.048	0.083	0.024	<0.0062	<0.0062	<0.035	<0.0085	0.053	<0.0083	0.055	<0.0083
<0.029	61.61	<0.0061	<0.0088	<0.0087	<0.025	<0.051	<0.0130	<0.051	0.045	0.024	0.083	<0.0074	<0.0059	<0.031	0.0059	<0.018	<0.0041	<0.0072	<0.0072
<0.032	9.35	<0.0093	<0.0073	<0.0069	<0.045	<0.045	<0.0130	<0.051	<0.0093	0.077	<0.0077	<0.0074	<0.0062	<0.035	<0.0059	<0.018	<0.0103	<0.0066	<0.0083
0.024	26.16	<0.0091	<0.0083	<0.0097	<0.039	<0.059	<0.0163	<0.051	0.031	0.083	0.077	<0.0032	<0.0083	<0.038	<0.0059	<0.018	<0.0174	<0.0072	<0.0072
0.032	2.29	<0.0048	<0.0084	<0.0066	<0.033	<0.036	<0.0103	<0.042	<0.0069	<0.028	<0.0067	<0.016	<0.0058	<0.031	<0.0073	<0.0226	0.0179	<0.0063	<0.0063
<0.214	<0.79	<0.00	<0.0252	<0.00	<0.104	<0.00	<0.043	<0.152	<0.00	0.073	<0.035	<0.00	<0.029	<0.063	<0.0151	0.064	0.062	<0.025	<0.010
40.78	17.75	2.83	40.78	0.47	1.77	0.21	0.17	0.66	0.177	0.27	0.41	0.41	0.086	0.5	0.047	1.08	1.19	0.64	0.41
11.54	<0.75	<0.043	0.031	0.027	0.12	<0.032	<0.052	0.18	1	0.06	0.175	2.03	0.175	0.03	0.033	0.24	0.165	0.14	<0.034
13.51	<0.73	<0.030	0.0066	0.026	<0.104	<0.197	<0.050	<0.18	0.067	<0.104	<0.026	0.03	0.03	0.24	0.052	0.132	2.32	0.153	<0.041
37.06	7.71	0.035	<0.032	<0.0066	<0.095	<0.174	<0.032	<0.110	<0.026	0.044	0.113	0.96	0.046	0.089	0.017	0.329	0.311	1.87	0.153
249.94	3.39	0.23	0.423	<0.0296	0.17	0.14	0.096	0.214	0.044	0.62	0.251	0.111	0.101	0.24	0.054	0.28	0.132	397.82	0.217
13.89	0.83	<0.030	<0.032	<0.0069	<0.094	<0.112	<0.032	<0.100	<0.017	0.24	0.062	0.23	0.046	0.52	0.017	1.44	0.57	1.58	0.217
2.83	<0.030	<0.033	<0.035	<0.0097	<0.104	<0.174	<0.050	<0.141	<0.026	0.35	<0.026	0.24	<0.024	0.29	0.03	0.5	0.229	1.13	0.153
8.39	20.85	<0.030	<0.032	<0.0087	<0.097	<0.115	0.038	0.17	0.044	0.64	0.35	0.2	<0.0167	0.52	0.054	1.44	0.53	0.37	0.191
23.59	23.2	0.78	1.27	0.135	0.52	<0.00	<0.024	0.45	0.041	0.28	0.069	0.28	0.128	0.073	0.16	3.3	0.68	0.53	0.172
8.6	1.93	45.73	93.55	9.62	38.42	11.69	0.88	4.72	0.47	1.71	0.74	1.37	0.31	2.03	0.65	4.43	3.3	26.64	0.524
220.48	21.68	163.54	16.81	<0.035	63.66	<0.00	2.18	7.8	1.06	4.88	0.24	0.27	0.128	0.24	0.62	1.77	8.91	0.136	0.524
2.98	0.85	0.074	0.163	0.035	<0.00	1.52	0.214	1.36	0.102	0.61	0.19	0.96	0.38	0.4	0.062	0.71	1	2.09	0.136
10.42	158.91	1.57	2.87	1.46	5.43	<0.22	0.096	0.53	0.51	0.47	0.113	0.23	0.046	0.101	0.03	0.89	1.65	2.09	0.211
1.14	1.02	0.88	0.484	0.113	0.51	<0.129	0.023	<0.13	0.103	1	0.078	0.24	0.115	0.82	0.165	0.438	1.338	1.65	0.222
1.25	0.88	2.34	2.34	0.276	0.63	0.2	0.032	0.2	0.038	0.18	0.34	1.04	0.2	0.83	0.03	0.5	13.38	4.07	0.102
32.21	<0.78	0.244	0.128	<0.024	<0.167	<0.115	<0.052	<0.170	0.065	0.35	0.103	0.55	0.131	0.112	0.112	0.8	<0.084	2.12	0.102
4.29	<0.83	<0.051	<0.051	0.032	<0.103	<0.123	0.035	0.32	<0.032	<0.00	0.05	0.119	<0.033	0.83	<0.022	<0.084	0.34	0.205	<0.102
14.18	<0.79	<0.042	0.062	0.019	<0.104	<0.00	<0.051	<0.127	<0.027	0.2	<0.026	0.46	0.046	0.23	0.044	0.21	0.236	0.188	2.12
32.32	0.64	29.9	56.89	6.57	24.14	4.95	0.78	2.86	0.49	1.14	0.18	4.68	0.41	2.42	0.41	0.12	0.257	0.127	0.188
70.3	49.51	15.24	18.59	3.55	13.32	1.88	0.67	4.32	0.73	6.28	1.41	4.68	2.42	0.51	1.13	8.76	5.13	0.43	2.09
87.77	3.37	<0.028	<0.030	<0.035	0.102	<0.204	<0.034	0.041	0.018	0.32	0.136	0.45	0.71	2.59	2.07	27.7	1.68	0.433	1.68
32.79	1.72	<0.050	<0.031	<0.0181	<0.174	0.077	0.0079	0.12	<0.026	0.32	0.086	0.4	0.082	0.55	0.081	0.7	0.93	1.09	0.433
220.77	<0.050	<0.031	<0.031	1.74	<0.174	0.077	0.0079	0.54	0.22	1.98	0.61	2.36	0.55	1.72	0.7	1.09	0.214	0.273	0.273
247.98	2.24	2.24	4.19	0.52	1.31	1.74	0.096	1.36	0.92	3.68	0.93	4.74	0.116	0.29	0.165	1.338	0.382	27.81	0.102
<0.157	12.12	5.67	5.67	0.43	1.31	0.49	0.184	1.36	0.22	2.36	0.4	2.36	0.82	1.72	0.165	13.38	0.248	2.15	4.07
47.22	<0.078	<0.078	0.388	0.085	0.383	<0.177	0.055	0.54	0.092	0.643	0.167	0.543	0.056	0.32	0.079	4.74	0.34	122.43	2.12
23.71	0.508	0.823	0.823	0.037	0.037	<0.00	<0.00	<0.227	0.0067	<0.126	<0.018	<0.076	<0.023	<0.119	<0.028	0.043	<0.033	<0.0029	<0.032
678.74	1.406	1.406	1.406	1.093	1.99	1.46	<0.00	1.36	0.92	14.54	3.27	11.94	1.81	10.97	1.44	6.73	6.49	6.49	27.81
51.45	2.42	6.08	6.08	0.327	1.99	0.7	0.472	0.54	2.35	1.98	0.61	2.36	1.72	0.29	1.44	7.23	3.49	2.15	2.15
52.31	43.71	1.55	3.12	0.629	1.044	0.297	0.135	0.269	0.221	0.532	0.223	0.243	0.089	0.47	0.364	0.58	2.41	15.34	11.47
134.35	1.34	1571.55	2807.85	359.82	1322.61	192.76	24.84	115.8	11.11	41.01	8.05	13.48	1.82	7.9	1.08	57.87	5.75	57.97	0.47
6.03	8.4	<0.064	0.075	0.084	<0.183	<0.186	<0.0260	<0.19	<0.030	0.15	0.227	<0.106	0.054	0.28	<0.039	0.44	0.54	1.56	2.33
934.25	15.33	13.95	23.48	2.9	10.79	1.84	0.27	2.43	0.506	3.68	0.93	4.74	0.98	5.29	1.28	6.95	1.05	3.92	1.9
127.52	<0.73	10.87	15.78	2.05	8.27	0.88	0.273	2.26	0.56	3.29	0.49	1.58	0.36	1.8	0.267	6.18	1.83	13.04	0.273
12.85	3.38	10.83	17.28	2.48	10.15	2.76	0.464	2.18	0.378	2.29	0.274	0.73	0.063	0.52	0.052	35.78	2.26	20.29	4.47
66.77	112.81	7.42	15.07	1.7	7.14	1.42	0.152	0.9	0.142	0.65	0.224	0.59	0.116	0.7	0.132	0.37	1.43	8.95	0.204
1.9	16.08	0.181	0.062	0.036	<0.17	0.27	<0.028	<0.16	<0.074	<0.20	<0.033	<0.097	<0.052	<0.111	<0.021	<0.109	1.26	3.38	0.77
4.44	1.25	0.134	0.262	<0.029	<0.21	0.057	<0.027	0.18	0.0092	<0.126	0.038	<0.117	<0.032	<0.133	0.035	0.127	0.227	0.302	0.028

Full Electron Microprobe, LA-ICP-MS and Glitter raw, corrected and normalised data is available electronically in excel spread sheet form if further information is required.